DEVELOPMENT OF AN ASSESSMENT METHOD FOR SEISMIC DAMAGE TO GRAVITY WASTE WATER PIPES

A Thesis in partial fulfilment of the requirements for the degree of

Master of Engineering in Civil Engineering

at the

University of Canterbury

By

Yifei Tang

Department of Civil and Natural Resources Engineering

University of Canterbury

New Zealand

2019

Abstract

This thesis documents the development and demonstration of an assessment method for analysing earthquake-related damage to concrete waste water gravity pipes in Christchurch, New Zealand, following the 2010-2011 Canterbury Earthquake Sequence (CES). The method is intended to be internationally adaptable to assist territorial local authorities with improving lifelines infrastructure disaster impact assessment and improvements in resilience. This is achieved through the provision of high-resolution, localised damage data, which demonstrate earthquake impacts along the pipe length. The insights gained will assist decision making and the prioritisation of resources following earthquake events to quickly and efficiently restore network function and reduce community impacts.

The method involved obtaining a selection of 55 reinforced concrete gravity waste water pipes with available Closed-Circuit Television (CCTV) inspection footage filmed before and after the CES. The pipes were assessed by reviewing the recordings, and damage was mapped to the nearest metre along the pipe length using Geographic Information Systems. An established, systematic coding process was used for reporting the nature and severity of the observed damage, and to differentiate between pre-existing and new damage resulting from the CES. The damage items were overlaid with geospatial data such as Light Detection and Ranging (LiDAR)-derived ground deformation data, Liquefaction Resistance Index data and seismic ground motion data (Peak Ground acceleration and Peak Ground Velocity) to identify potential relationships between these parameters and pipe performance.

Initial assessment outcomes for the pipe selection revealed that main pipe joints and lateral connections were more vulnerable than the pipe body during a seismic event. Smaller diameter pipes may also be more vulnerable than larger pipes during a seismic event. Obvious differential ground movement resulted in increased local damage observations in many cases, however this was not obvious for all pipes. Pipes with older installation ages exhibited more overall damage prior to a seismic event, which is likely attributable to increased chemical and biological deterioration. However, no evidence was found relating pipe age to performance during a seismic event. No evidence was found linking levels of pre-CES damage in a pipe with subsequent seismic performance, and seismic performance with liquefaction resistance or magnitude of seismic ground motion.

The results reported are of limited application due to the small demonstration sample size, but reveal the additional level of detail and insight possible using the method presented in this thesis over existing assessment methods, especially in relation to high resolution variations along the length of the pipe such as localised ground deformations evidenced by LiDAR.

The results may be improved by studying a larger and more diverse sample pool, automating data collection and input processes in order to improve efficiency and consider additional input such as pipe dip and cumulative damage over a large distance.

The method is dependent on comprehensive and accurate pre-event CCTV assessments and LIDAR data so that post-event data could be compared. It is proposed that local territorial authorities should prioritise acquiring this information as a first important step towards improving the seismic resilience of a gravity waste water pipe network.

Acknowledgements

I would like to open the acknowledgements to thank my two superb supervisors Dr Matthew Hughes and Associate Professor Allan Scott. They have taken time out of their busy schedules to have consistent meetings with me to develop my research goal and establish details about my thesis. I would simply not have the energy nor guidance to complete this task without their energetic support and I thank them for all the patience and time they have dedicated to helping this research project come to fruition. Matthew has in particular taken the additional step to having one-on-one tutorials on geospatial analysis using GIS, and this was a tool I had absolutely no idea how to use prior to this project. Allan also made the effort of communicating and sharing ideas with me while he was overseas in Canada.

From the Christchurch City Council my thanks go to Irmana Garcia Sampedro and Eilidh Hilson. Irmana and I have met and discussed the project together on multiple occasions and, being a Strategic Asset Engineer, she provided me with not only the raw CCTV footage required for this project but also professional guidance on how to interpret the results from the CCTV surveys. Irmana also provided some insight on how the project could be defined in a way which would have practical applications and therefore be directly beneficial to the interests of the local council. Eilidh constantly made herself available to compile relevant raw data required for my analysis and passing this information to me whenever I needed it.

While completing my Masters project I was often absent from work on study leave to attend meetings, lectures and discussions, and I thank my work supervisor Zahid Hanif for having the patience to bear with me for all the time I was disengaged at work.

Writing a thesis part time has been a journey, but it has been a fantastic one thanks to the help of my partner Wei, who never fails to lift my spirit.

Yifei Tang

10 April 2019

Table of Contents

List of Figures

List of Tables

List of Acronyms

AC	Asbestos Cement
ACPA	American Concrete Pipe Association
ASCE	American Society of Civil Engineers
CCC	Christchurch City Council
CDEM 2002	Civil Defence Management Act 2002
CES	2010-2011 Canterbury Earthquake Sequence
CI	Cast Iron
DEM	Digital Elevation Model
GI	Galvanised Iron
GIS	Geographic Information System
EW	Earthenware
FEM	Finite Element Analysis
HDPE	High-Density Polyethylene
IRTS&G	Infrastructure Recovery Technical Standards and Guidelines
NZLC	New Zealand Lifelines Council
NZPIM	New Zealand Pipe Inspection Manual
PSHA	Probabilistic Seismic Hazard Analysis
PVC	Polyvinyl Chloride
RCRR	Reinforced Concrete Rubber Ring
S	Steel
SCIRT	Stronger Christchurch Infrastructure Rebuild Team
SPIDA	Soil-Pipe Interaction Design and Analysis
UNIDSR	United Nations International Strategy for Disaster Reduction
VT	Vibration Technology

Chapter 1 - Introduction

Lifeline infrastructure provides the basic services required for the operation of society. These include telecommunications, transport, water and energy. In the aftermath of a disaster, decisions need to be made urgently to alleviate the strain suddenly imposed on available resources. Therefore, a robust and resilient system of lifelines is crucial for the ability of a region to recover from traumatic events.

This thesis presents a detailed method for assessing seismic impacts on reinforced concrete gravity waste water pipes based on the performance of infrastructure in Christchurch City, New Zealand, during the 2010-2011 Canterbury Earthquake Sequence (CES). This assessment characterises specific modes of failure and causative factors, in order to contribute to development of a risk and resilience framework for this critical infrastructure lifeline system within New Zealand and elsewhere.

This Chapter presents an overview of key topics and the rationale for undertaking this study including a discussion of risk and resilience to infrastructure with a New Zealand context, and the suitability of using data from Christchurch as a case study towards understanding the general seismic performance of reinforced concrete waste water pipes. Following this review, the objectives of the project are presented.

1.1 Understanding risk and resilience

The primary objective of this thesis project is to contribute to increased resilience of waste water lifeline infrastructure. Building infrastructure resilience starts with the understanding of disaster risk.

The components of disaster risk in the current New Zealand risk management framework are derived from definitions in the United Nations National Disaster Risk Assessment, which is a set of guidelines produced in 2016 by the United Nations International Strategy for Disaster Reduction (UNISDR), under its “Words into Action” initiative to support implementation of the Sendai Framework for Disaster Risk Reduction 2015-2030 on a national level. This framework is currently the most encompassing international accord on disaster risk reduction in place (UNISDR, 2018).

The Sendai Framework aims for the “substantial reduction of disaster risk and losses in lives, livelihoods and health and in the economic, physical, social, cultural and environmental assets of persons, businesses, communities and countries” (UNISDR, 2018). In order to achieve this, seven global targets have been agreed between member states (UNISDR, 2018):

1. “Substantially reduce global disaster mortality by 2030, aiming to lower average per 100,000 global mortality between 2020-2030 compared to 2005-2015;
2. Substantially reduce the number of affected people globally by 2030, aiming to lower the average global figure per 100,000 between 2020-2030 compared to 2005-2015;
3. Reduce direct disaster economic loss in relation to global gross domestic product by 2030;
4. Substantially reduce disaster damage to critical infrastructure and disruption of basic services, among them health and educational facilities, including through developing their resilience by 2030;
5. Substantially increase the number of countries with national and local disaster risk reduction strategies by 2020;
6. Substantially enhance international cooperation to developing countries through adequate and sustainable support to complement their national actions for implementation of the framework by 2030;
7. Substantially increase the availability of and access to multi-hazard early warning systems and disaster risk information and assessments to the people by 2030.”

Lifeline infrastructures such as waste water networks are fundamental to public health and safety, the local economy, and the basic operation of society. Therefore, improving general resilience for lifeline infrastructure directly supports the achievement of goals 2, 3, and 4 of the Sendai Framework. Addressing these Sendai targets in the context of waste water systems also aligns with the 2015-2030 Sustainable Development Goals, specifically Goal 6 that addresses ensuring access to clean water and sanitation for all (UNISDR, 2019).

The disaster risk concept adopted by the UNISDR defines risk based on the interaction between likelihood and impact, and the interaction of the key components of hazard, exposure, and vulnerability. Hazard refers to a phenomenon (whether natural or man-made)

causing harm. Exposure defines the spatial (and possibly temporal) extent of potentially affected communities and assets in hazard-prone areas, and vulnerability is based on the attributes of the exposed communities and their assets that affect their susceptibility to the hazard (UNISDR, 2018).

The interaction of the risk components results in varying levels of impact directly or indirectly affecting a system or community. A summary chart showing the risk components and impacts is provided in Figure 1-1. The impact may or may not be quantifiable, due to the differing perceptions of risk amongst different affected communities (New Zealand Parliamentary Counsel Office, 2018) and may directly or indirectly affect the community. In the case of wastewater networks, direct impacts include damage to infrastructure, and indirect impacts could include loss of income for businesses from requiring customers to use portable toilets while repairs are undertaken. The latter is also an example of a quantifiable impact, while health risks due to water borne disease may be difficult to quantify.

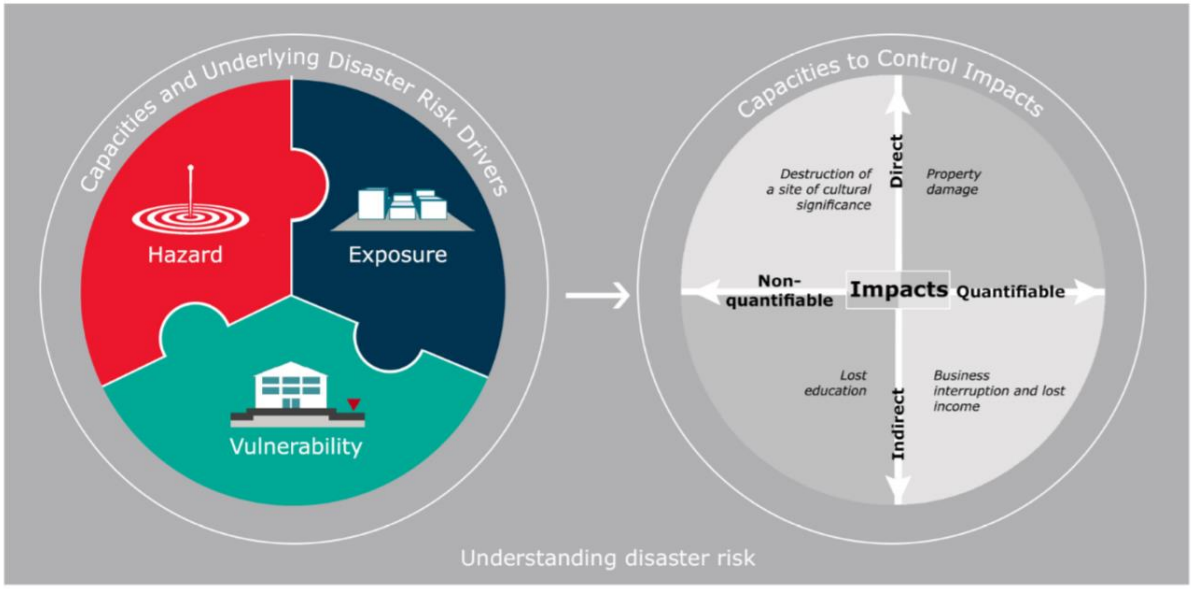

Figure 1-1. Disaster risk drivers and impacts (UNISDR, 2017)

New Zealand follows the principles and guidelines of risk management provided in the standard AS/NZS ISO 31000:2009, which is identical to and reproduced from the international standard ISO 31000. The risk management process is illustrated in Figure 1-2. and starts with establishing the context in order to define the scope of assessment; for

example, engaging with stakeholders and defining acceptable criteria for decision making. This is followed by the assessment of risk, which involves scoping the hazard, exposure and vulnerability and assessing each point of interaction of the various disaster risk components for the purpose of managing the risk. The final stage is risk treatment, which could include methods to reduce affected population numbers or spatial extent of exposed assets. Throughout the process, communication and consultation with stakeholders is recommended, along with consistent monitoring and review of the process.

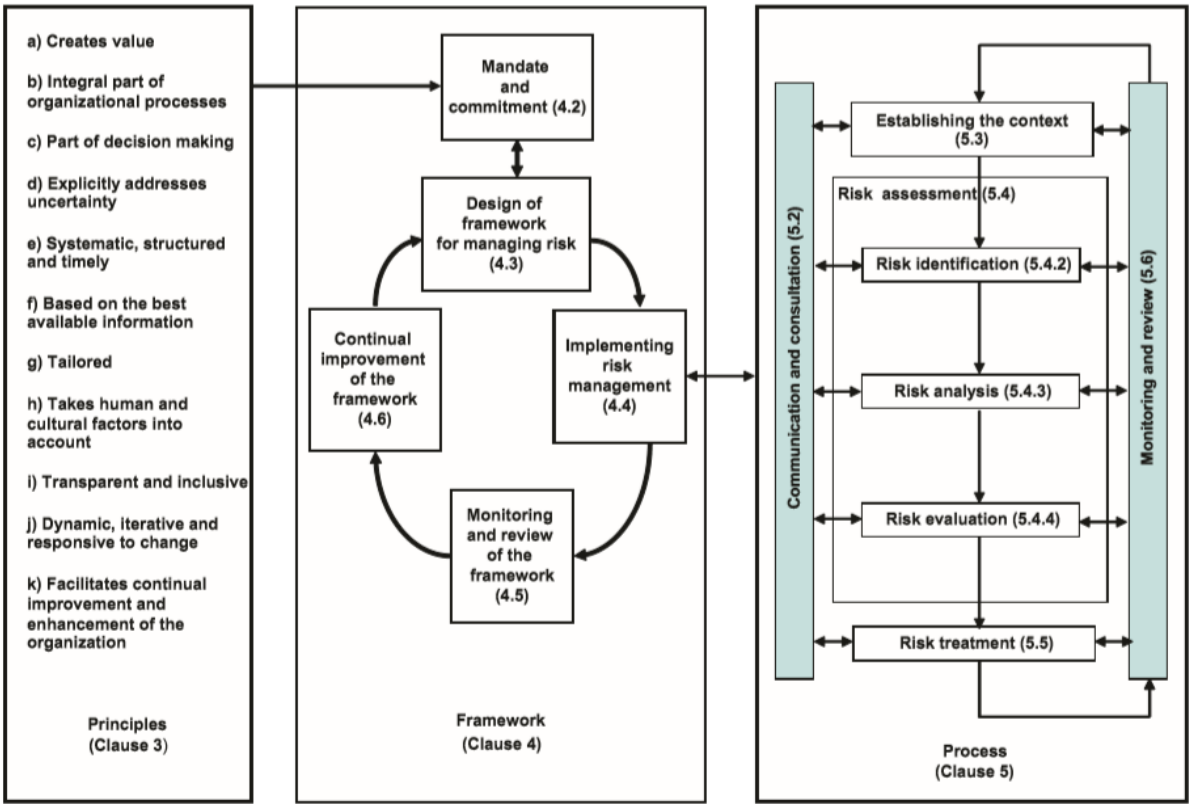

Figure 1-2. The risk management framework (centre) is the result of the mandate and commitment of the risk management authority which is based on the 11 risk management principles (left). A framework is then designed and implemented using the risk management process (right), which is continuously improved through monitoring and review (Standards New Zealand, 2009)

Resilience is defined by the UNISDR as "the ability of a system, community or society exposed to hazards to resist, absorb, accommodate, adapt to, transform and recover from the effects of a hazard in a timely and efficient manner, including through the preservation and restoration of its essential basic structures and functions through risk management"

(UNISDR, 2018). With regards to lifelines infrastructure, resilience can be understood as the state of being able to avoid utility supply outages, or maintain or quickly restore service delivery when hazardous events occur (New Zealand Lifelines Council, 2017).

Resilience can be separated into two aspects: absorption and adaptability. These represent, respectively, the impact felt by a community, and the speed of recovery following a traumatic event. Both aspects require adequate management to increase resilience as a whole. The differences between a high-resilience community and that of a low-resilience community is illustrated in Figure 1-3.

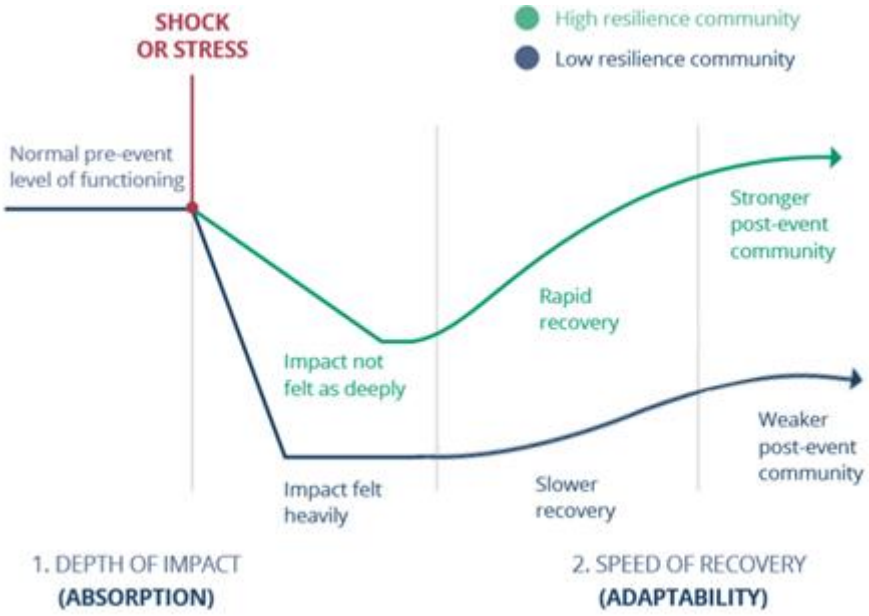

Figure 1-3. The differences in resilience between a high resilience and low resilience community, the low resilience community feels more impact upon initial stress and recovers slower, resulting in a weaker post-event community (New Zealand Ministry of Civil Defence and Emergency Management, 2018)

A comprehensive treatment of infrastructure resilience and its relationship to risk management, and the scales, dimensions and principles of infrastructure resilience, has been presented in the International Infrastructure Management Manual (IIMM) (Institute of Public Works Engineering et al., 2015). Decision making bodies typically choose to take a risk-based or resilience-based approach to managing infrastructure. The approaches are compared below in Table 1-1.

Table 1-1. Risk vs resilience-based approach to infrastructure management (Institute of Public Works Engineering et al., 2015)

Risk Approach	**Resilience Approach**
(likelihood × consequence), known hazards, risk management/mitigation	Events that are unpredictable, low-probability high consequence
Should consider the degree of certainty related to the hazard likelihood and range of potential consequences. If there is significant uncertainty, a 'resilience approach" should be used as well	Consideration of over-design events. What happens when this occurs? What procedures are in place to manage?
Consideration of multiple interdependencies related to a piece of infrastructure and ways to reduce or manage these more efficiently. Have range of potential failure possibilities/modes (across interdependencies) been considered and planned for?	Given the criticality of a specific system or asset, should further investment be made to manage failure due to an unspecified cause (e.g. by providing redundant systems, safe-failure approaches)
Should focus on prioritising risk reduction for those assessed as being high	Should focus on measuring attributes of resilient systems

A risk-based approach would consider the likelihood of threats and consequences. It would require quantifying the risk of failure of each component in the network. The goal is to identify the component's contribution to the overall risk and determining whether one component poses substantially more risk than others, which then becomes the basis of quantitative benchmarks for the system (Institute of Public Works Engineering et al., 2015).

In contrast, a resilience-based approach aims to prepare the system to recover quickly from various known and unknown threats. Resilience is an inherent property of the system itself and does not require an assessment of risk, but the attention is placed on how the system can adapt, absorb and recover from any event. This has implications with regards to capital investment; a risk-based approach for managing a waste water network would require significant expenditure of resources on scoping the hazard, for example the annual exceedance probability of a design earthquake or liquefaction potential of the surrounding soil. A resilience-based approach does not require expenditure of resources to identify the hazard, and directly expends resources to prepare for breakages in the network and identify costs required to provide redundant flow paths.

Both approaches have advantages. A risk-based approach is more comprehensive and the highest risk component is usually identified for improvement, but the nature of certain hazards such as earthquakes are low probability and high impact, therefore expending significant resources to upgrade the weakest component in the network to meet the demands of these events may be prohibitively expensive in terms of both initial capital and maintenance costs, not to mention the hazard scoping costs discussed previously. A resilience-based approach may allow for planned failure of these highest risk components, provided an alternate solution is supplied, which in many instances may be significantly cheaper to realise.

The IIMM presents infrastructure resilience in terms of scale, which may be either human-based or physical-based. These are shown below in Table 1-2:

Table 1-2. Scales of resilience (Institute of Public Works Engineering et al., 2015)

Scale	**Level**	**Example**
Human	Neighbourhood	Provision of social infrastructure, such as a community hall or fire station
	Country	National arrangements for welfare support following a major disaster
Physical	Asset	Robustness of materials and structures e.g. bridge components
	Network/System	Provision of asset redundancy across a network i.e. network diversity
	System of Systems (National)	Assessment of the interdependencies between sectors, such as telecommunications on electricity and fuel

With regards to the waste water network, the provision of portable toilets serving a small local population following an earthquake is an example of human scale resilience at the neighbourhood level, which absorbs the pressure for broken sewage pipes to be fixed and operational in the shortest amount of time. The ductility of a buried reinforced concrete pipe is an example of physical scale resilience at the asset level, as the pipe, which is a single physical asset, can deform a larger amount before cracks start appearing and leakages occur.

Resilience is also defined based on a technical or organisation dimension. This is shown in Table 1-3. Again, using examples specifically relating to the resilience of the waste water network, developing training materials for standards for pipe assessment is an example of organisational resilience based on the principle of change readiness, as this results in a highly trained workface able to assess damaged pipes and recommend repairs following an earthquake. Using a cement mix with higher compressive strength in the design of

reinforced concrete pipes is an example of technical resilience based on the principle of robustness, as this means the components of the network, i.e. the pipes, are able to withstand a larger stress before loss of function.

Table 1-3. Dimensions of resilience (Institute of Public Works Engineering et al., 2015)

Dimension	Principle	Definition & Justification
Technical	Robustness	Strength, or the ability of elements and other units of analysis to withstand a given level of stress or demand without suffering degradation or loss of function.
	Redundancy/ Back up	The extent to which elements, systems, other infrastructure units, or reserve capacity exist that are substitutable i.e. capable of satisfying functional requirements in the event of disruption, degradation or loss of functionality.
	Modularity/ Flexibility	System components have enough independence that damage or failure of one part or component of a system has a low probability of inducing failure of other similar or related components in the system. This may favour decentralised over centralised systems. Can also mean constructing systems that can be simply modified and improved/added to or strengthened. Relates closely to 'safe-to-fail' principle below.
	Safe-To-Fail	The extent to which design approaches are used, allowing (where relevant) controlled, planned failure during unpredicted conditions, recognising the possibility of failure can never be eliminated. This may involve novel approaches to design, to complement traditional, incremental risk-based design.
Organisational	Change Readiness	The ability to sense and anticipate hazards, identify problems and failures, and to develop a forewarning of disruption threats and their effects through sourcing a diversity of views, increasing alertness an, and understanding social vulnerability. This also involves ability to adapt (either via redesign or planning) and learn from the success or failure of previous adaptive strategies and the capacity to mobilise resources (financial or human) when conditions exist that threaten to disrupt some element, system, or other unit.
	Networks	The ability to establish relationships, mutual aid arrangements and regulatory partnerships, understand interconnectedness and vulnerabilities across all aspects of supply chains and distribution networks, and promote open communication and mitigation of internal/external silos.
	Leadership & Culture	The ability to develop an organisational mind-set/culture of enthusiasm for challenges, agility, flexibility, adaptive capacity, innovation and taking opportunities

A table of assessed interdependencies of infrastructure following a disaster in New Zealand was presented in the National Vulnerability Assessment – Stage 1 and is provided in Figure 1.4. The waste water sector is assessed to be highly dependent on the fuel, roading,

telecommunications and electricity sectors, while most other sectors have low dependence on the waste water sector, other than air transport which has medium dependence.

The degree to which the utilities listed to the right are dependent on the utilities listed below	Roads	Rail	Sea Transport	Air Transport	Water Supply	Wastewater	Stormwater	Electricity	Gas	Fuel Supply	Broadcasting	VHF Radio	Telecomms	Total Dependency
Fuel	3	3	3	3	3	3	3	3	3		3	3	3	36
Roads		3	3	3	3	3	3	3	3	3	2	2	3	34
Tele-comms	3	2	2	2	3	3	3	3	3	2	2	3		31
Electricity	1	2	3	3	3	3	2		2	2	3	3	3	30
VHF Radio	2	2	3	3	2	2	2	2	2	2	2		2	26
Broadcasting	2	2	2	2	2	2	2	2	2	2		2	2	24
Air Transport	2	1	1		2	2	2	2	2	2	2	2	2	22
Water Supply	1	1	1	2		3	1	1	1	1	1	1	2	16
Stormwater	2	1	1	2	1	1		1	1	1	1	1	1	14
Wastewater	1	1	1	2	1		1	1	1	1	1	1	1	13
Rail	1		1	1	1	1	1	1	1	1	1	1	1	12
Sea Transport	1	1		1	1	1	1	1	1	1	1	1	1	12
Gas	1	1	1	1	1	1	1	1		1	1	1	1	12

Figure 1-4. Lifelines Sector Interdependency Matrix during / post disaster event colour coded to show that the larger the number the greater the interdependency between the sectors compared (New Zealand Lifelines Council, 2017)

1.2 Infrastructure Resilience in New Zealand

The Civil Defence and Emergency Management (CDEM) Act 2002 is the legislative framework for managing hazards in New Zealand "in a way that contributes to the social, economic, cultural and environmental well-being and safety of the public and to the protection of property" (New Zealand Parliamentary Counsel Office, 2018). With regards to lifelines, section 60: Duties of Lifeline Utilities states that "every lifeline utility must ensure that it is able to function to the fullest possible extent, even though this may be at a reduced level, during and after an emergency" while they must also "participate in the development of the national civil defence emergency management strategy and civil defence emergency management plans" (New Zealand Parliamentary Counsel Office, 2018).

A National Disaster Resilience Strategy was proposed in 2018, the third strategy on emergency management under the CDEM Act that builds upon knowledge gained from 16 years of lessons since the Act came into effect (New Zealand Ministry of Civil Defence and

Emergency Management, 2018). The strategy signals New Zealand's commitment to improving the resilience of the country's infrastructure in accordance to the 2015-2010 Sendai Framework, especially the resilience of lifelines infrastructure.

In New Zealand, the vulnerabilities and interdependencies of lifelines systems are reviewed by the New Zealand Lifelines Council (NZLC) and 16 regional lifelines groups. The NZLC is currently undertaking a project known as the New Zealand Lifelines Infrastructure Vulnerability Assessment, which reflects an overarching intent for increased resilience of New Zealand infrastructure. The first of three stages was completed in September 2017. The overall goal of the project is to provide government and industry with a strategic understanding of nationally significant infrastructure, its vulnerability and resilience to hazards, and strategies to mitigate risks to a nationally agreed 'acceptable' level (New Zealand Lifelines Council, 2017).

The New Zealand Lifelines Infrastructure Vulnerability Assessment has identified various barriers to resilience in the country. Many of New Zealand's critical infrastructure assets are ageing and vulnerable, which will require extensive resources to strengthen and or maintain. Disaster recovery is often underestimated in terms of time and cost, and not factored into investment decision-making. Many organisations and property owners aim for the lowest-cost option instead of the most resilient solution, as the process of building resilience is perceived by many as limiting economic development and business growth (New Zealand Ministry of Civil Defence and Emergency Management, 2018).

In the case of the waste water pipe network, older brittle pipe materials are slowly being replaced with more resilient, ductile materials. However, progress to date has been slow due to competing demands for infrastructure investment in other sectors, with many damaged pipes being re-lined to extend their use instead of being replaced as a more economic option (New Zealand Lifelines Council, 2017).

Waste water systems are also increasingly being managed remotely by telemetry. Modern asset management systems depend on extensive computing and software resources, so in this way they are dependent on the electricity and telecommunications networks (New Zealand Lifelines Council, 2017).

1.3 Relevance of Christchurch as a case study

During late 2010-2011 the city of Christchurch in New Zealand was affected by a series of devastating earthquakes, known as the Canterbury Earthquake Sequence (CES). The CES has "generated one of the most comprehensive databases in the world" regarding seismic impacts on urban environments (Cubrinovski et al., 2014).

Information available to researchers includes detailed and comprehensive seismic ground motion databases containing Peak Ground Acceleration (PGA) and Peak Ground Velocity (PGV) data, mapped liquefaction severity, ground deformation evidenced by Light Detection and Ranging (LiDAR) data, and geotechnical data currently archived in the New Zealand Geotechnical Database (New Zealand Geotechnical Database, 2012).

Following the CES, the Stronger Christchurch Infrastructure Rebuild Team (SCIRT) was formed as an alliance consisting of the Christchurch City Council (CCC), New Zealand Transport Agency (NZTA) and Canterbury Earthquake Recovery Authority (CERA) together with five private companies to repair horizontal infrastructure including the waste water network (SCIRT Learning Legacy, 2019). SCIRT compiled detailed damage and repair logs of the waste water pipes and undertook Closed Circuit Television (CCTV) damage surveys. Approximately half of all waste water pipes across Christchurch city were subject to CCTV surveys following the CES, many of which were also surveyed before the CES. These surveys provide high-resolution damage information along individual pipes. Other investigation methods were also undertaken such as manhole level surveys, pole camera surveys and pipe profilometer surveys (Liu et al., 2013). The contractors conducting this work were required to record location coordinates, repair date, repair length, damage cause, repair type, material, manufacturer, and details of the contractor themselves during inspections.

The comprehensive assessment reports compiled throughout the SCIRT process were critical from an operational perspective by ensuring that post-repair damage locations could be identified and repairs were not scheduled twice (Sampedro & Hughes, 2018). From a research perspective the comprehensiveness and accessibility of earthquake damage data, as well as level of service data, enables a detailed mechanistic understanding of the earthquake impacts on urban lifeline infrastructure (Sampedro & Hughes, 2018b). The combination of these detailed performance data with comprehensive spatial databases of

the waste water system enable detailed spatial analysis, linking system performance with seismic parameters and ground deformation data.

The waste water pipe materials used in Christchurch are common to cities across New Zealand and around the world, and the standards used share similarities with other international pipework design and testing standards. Therefore, this case study on Christchurch will provide insight into the potential seismic performance of reinforced waste water pipes in other cities nationally and overseas, and the inputs required in the proposed method are easily retrievable in cities with developed information gathering systems and databases in place.

1.4 Objectives

The scope of this thesis is to develop an easily adaptable assessment method for assessing the robustness of gravity waste water pipes, which is a technical dimension of resilience in the waste water network.

By identifying the effect of various parameters on pipe robustness to seismic damage, using the significant CES data available in Christchurch as a case study, this study contributes to an enhanced understanding of physical scale resilience of the network at the asset level.

Ultimately this understanding assists decision making by territorial local authorities regarding the optimal allocation of resources following a disaster, thereby also improving the resilience of the waste water network on an organisational dimension.

The key objectives of this method are to:

a) Assess the extent of damage experienced by reinforced concrete gravity waste water pipes through the CES by examining CCTV recordings before and after the events;
b) Determine correspondence between earthquake ground performance and concrete waste water pipe failure incidence/modes;
c) Determine correspondence between intrinsic characteristics of concrete waste water pipes such as diameter and age of installation with failure incidence/modes.

The following chapter presents a literature review of key aspects of Christchurch's waste water infrastructure system development, and impacts of the CES, relevant to this study.

Chapter 2 - Literature Review

Chapter 1 introduced the UNISDR risk components of hazard, exposure and vulnerability. In this study the hazard is defined as the CES, the exposure is the reinforced concrete waste water pipe network in Christchurch, and the vulnerabilities are the various parameters which are hypothesised to affect the network performance through the CES. This chapter provides a literature review of these risk components, tying these concepts into the context of reinforced concrete waste water pipe performance through the CES.

Section 2.1 provides a technical background to the development of the design standards and innovations which have shaped and specified the "exposure" under consideration in this study. The history and expansion of the "exposure" is explored with a local focus in Section 2.2.

Section 2.3 explores various pipe and network parameters in detail to examine their influence on earthquake performance, which together make up the "vulnerability" under consideration.

Section 2.4 describes the CES or "hazard" and its geotechnical, structural and financial impacts, while Section 2.5 discusses the processes and techniques of assessing said impacts.

2.1 History and design of reinforced concrete waste water pipes

This section outlines the technological and legislative aspects which have affected the development of the reinforced concrete pipe in New Zealand, of which our definition of the risk component of "exposure" is a subset.

2.1.1 Development of reinforced concrete pipe design

Documented evidence of rigid sewer pipe materials such as reinforced concrete existed since the 19th century in North America. The modern design for reinforced concrete pipes has been developed over the past century through a series of innovations and milestones. A visual timeline was produced by Erdogmus and Tadros (2006) and presented in Figure 2-1:

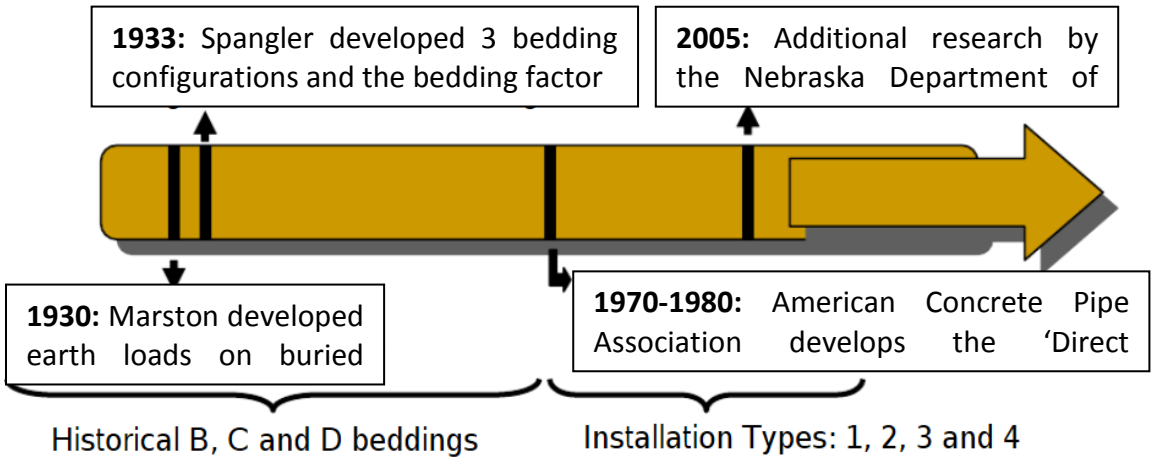

Figure 2-1. Visual timeline of reinforced concrete pipe development (Erdogmus & Tadros, 2006)

The first rational design approach of the buried concrete pipe, known as the 'indirect design method' was proposed by Anson Marston of Iowa State University in 1913 in the paper "The Theory of Loads on Pipes in Ditches and Tests of Cement and Clay Drain Tile and Sewer Pipe" (Marston & Anderson, 1913). The formula is known as the Marston load equation. Additional research in the 1920s was undertaken at Iowa State University which resulted in the publication of a comprehensive paper by Spangler in 1933. The paper introduced three standard bedding configurations (B, C, and D) to describe the surrounding soil pressure. Spangler also defined a fourth bedding configuration (A) where the bottom of the pipe sits in a concrete cradle or arch, however he stated that no attempt was made "either to measure or to estimate the distribution of the vertical reaction on the pipe when cradled in concrete" (Spangler, 1960). The historical bedding configurations are shown in Appendix C Figure C-1.

The work by Marston and Spangler (1933) formed the basis of the 'indirect method' of pipe design where the loading is defined by the magnitude and distribution of earth pressure on the pipe, while the capacity is a function of a 'bedding factor', factor of safety, and test load from the three-edge bearing test (Spangler, 1960). The three-edge bearing test continues to be widely used today (Carleton et al., 2017).

The indirect method was gradually refined to more accurately reflect installed conditions, but these modifications were not universally adopted by consulting engineers (Erdogmus &

Tadros, 2006). The indirect method also consisted of many limitations such as considering the load to act only at the top of pipe, neglecting axial thrust and lacking clear definitions for bedding material and compaction levels (Al-Saleem & Langdon, 2015).

In the 1960s, innovations in rubber joint gaskets resulted in significantly reduced pipe leakage and infiltration. Heger also proposed the use of welded deformed wire fabric to enhance crack control and bonding (Heger, 1963).

In the 1970s-1980s, Finite Element Modelling (FEM) of concrete pipes began to increase in popularity due to technological advances of the time. The American Concrete Pipe Association (ACPA) commenced a research program which resulted in the computer software SPIDA (Soil-Pipe Interaction Design and Analysis). This resulted in the development of the 'direct method' which uses standardised earth pressure distributions developed by Heger (1963) for pipes depending on four standard methods of installation rather than the bedding configurations used in the past. This resulted in better representations of actual buried conditions and considers both strength and serviceability (Al-Saleem & Langdon, 2015). The installation types are outlined in Appendix C, Table C-1.

The 'direct method' was first incorporated in a 1993 American Society of Civil Engineers (ASCE) standard titled "ASCE Standard Practice for Direct Design of Buried Precast Concrete Pipe in Standard Installation" (SIDD).

A general comparison of the direct and indirect methods was produced by Erdogmus and Tadros (2006), and is provided in Table 2-1. Major differences exist in the determination of the pipe supporting strength; however, the load calculations and installation types are consistent with each other.

Both the direct and indirect methods continue to be widely used, however there is a need to update them to reflect modern material advances in concrete and steel reinforcing (Erdogmus et al., 2010). In recent years, fibre reinforced concrete pipes began to be deployed worldwide (Wong & Nehdi, 2018) slowly replacing steel reinforcing as an alternative material, however this has not been standardised in design codes.

Table 2-1. A simplified comparison of the direct and indirect methods for the design of buried reinforced concrete pipes (Erdogmus & Tadros, 2006)

Indirect Design	Direct Design
1. Determine earth load (Prism Load x Arching Factor)	
2. Determine live load demand from AASHTO (American Association of State Highway and Transportation Officials)	
3. Select Standard Installation Type	
4. Determine Bedding Factor	4. Determine Moments, Thrusts and Shear Forces
5. Determine supporting strength from three-edge bearing test 6. Determine wall thickness, concrete strength and reinforced based on required supporting strength in step (5)	6. Determine wall thickness, concrete strength and reinforced based on a limit state analysis

2.1.2 Reinforced concrete pipe standards in New Zealand

Table 2-2 shows the standards used in New Zealand which are applicable to buried concrete pipes. There are now two sets of standards specifying the buried pipe and the concrete pipe, respectively, which used to be part of the same standard until the 1970s.

Table 2-2. Timeline of reinforced concrete pipe design standards in New Zealand

Year of Publication	Buried Pipe Standards	Concrete Pipe Standards
1937	Australian Standard A35, Precast Concrete Drainage Pipes	
1957	Australian Standard A35, Precast Concrete Drainage Pipes	
1974	NZS 4451:1974 Loads on buried rigid pipes	
1978		NZS 3107:1978 Specification for precast concrete drainage and pressure pipes
1989	AS/NZS 3725:1989 Loads on buried concrete pipes	
1992		AS/NZS 4058:1992 Precast concrete pipes (pressure and non-pressure)
2007	AS/NZS 3725:2007 Design for installation of buried concrete pipes	AS/NZS 4058:2007 Precast concrete pipes (pressure and non-pressure)

Concrete pipes were first specified in the 1937 edition of Australian Standard A35, Precast Concrete Drainage Pipes. This standard specified one strength class known as Class X. A revision to the standard was undertaken in 1957 in response to a request from the Conference of State Road Authorities of Australia for the provision of two additional strength categories Class Y and Z, which have 50% and 100% higher cracking strengths than Class X respectively. Little else was changed in the standard by way of technical requirements of the specifications, other than a change to the method for determining water absorption, after investigations found that the previous method produced results which were not sufficiently accurate or reproducible (Standards Association of Australia, 1957).

In 1974 a separate standard for buried pipes was developed in the form of NZS 4451:1974, while in 1978 the concrete pipe standard NZS 3107:1978 was developed, making reference to NZS 4451:1974 where necessary for designing buried pipes. The standards then developed separately while being compatible with each other.

Spangler's (1933) bedding configurations (refer Appendix C Figure C-1) were included in the Australian design standard A35:1937 in the Appendix, and subsequently in the body of NZS 4451:1974. These were widely used until the 1990s and were based on the 'indirect method'. The findings from SPIDA and the development of the 'direct method' were incorporated into AS/NZS 3725:1989 (Al-Saleem & Langdon, 2015). In the development of the current New Zealand design standard for installation of buried concrete pipes (AS/NZS 3725:2007), the joint technical committee WS-006 combined concepts from both the 'direct method' and 'indirect method' to develop its own support condition definitions (Al-Saleem & Langdon, 2015).

A review of AS/NZS 3725:2007 by Al-Saleem and Langdon (2015) indicated that the standard needed additional development to suit New Zealand conditions. For example, selected bedding materials referred to in the standard are not readily available in most areas around the country.

AS/NZS 4058:2007 specifies the reinforced concrete pipe itself. The following items are tested as a part of the standard (Standards New Zealand, 2007b):

- proof load / ultimate load testing
- water tightness (also known as hydrostatic testing)
- specified and ultimate pressure tests
- water absorption
- flexible joint assembly
- measurement of concrete cover to reinforcement
- measurement of dimensions other than concrete cover

The load testing arrangement in Australia and New Zealand is based on a two-edge bearing test, which shares resemblances to the standard three-edge bearing test used in the United States, and the alternate three-edge bearing test adopted in the United Kingdom.

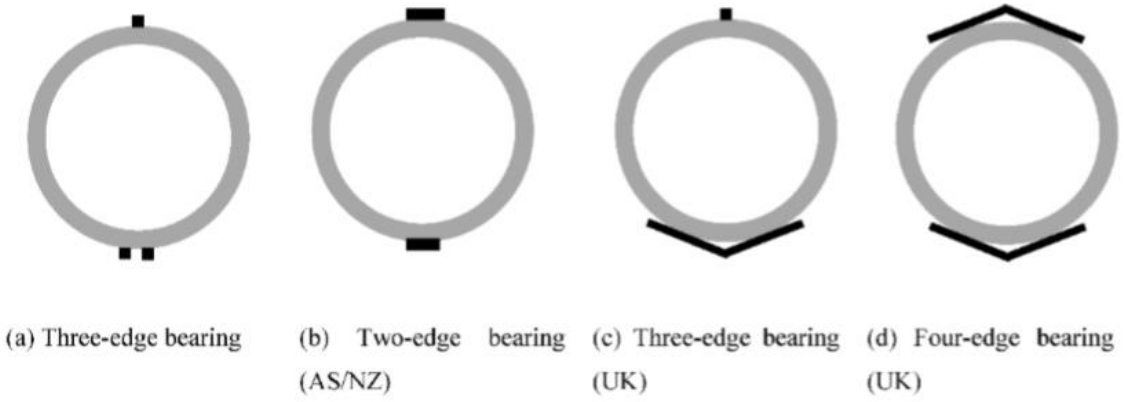

Figure 2-2. Illustrations of pipe testing in New Zealand and overseas (Wong & Nehdi, 2018)

A pipe specimen is loaded at a rate exceeding 10kN/min/m until the design crack size is achieved at 6 different points along the pipe based on the concrete cover provided. The crack size is measured while loaded, then the load is subsequently removed and the crack size is measured again. The crack sizes are not to exceed the sizes presented in Table 2-3.

Table 2-3. Design crack sizes with concrete cover as per AS/NZS 4058:2007 (Standards New Zealand, 2007b)

Concrete Cover	**Pipe Loaded**	**Load Removed**
≤10 mm	0.15 mm	0.10 mm
Between 10 mm and 20 mm	0.20 mm	0.15 mm
≥20 mm	0.25 mm	0.20 mm

The ultimate load test was first specified in AS A35-1937 as a force application of 1.5 times the proof load test (Standards New Zealand, 2007b), which means that the pipe has a design factor of safety of 1.5. This was reduced to 1.25 in AS/NZS 4058:1992 due to the advent of higher material classes and was consistent with international standards of high load classes, and is currently the factor of safety in the current New Zealand precast concrete pipe design code.

The water tightness test was first introduced in the Australian standard A35:1937 where the pipe is expected to be watertight to depths of up to 30 feet (approximately 9.1 m). This was adjusted to 100 kPa (approximately 10 m) in the subsequent New Zealand standard NZS 3107:1978 and reduced to 90 kPa (approximately 9 m) in the later standard AS/NZS 4058:1992, which is still applicable in the current standard AS/NZS 4058:2007.

The current water absorption test outlined in AS/NZS 4058:2007 is undertaken on a concrete core sample retrieved from a pipe and measures the increase in weight once the specimen has been oven dried and exposed to water. The absorption is limited to 6% which is slightly more stringent than the preceding standards, where it was 6.5%.

AS/NZS 4058:2007 poses restrictions on maximum acid-soluble chloride ion content of 0.8 kg/m^3 and sulphate ion content of 4-5% in the concrete mix depending on curing method used. Chemical admixtures are also prohibited from containing “nitrates, significant chlorides or other strongly ionized salts” due to durability concerns (Standards New Zealand, 2007a).

2.1.3 Comparison with international reinforced concrete pipe standards

In a study of six countries together encompassing a quarter of the world’s population by Wong and Nehdi (2018), the reinforced concrete pipe standards were compared. The selected countries and the name of the standards are presented in Table 2.4.

Table 2-4. Comparison of international reinforced concrete pipe standards (Wong & Nehdi, 2018) where RCP refers to Reinforced Concrete Pipe, FRCP refers to Fibre Reinforced Concrete Pipe, SFRCP refers to Steel Fibre Reinforced Concrete Pipe and SynFRCP refers to Synthetic Fibre Reinforced Concrete Pipe.

Study Area	Design Standard and Reference	Materials and Manufacturing Specification	Structural Strength and Testing	Hydrostatic Performance Testing Standard
Canada	CSA 56, OCPA Concrete Design Manual	CSA A257.2 (RCP)	CSA A257.0	CSA A257.0
USA	ASCE15, ACPA Concrete Pipe Design Manual	ASTM C76 (RCP), ASTM C1765 (SFRCP), ASTM C1818 (SynFRCP)	ASTM C497	ASTM C443, ASTM C1628
United Kingdom	BS EN 1295	BS EN 1916 (RCP, FRCP)	BS EN 1916	BS EN 1916
Australia and New Zealand	AS/NZS 3725	AS/NZS 4058 (RCP), AS4139 (FRCP)	AS/NZS 4058	AS/NZS 4058
China	CECS 143	GB/T11836 (RCP)	GB/T16752	GB/T16752

The comparison of standards did not reveal that any design standard from a particular geographic region was more stringent or complex than others, with each standard having more stringent requirements in some areas and more lenient requirements in others. Australia and New Zealand allowed the greatest diversity in reinforced concrete pipe diameter (from 100 mm to 4200 mm) compared to other regions. Australian and New Zealand pipes also possessed more lenient design tolerances on pipe wall thickness compared to other countries, but tighter tolerances on pipe length for most diameter classes and concrete cover requirements, which were mainly determined by logistical constraints imposed by local transport authorities (Wong & Nehdi, 2018). In terms of hydrostatic performance and crack examination following a loading test, the New Zealand design code was found to be not as stringent as Canada and China.

Similar to other international pipe design standards, design of buried reinforced concrete pipework in New Zealand has undergone multiple revisions since the first adoption of the Australian Standard A35, Precast Concrete Drainage Pipes in 1937. These were mainly in line with international innovations in pipe design. Wong and Nehdi (2018) stated in their international pipe standard comparison that currently Australia and New Zealand are “part of the front end of pipe technology advancement.”, however most modern reinforced

concrete pipe standards including AS/NZS 3725:2007 were not being reviewed frequently enough in comparison to state-of-the-art developments in other sectors such as the flexible pipe industry.

2.2 History of the Christchurch waste water system

This section presents the history and expansion of the waste water network in metropolitan Christchurch, which documents the waste water pipe "exposure" of interest in this research.

Prior to the existence of the Christchurch Drainage Board in 1875, drainage issues in the city were addressed by the Canterbury Provincial Government (1853-1876), the Christchurch City Council, which was established in 1862 but only governed the area within the original town belts, and the Roads Boards, which from 1864 undertook drainage work lying beyond the town belts (Wilson, 1989). The city at the time lacked a proper sewerage system, and sewage disposal was by way of backyard long drops, cesspits, chamber pots, and routine nocturnal services of the 'night men', who were council contractors responsible for visiting properties under the cover of dark where people put their excrement (night soil) in buckets and dump it via horse drawn carriages to 'manure depots' in the city outskirts (Wilson, 1989). Sewage was not always buried and lead to increased pollution of waterways and "water borne diseases such as typhoid, diphtheria and dysentery in the city" (Wilson, 1989).

To address the problem, the Christchurch Drainage Board was formed in 1875. It was the first body of its type in New Zealand with the sole responsibility to manage stormwater drainage and sewerage disposal, in contrast to other main centres where these were managed by the local territorial authority (Wilson, 1989).

The original plan for the Christchurch sewerage system was proposed in 1877 by John Carruthers, who was the chief engineer of the Board. His idea was based on a combined storm water and waste water system which was conveyed east to an estuary outfall. His idea was met with criticism due to "fears of sewage contamination at the estuary outfall, blockages, and inadequacies in the local water supply for flushing" (Wilson, 1989).

Figure 2-3. View of ground excavation work in 1918 (Wilson, 1989)

In 1878 the Board hired a new consulting engineer William Clark, who revised the original plans to separate the waste water from the storm water. The plan included the construction of a pumping station to pump the sewage to the east of the city to a sewage farm which could use it to irrigate paddocks as fertiliser. Clark's scheme was approved, but construction was slow. This is due to the fact that the flat, low-lying nature of the city made it difficult to achieve sufficient fall in gravity pipes, and the swamp-like ground conditions, often riddled with tree stumps as shown in Figure 2-3, were unsatisfactory for pipe foundations (Wilson, 1989).

In 1882 the initial design was finished, but not all properties were immediately connected as landowners needed to pay a connection fee. In 1884, Christchurch had 293 water closets (individual toilets), which increased to 1915 in 1901. Most of the original pipes were constructed of earthenware (EW) and the smaller diameter pipes were made locally, whereas the larger ones were imported from Scotland (Wilson, 1989).

The network was continually expanded over the past century and a visual timeline of the sewered areas by date of construction is shown in Figure 2-4. The inner suburbs tend to have older installation dates, with the majority of pipes within 2 km of the Central Business

District being constructed between 1890 and 1930. Older pipes installed prior to the implementation AS/NZS 3725:1989 were based on the 'indirect' design methodology in comparison to the subsequent standards which combined concepts from the 'direct' design methodology. Refer section 2.1.2 for a comparison of the New Zealand reinforced concrete pipe design and testing standards.

By 1989, when the responsibilities of the Board passed onto the newly enlarged Christchurch City Council, Christchurch had transformed from New Zealand's unhealthiest town to the country's best drained city (Wilson, 1989). Following the CES, many of the city's original 19th century sewer lines were replaced or decommissioned. Pipes that experienced minor damage were re-lined and continue to be used to this day.

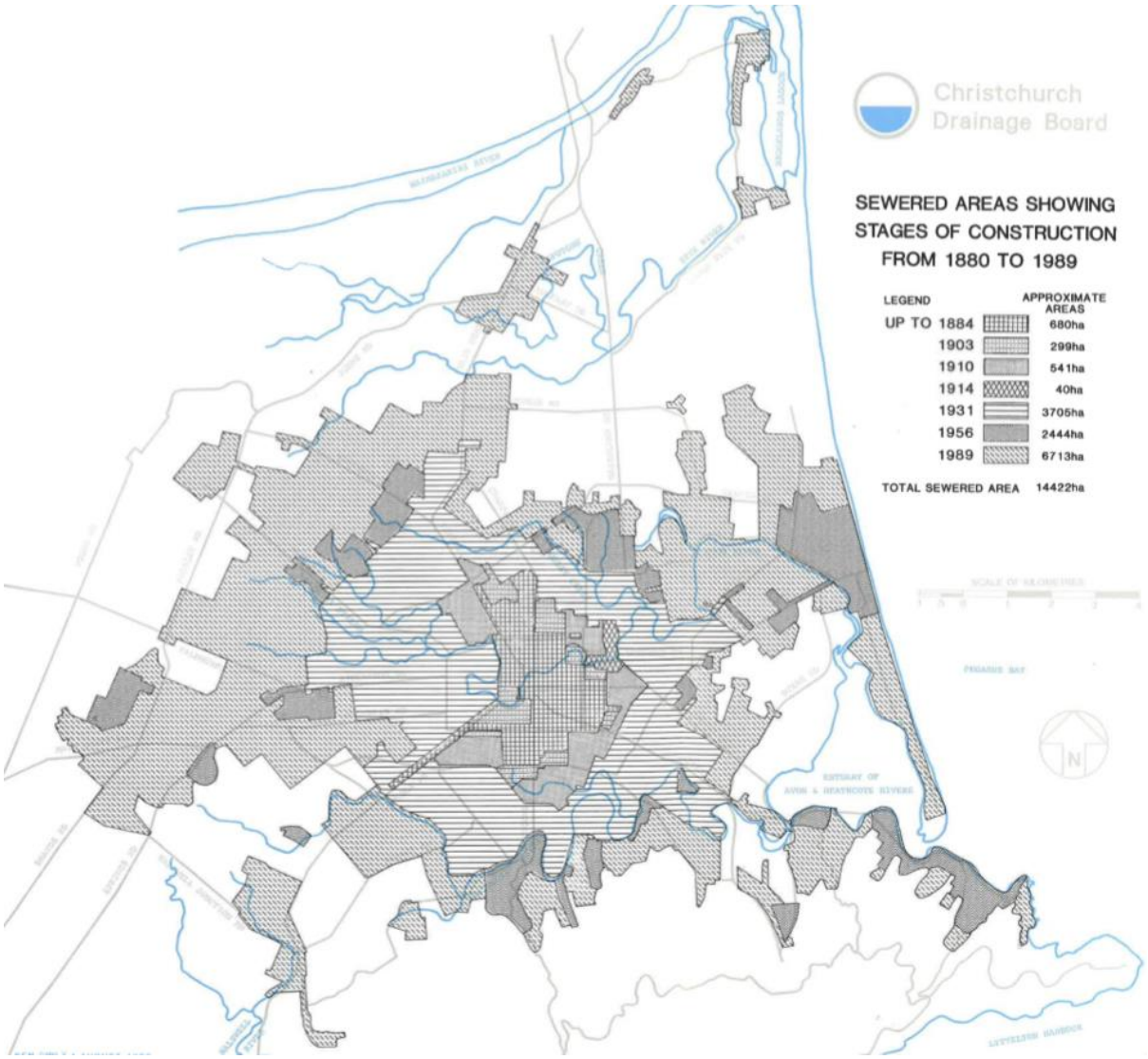

Figure 2-4. Sewered areas showing stages of construction from 1880 to 1989 (Wilson, 1989)

Figure 2-5 provides a graphical indication of the decades of installation for individual waste water pipes across Christchurch City and Lyttleton Harbour for all material types. The installation dates of the pipes appear to be consistent within a suburb in accordance to Figure 2-4.

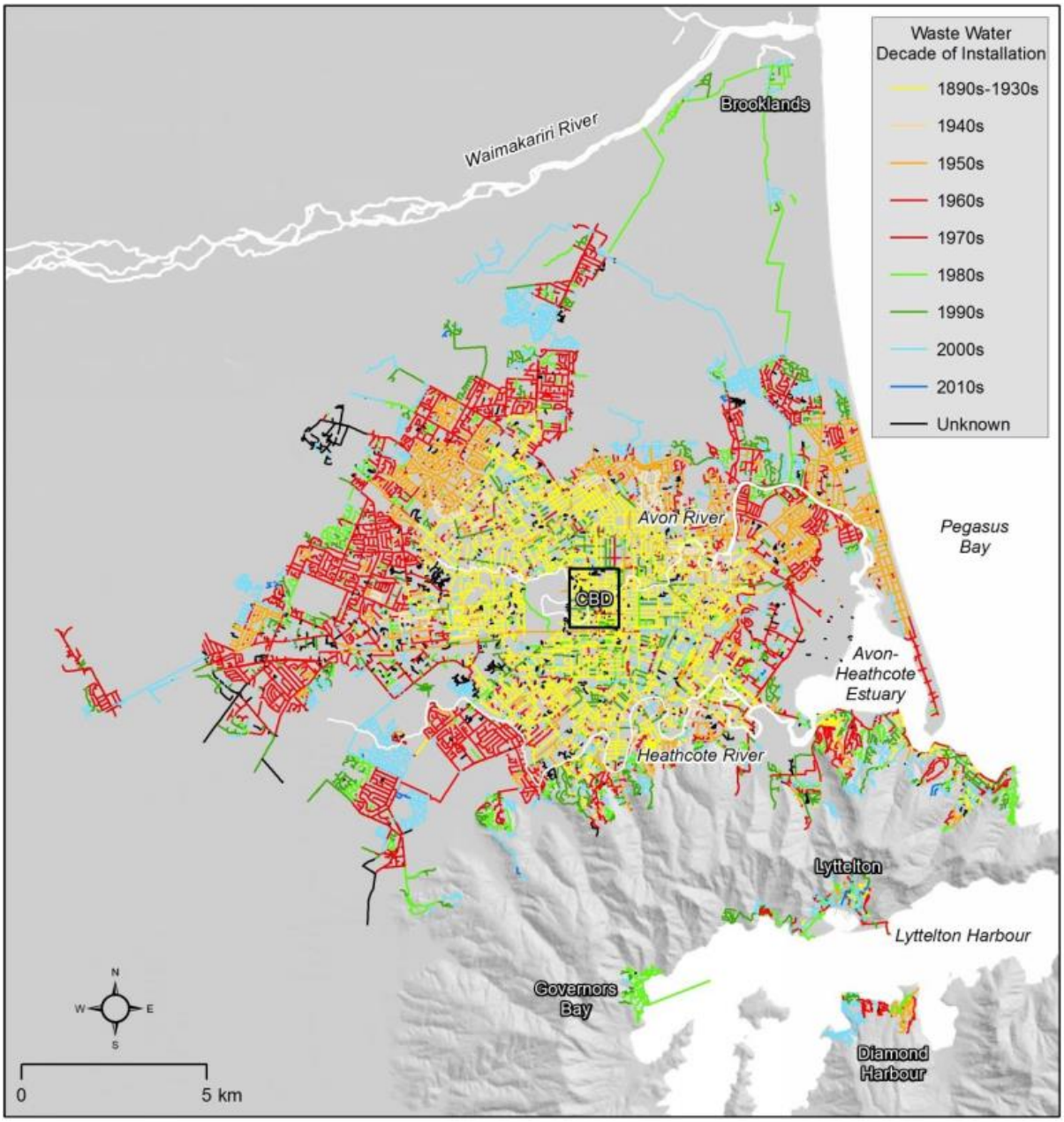

Figure 2-5. Christchurch City and Lyttleton Harbour waste water network graphed according to the decade of installation (Cubrinovski et al., 2014)

The current waste water network consists of a city-wide network of approximately 1800 km of pipe leading to the treatment plant located in Bromley. The pipes have an asset design life of 100 years (Cubrinovski et al., 2011). The wastewater pipes are typically laid in the

centre of roads with a 1.2 m minimum vertical cover, the majority of pipes are gravity pipes which are 2.0-3.5 m deep and laid between manholes which are spaced at maximum distances of 100 m for small diameter pipes, and up to 180 m for trunk mains (Cubrinovski et al., 2011). The few that pipes are pressurised are generally located within a depth of 1 m similar to the potable water network. The distribution of gravity and pressurised pipes in the city is shown in Figure 2-6.

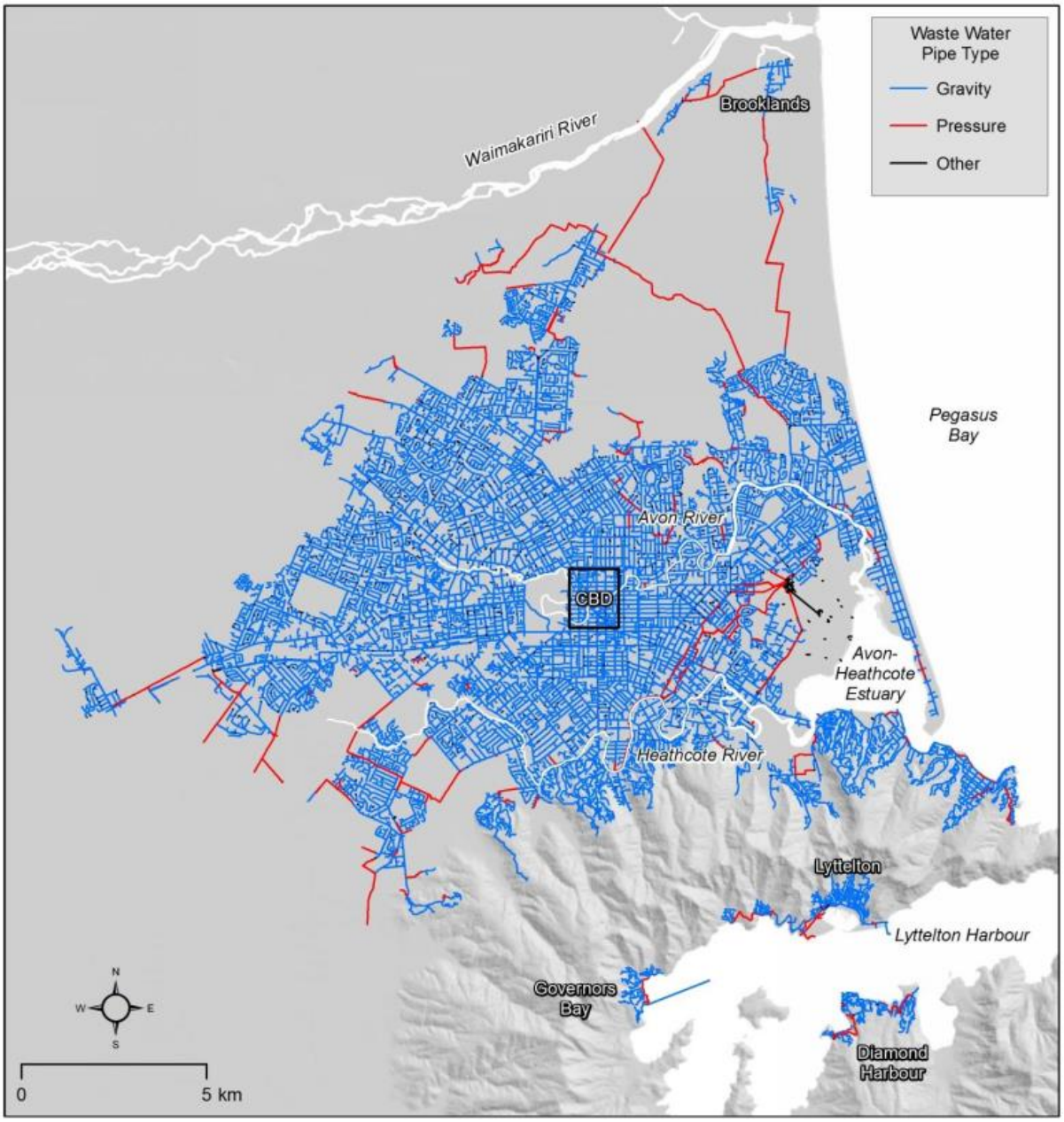

Figure 2-6. Christchurch City and Lyttleton Harbour waste water network graphed to distinguish between gravity and pressurized pipelines (Cubrinovski et al., 2014)

The proportion of gravity waste water pipes of each diameter class in Christchurch city was provided by Heiler et al. (2012), refer to Table 2-5 below. The majority of waste water pipes in the city have a diameter between 150-199 mm for all material categories.

Table 2-5. Gravity waste water pipes in Christchurch by diameter (Heiler et al., 2012).

Diameter	**<150 mm**	**150-199 mm**	**200-299 mm**	**300-399 mm**	**>400 mm**	**Total**
Length	32 km	1020 km	353 km	89km	116 km	1610 km
% of Total	2%	63%	22%	6%	7%	100%

2.3 Factors affecting reinforced concrete waste water pipe performance

This section explores the factors which are hypothesised to affect the susceptibility and performance of reinforced concrete waste water pipes to earthquakes, which is our definition of the risk component of "vulnerability" in this study.

2.3.1 Chemical and biological deterioration

Extensive literature exists regarding the chemical and biological deterioration of reinforced concrete waste water pipes. Pipes with significant existing deterioration will have higher susceptibility to earthquake damage due to their weakened structure.

Biogenic sulphuric acid deterioration is considered to be the most damaging attack mechanism for the entire concrete waste water network, including pipelines, aeration tanks, septic tanks, pumping stations and influence channels (Parande et al., 2006). Chemically, the gravity waste water environment is characterised by high sulphate and dissolved sulphide concentrations, high hydrogen sulphide gas content, low dissolved oxygen levels and low acidity level (O'Connell et al., 2010). The higher these chemical contents the greater the biogenic deterioration.

In sewage effluent, sulphate-reducing proteolytic bacteria *Acidithiobacillus thiooxidans* convert sulphates to sulphides under anaerobic conditions which diffuse into the air. Lower water flows (velocities and quantity) were found to result in increased conversion activity, for example a study by Romanova et al. (2014) showed that between late evening to early morning effluent flow is typically lower due to reduced household and industrial activity,

and hydrogen sulphide gas concentration in manholes was higher. During this time the temperatures were also lower, which the authors attributed to less hot water discharge and lower surrounding ambient temperature.

The sulphides are subsequently further reduced by oxygen, where present, to sulphur and sulphur compounds (Neville, 2004). The bacteria genus *Thiobacillus* converts these to sulphuric acid. A visual representation of this is provided by De Schutter (2012) and featured in Figure 2-7, showing that this occurs in both the air and effluent liquid environment:

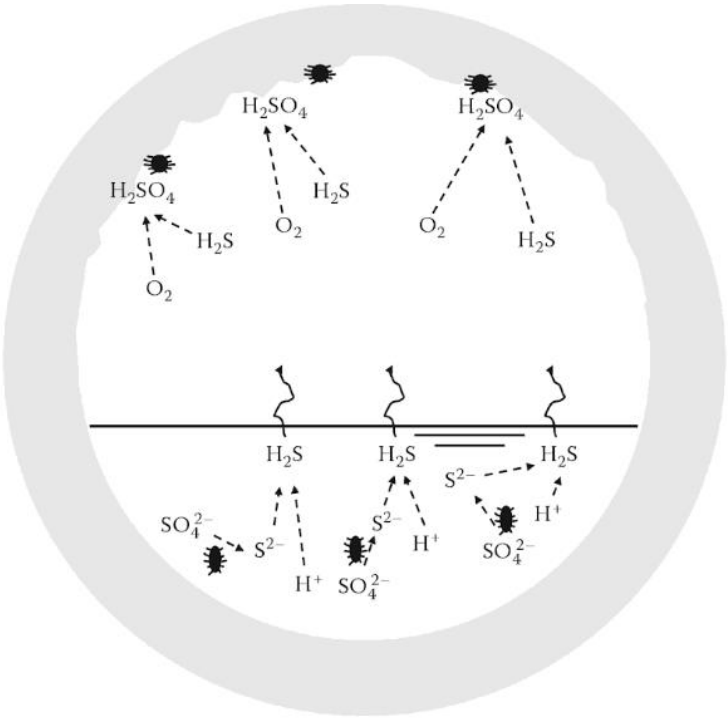

Figure 2-7. Sulphuric acid attack mechanism, retrieved from Damage to Concrete Structures by De Schutter (2012)

The acid directly attacks the cement matrix by reacting with calcium hydroxide in cement to yield calcium sulphate in accordance to the following equation:

$$Ca(OH)_2 + H_2SO_4 \rightarrow CaSO_4 + 2H_2O \quad (1)$$

The calcium sulphate appears on the surface of the pipe walls as a substance with a slime and cheese-like texture. This reacts to form gypsum around pH levels less than 3 (Mori et al., 1992). The formation of gypsum results in the loss of cohesive strength in the cement and may further also react with calcium aluminium hydrate in the cement to form Ettringite at pH levels greater than3 (Mori et al., 1992). Ettringite is considered to be a significant cause

of the expansion and hence disruption to concrete structures; it has an expansive formation that etches concrete surfaces, and penetrates the mortar surface causing cracking and pitting (Saricimen et al., 2003).

The worst damage typically occurs slightly above the sewage level, where the concrete pipe walls are vulnerable to deterioration from both vapor and liquid phases of sewage and can experience corrosion of up to 4.3-4.7 mm per year. In comparison, the deterioration at the crown of the pipe experiences the least damage, typically 1.4 mm per year (Mori et al., 1992).

Several methods such as high-performance coatings, linings consisting of fibreglass, brick, ceramic and specialised mortars exist to protect concrete from sulphuric acid damage produced by *Thiobacillus*.

Carbonation and chloride attack are two alternative damage mechanisms affecting reinforced concrete waste water pipes, which together result in corrosion of reinforcing bars. Steel passivates due the high alkalinity of the cement where the pH is typically above 13. Carbonation occurs when carbonic acid is formed from the reaction of calcium hydroxide in the cement with dissolved carbon dioxide in the pipe environment. The process reduces the alkalinity of concrete, and when the pH is reduced below 8.3, the passive layer becomes ineffective and the corrosion of the steel can occur (Broomfield, 2007). Carbonation causes slow deterioration over many years and is dependent on waste water flow, solubility of carbon dioxide (CO_2), pH and water hardness in the pipes.

Chloride attack is a third attack mechanism whereby chloride ions penetrate through the concrete cover and destabilise the passive layer around the steel, resulting in corrosion of the reinforcing bars. The formation of the corrosion product is an expansive process, as the volume of the corrosion products increase up to a factor of six in the concrete which exceeds its tensile capacity, resulting in spalling and cracking (Broomfield, 2007). Acidophilic bacteria also oxidise ferrous to ferric oxide leading to the rapid acceleration of corrosion of steel reinforcement (Parande et al., 2006).

In industrial waste water, acid deterioration results from manufactured acids reacting with the alkaline cementitious compounds. The extent is dependent on the sewage flow rate and

solubility of chlorides. pH levels below 12.5 result in the depletion of potassium and sodium, followed by the depletion of hydroxides and calcium silicate hydrate (C-S-H) at pH levels below 10 and 8, respectively (Parande et al., 2006). Industrial processes also result in increased chloride content in the waste water.

The durability of a buried reinforced concrete pipe is also affected by the continual exposure of the outer pipe to soil constituents such as sulphate, chloride salts, and dissolved CO_2. Sulphates exist in the natural soil in the form of calcium, sodium, magnesium and potassium, while ammonium sulphate also exists in industrial and agricultural soil due to the production and use of fertilisers (Parande et al., 2006).

AS/NZS 4058:2007 Appendix E provides limits of 20,000 ppm and 1,000 ppm to the allowable soil concentration of chlorides and sulphates, respectively, for general-purpose reinforced concrete. The pH of the soil needs to be controlled within 4.5-5.5 depending on its drainage characteristics, with permeable soil types such as clean gravel and sands having more stringent requirements in comparison to impervious types such as homogeneous clays (Standards New Zealand, 2007a).

The maintenance costs associated with addressing the impacts of chemical and biological deterioration of wastewater pipes are very high around the world, having exceeded $25 billion per year in the United States alone (O'Connell et al., 2010). Test results by Moradian et al. (2012) revealed most damage in poorly constructed networks is a complex combination of all the aforementioned damage mechanisms of biogenic sulphuric acid attack, chloride attack, and carbonation. Moradian et al. (2012) stated that most authors focused on the biogenic sulphuric acid attack as the main mechanism, and overlooked the other aforementioned aggressive phenomena, which should be addressed for a comprehensive deterioration review.

2.3.2 Fabrication

Reinforced concrete pipes are fabricated using three main processes, which result in slightly different characteristics. The spun process uses centrifugal spinning to reduce the water to cement ratio. The process is currently used for the widest range of diameters (between 150 mm-2300 mm). The roller suspension process uses centrifugal roller compaction and heavy vibration and is primarily used for reinforced concrete pipes between 225 mm-600 mm in

diameter, however these pipes are not suitable for marine environment applications, indicating their higher susceptibility to corrosion. The Vibration Technology (VT) process is a vertical dry cast process which results from a dry mix concrete being placed in a mould and the inner core is vibrated. The pipe is subsequently removed from the core and transported by crane directly to the curing area where the outer mould is stripped. It is used primarily for larger pipes between 675-2400 mm in diameter (Concrete Pipe Association of Australasia, 2018).

The centrifugal and roller suspension processes have existed since the early 1900s, while the VT process was a much later innovation around 2002 following the British and European standards BSEN 1916:2002 and BS 5911-1:2002, which result in thicker walls providing increased cover for steel compared to the previous two methods (Concrete Pipe Association of Australasia, 2018).

Water content and concrete mix during the fabrication of reinforced concrete pipes result in differences in reported durability performance in waste water systems. In New Zealand, these are regulated through NZS 3121:2015 Water and aggregate for concrete (Standards New Zealand, 2007a). The aforementioned three fabrication processes result in a low water to cement ratio (between 0.3 and 0.4), resulting in concrete compression strengths up to 60 MPa. This ensures that the concrete is impermeable to water and achieves the highest levels of durability for any commercial concrete casting process in the New Zealand industry (Concrete Pipe Association of Australasia, 2018).

Literature on concrete mix durability concluded that in sewer conditions with significant biological (microbial) activity, calcium aluminate cements experienced less sulphuric acid degradation compared to normal Portland cement, due to the ability of the former mix to affect the metabolism of the sulphate reducing proteolytic bacteria, resulting in less sulphuric acid production (Alexander & Fourie, 2011). Aggregate type has also been demonstrated to be effective in controlling sulphuric acid deterioration, where “limestone aggregates showed smaller degradation depths than inert aggregates due to the production of a local buffering environment to protect the underlying cement paste” (Beliea et al., 2004).

The steel reinforcing used affects the tensile strength of concrete and hence crack control properties and water tightness. AS/NZS 4058 requires that all steel reinforcing complies with AS/NZS 4761 to ensure that the reinforcement component of the product is known and controlled (Standards New Zealand, 2007a). Reinforcing cages are typically sourced from steel suppliers with an accredited quality system meeting AS/NZS ISO 9001, with testing conducted by laboratories or inspection bodies that are accredited by International Accreditation New Zealand (IANZ). The steel reinforcement cages are typically fabricated using high-precision automated welding machines (Concrete Pipe Association of Australasia, 2018). Reinforcing steel with high carbon content has been observed to be more susceptible to chloride attack than ductile iron (Song et al., 2017).

The size and layout of reinforcing used is dependent on in-house design specifications of pipe manufacturers. This depends on the pipe application, size class, joint type, load class and water-tightness class. The reinforcing cage used may differ significantly among manufacturers and could range from singly to doubly reinforced or be circular or elliptical in shape. Four common configurations are depicted in Figure 2-8, which are all used in the waste water infrastructure systems in New Zealand. Doubly reinforced sections have higher tensile and therefore bending capacity than singly reinforced sections.

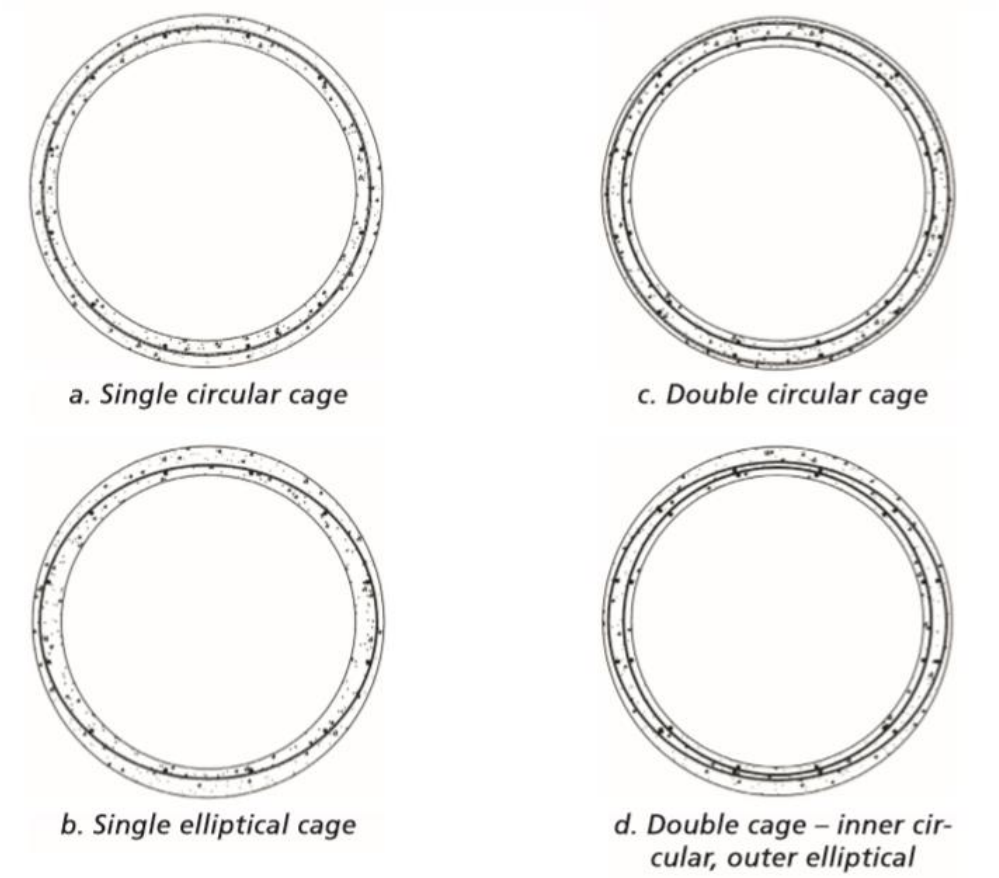

Figure 2-8. Examples of various steel cage configurations for reinforced concrete pipes in New Zealand (Standards New Zealand, 2007a).

In cases where the joint design includes a socket of some variety, some prescribed amount of socket reinforcement is also included. Due to the lengths of pipe fabricated, some cages may require lapping the cages to create a structural continuity between the barrel and socket reinforcement (Concrete Pipe Association of Australasia, 2018). Joints have been observed to have higher defect rates than general parts of the pipe. A study by O'Reilly et al. (1989) showed that up to 23% of joints in a random investigation were defective, and concluded that "the elimination of connections and their substitution by junctions would remove a major source of structural defects in pipe sewers".

2.3.3 Installation

The installation method and choice of bedding arrangement of a buried pipe after fabrication is considered to affect the amount of stress it is subjected to during daily service and seismic loads. The higher the percentage compaction of soil surrounding the pipe, the better the support is in the direction of imparted stress.

The buried pipe standard NZS3725:2007, which was introduced earlier in section 2.1.2, classifies installation conditions as either trench or embankment conditions, as per Figure 2-9. In trench conditions the backfill settlement over time results in a load acting at the top of the pipe which is offset by frictional forces developing between the sides of the trench and the fill. The loads acting on the pipe depend on the trench dimensions, pipe diameter, compaction and the requirements for trench support. An embankment condition results from pipes being laid near ground level and fill being placed over the top of the pipe. The loading on the pipe in an embankment is primarily due to pipe diameter and height of the fill (Concrete Pipe Association of Australasia, 2018).

In order to maintain the proper pipe alignment and sustain the weight of soil, traffic and construction loading over the length of a pipe, various zones surrounding the pipe are specified for both installation conditions. The Bed Zone lies beneath the pipe and is generally 100-150 mm thick, acting to provide even support and cushioning underneath the pipe. Above lies the Haunch Zone, the thickness being approximately 10-30% of the external pipe diameter. The role of the Haunch Zone is to reduce bending moment effects in the pipe walls and transfer the loads to the Bed Zone. The Side Zones above the Haunch Zone protect the sides of the pipe, and the overlay zone protects the top of the pipe from physical damage due to oversized aggregates and other objects in the backfill or embankment fill (Concrete Pipe Association of Australasia, 2018). The overall trench widths are 300 mm wider than the diameter of the pipe (Cubrinovski et al., 2011).

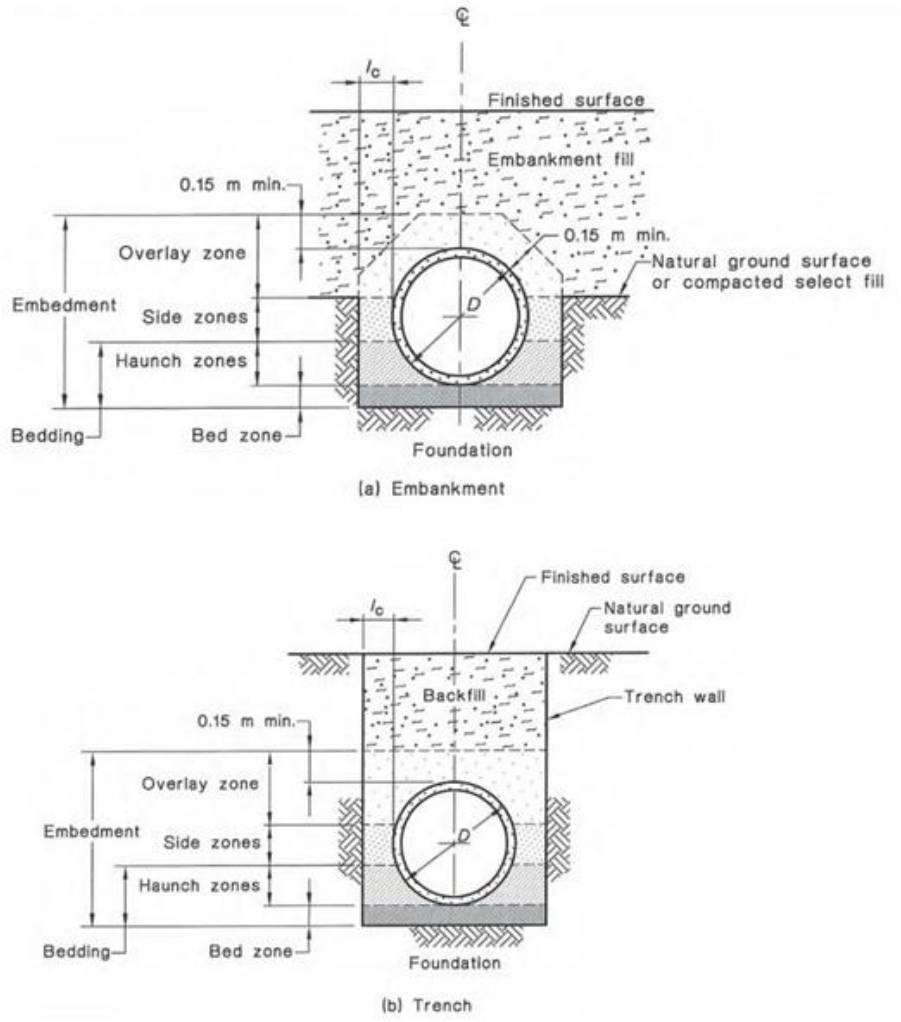

Figure 2-9. Cross section of a buried pipe as specified in Australia and New Zealand (Standards New Zealand, 2007a).

For the above two installation conditions, six support conditions (H1, H2, HS1, HS2, HS3, and U) are also defined, where H stands for Haunch Support, HS stands for Haunch and Side Support, and the following number represents the compaction of fill. These support conditions have incorporated a mix of both Spangler's bedding configurations (refer Appendix C, Figure C-1), and the ACPA Type 1-3 standard installations (refer Appendix C, Table C-1). This means the standard combines theory from both the indirect method and the direct method, which are two different theoretical approaches of pipe soil interaction analysis, resulting in confusion for the engineer, asset manager or contractor.

The standard has been viewed as overly conservative, laden with technical irregularities, and not achievable in many cases, such as target compaction percentage (Al-Saleem &

Langdon, 2015). Therefore implementation of NZS3725:2007 has been regarded as difficult and costly in most parts of New Zealand (Al-Saleem & Langdon, 2015), and as a result many territorial authorities have developed their own standard details which is loosely based on the NZS3725:2007, but has been simplified and adapted based on local conditions. This means the installation specifications of buried pipes across New Zealand are different depending on the area of jurisdiction. Table 2-6 compares the installation methods across some of the major cities in New Zealand and compared to the New Zealand Standards.

In Christchurch, backfill for a waste water pipe was dependant on the age of construction. Older pipes tended to be backfilled with local native soils, while newer pipes were specified with either AP20 or AP40 backfills compacted to 95% dry density (Cubrinovski et al., 2014). These engineered backfills are required to meet a particular particle size distribution envelope in accordance to the New Zealand Transport Agency (NZTA), with the maximum aggregate size not exceeding 20 mm for AP20, and not exceeding 40 mm for AP40. AP40 backfill has reportedly resulted in better earthquake performance for certain materials (e.g. High-Density Polyethylene (HDPE) and Asbestos Cement (AC)) compared to native soils, but offered no obvious benefits for other materials such as Galvanised Iron (GI) (Cubrinovski et al., 2014).

Soils with better drainage such as gravels and sands were observed to result in lower defect rates to buried pipes than silts and clays (O'Reilly et al., 1989). Soil expansion also causes stresses on waste water pipes due to swelling in clay particles when water is absorbed and shrinkage when moisture is lost due to evaporation or transpiration (Davies et al., 2001). A similar effect exists for the freezing and thawing of soils, and was most pronounced in trench installations where the backfill and side-fill had different frost susceptibilities (Davies et al., 2001).

Table 2-6. Pipe installation specifications by NZS standards and major cities in New Zealand (Al-Saleem & Langdon, 2015)

Standard	Bedding Type	Type of Bedding Material	Depth of Bedding	Bedding Factor	Notes
NZS 4452:1986	Type A	Concrete	D/4	Not Specified	
	Type B	Compacted Granular Bedding	D/4	Not Specified	Shape subgrade for earth foundation (no bedding)
	Type C	Compacted soil free from large stones	D/6	Not Specified	Flexible Pipes
	Type D	N/A			Not Recommended
NZS 4404:2010	Type 1	Concrete	D/4	Not Specified	
	Type 2	Granular Materials	D/2	Not Specified	
	Type 3	N/A			For flexible pipes
	Type 4	Granular Materials	D + 150mm	Not Specified	Where immigration of fines expected (wrap with Geotextile)
Tauranga City					Same as NZS 4452:1986
Hamilton City	H2	Free draining granular materials with 95% compaction	D + 300mm	2.0 or 1.7	With reference to AS/NZS 3725:2007
Nelson City	H2	AP20 + Clegg Impact Value 35 for roads and 25 for others	D/3	2.0 or 1.7	Geotextile wrap where immigration of fines possible
Wellington Region	N/A	5-20 Drainage to D/4 + 20 & 40 Drainage to D + 150mm	D + 150mm	Not Specified	Geotextile wrap where immigration of fines possible
Palmerston North	N/A	Same as Wellington Region	D/4	Not Specified	Compaction 95% to top of trench.
	Others			Not Specified	Spec. Text required AS/NZS 3725
Dunedin City	N/A	Concrete	Various	Not Specified	
Hastings City	N/A	Granular Materials	D/4	Not Specified	NZS 4451:1976
Auckland City	H2	GAP20	D/2	2.0 or 1.7	Calculated as per AS/NZS 3725:2007
Christchurch City	N/A	AP20, AP40	Variable D to D/4	Not Specified	Under Review

O'Reilly et al. (1989) observed that the defect rate gradually reduced to an installed depth of 5.5 m, and then increased again beyond this depth. They theorised that the depth between

0 – 5.5 m reflected a reduction in the loads from surface level traffic and utility maintenance activities. Beyond this depth, the increase in defect rate is associated with the increasing magnitude of overburden pressure. Other studies however indicate most defect rates apply to waste water pipes installed within the first 2 m, where the “effect of seasonal moisture variations in the soil may be significant” (Davies et al., 2001). Earthquake wave actions were observed to vary at different installation depths. For instance, pipes closer to the surface are typically subjected to Rayleigh waves, and pipes deeper to S waves (O’Rourke et al., 2014).

If the pipes are pressurised, their seismic performance has been noted to increase compared to gravity pipes (Liu et al., 2015). This has been studied in international literature where fragility functions for potable water pressurised pipelines were adopted to study the physical damage to a gravity waste water network, and were found to slightly underestimate the damage observed (Liu et al., 2015).

2.3.4 Service conditions

The above-ground conditions have reportedly resulted in different defect levels in buried waste water pipes. The operation of construction vehicles was reported to increase observed defect levels to pipes underneath construction sites (Davies et al., 2001). Pipes beneath gardens and residential homes were identified as having more structural defects than pipes beneath roads, where it was suggested that this was due to excessive disturbances during house construction or garden maintenance (O'Reilly et al., 1989). The same study also identified that increases in traffic flow resulted in a marginal increase in overall defect rate for small to medium roads, with the exception of trunk roads where the pavement was theorised to be stronger with higher design requirements (O'Reilly et al., 1989).

2.3.5 Age

The age of reinforced concrete pipes is considered to have an indirect effect on their durability by determining the design standard and specifications used in its design, and consequently the strength of materials specified in construction, installation method and backfill type. Refer to section 2.1.2 for a discussion of the reinforced concrete pipe design standard in New Zealand and its development over time.

Age also increases the length of time the pipes are affected by biogenic and corrosive processes over time (refer Section 2.3.1). Gradual processes such as carbonation are especially pronounced in older pipes. However, mixed results are reported in the literature for the relationship between defect rate and age. In a United Kingdom waste water network performance study, O'Reilly et al. (1989) estimated that the defect rate was 7.4% - 11.3% for pipes prior to 1944, which then dropped to 2% in the next 25 years and then even further to 0.6%-1.2%, indicating a clear increase in defects with age of the pipe. However, an alternate study by Lester and Farrar (1979) could not find any correlation between defect rate and age.

2.3.6 Dimensions

The physical dimensions of reinforced concrete pipes affect durability by influencing how the forces are distributed, the steel reinforcing arrangement, bar sizes, and fabrication processes used in their construction (refer Section 2.3.2).

The sizes of pipe sections are generally defined by their interior and exterior diameters. In general, larger-diameter pipes provide increased pipe wall thicknesses that allow for more space to accommodate reinforcement, resulting in higher flexural and shear strength (Wong & Nehdi, 2018). Thicker pipe walls also result in higher rigidity, which has been reported in different kinds of observed failure modes (Edkins et al., 2016).

In the Christchurch context, the susceptibility of different pipe diameters for a specific pipe material type is difficult to establish due to the fact that “materials for different network components are usually restricted to only a few diameter classes” (Cubrinovski et al., 2014). However, pipes of different diameters have been observed to have different failure mechanisms despite being composed of the same material (Romero et al., 2010), which reinforces the hypothesis that the distribution of forces vary based on diameter classes.

2.4 2010-2011 Canterbury Earthquake Sequence

This section explores the background and impacts of the CES, which is the hazard under consideration in this study.

In New Zealand, earthquakes represent one of the most significant risks due to the abundance of active seismic faults that lie beneath the country. New Zealand lies on the

tectonic boundary between the Indo-Australian and Pacific plates. The relative motions of the two plates are not concentrated on one or two fault lines in a narrow zone, but across a complex network of faults across a much larger zone (Quigley et al., 2016). This means that earthquakes may potentially occur at multiple locations, making them difficult to predict.

The Alpine Fault, Wellington Fault and Hikurangi Subduction Zones are believed to pose the greatest risk to the country as a whole. This is because the Alpine Fault traverses over 400 km across the South Island, the Wellington Fault lies directly beneath the capital city and the Hikurangi Subduction Zone represents significant risk to the entire eastern North Island, in addition to being assessed as having a high probability to generate tsunamis. Major earthquake sequences on any of these faults could lead to damage to life and property on an unprecedented level (New Zealand Lifelines Council, 2017). A relatively recent example of the devastation caused by earthquakes occurred in Christchurch, which is the largest city in the South Island of New Zealand with a population of approximately 350,000 living in an area of 1426 km^2 (Hughes et al., 2015).

A sequence of earthquakes devastated the region starting in 2010 and these became known as the Canterbury Earthquake Sequences (CES). The major events occurred on 4 September 2010 (Moment Magnitude (M_w) 7.1), 22 February 2011 (M_w 6.2), 13 June 2011 (two earthquakes with M_w 5.3 at 1:00 p.m. and M_w 6.0 at 2:20 p.m.), and 23 December 2011 (two earthquakes with M_w 5.8 at 1:58 p.m. and M_w 5.9 at 3:18 p.m.) (Hughes et al., 2015). Between September 2010 and mid-July 2012, the Canterbury region experienced three events between magnitudes 6.0 - 6.9, 54 events between magnitudes 5.0 - 5.9, 431 events between magnitudes 4.0 - 4.9, over 3000 events between magnitudes 3.0-3.9, and thousands of smaller tremors. The majority of the epicentres for the main events were located within 10 km of the Christchurch city centre (Quigley et al., 2016).

2.4.1 Ground Deformation

2.4.1.1 Transient ground deformation – Peak Ground Acceleration and Peak Ground Velocity

Earthquake-induced ground motions exhibit spatial variability over short distances of several metres due to local heterogeneous soil conditions that can give different site responses. Over large distances the fault rupture mechanism and wave propagation through a heterogeneous crust also affects the site response (Bradley, 2014).

Seismic ground motions are typically reported as PGA or PGV distributions and provide an indication of the intensity of shaking at a given site in accordance to an accelerogram. PGA is usually expressed in terms of g (acceleration due to gravity) and PGV in cm s^{-1} (centimetres per second). Larger PGA and PGV values place greater demand on the pipe and increases the susceptibility to damage.

Ground motion information is not generally provided as a deterministic number, but as a probability distribution with mean and standard deviation estimated from conventional ground motion theory. The PGA probability distribution is conditional on the actual measured PGA obtained from accelerometers throughout the city, so that the measured values provide some constraint (Bradley & Hughes, 2012).

A current map of accelerometers and strong motion sensors throughout Christchurch is shown below in Figure 2-10. Strong motion sensors measure PGV and have higher sensitivity than accelerometers, which measure PGA but have greater range (Seismology Research Centre, 2014).

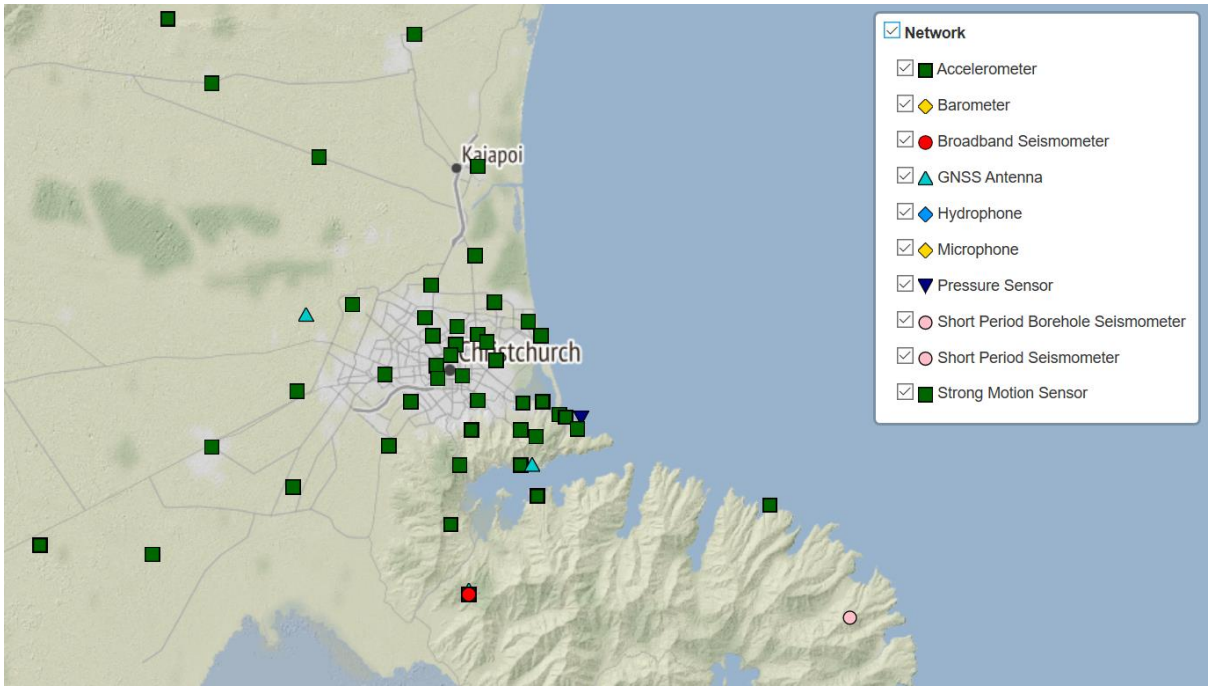

Figure 2-10. Sensors around Christchurch as a part of GeoNet's continuous GNSS network (GNS Science, 2018).

Figure 2-11 shows the conditional PGA calculated from the 22 February 2011 Christchurch Earthquake. General findings concluded that PGA amplitudes displayed a general attenuation with increasing distance from the earthquake epicentre (Bradley & Hughes, 2012). Inherent uncertainties in ground motion calculations should also be taken into account and any PGA retrieved at a considerable distance from existing ground motion stations is considered to have more uncertainty than those which are calculated nearby.

For small to moderate earthquakes the PGA is a reasonably good determinant of the observed damage to buildings and infrastructure, while for larger earthquakes PGV becomes more accurate at predicting damage outcome (U.S Geological Survey, 2011).

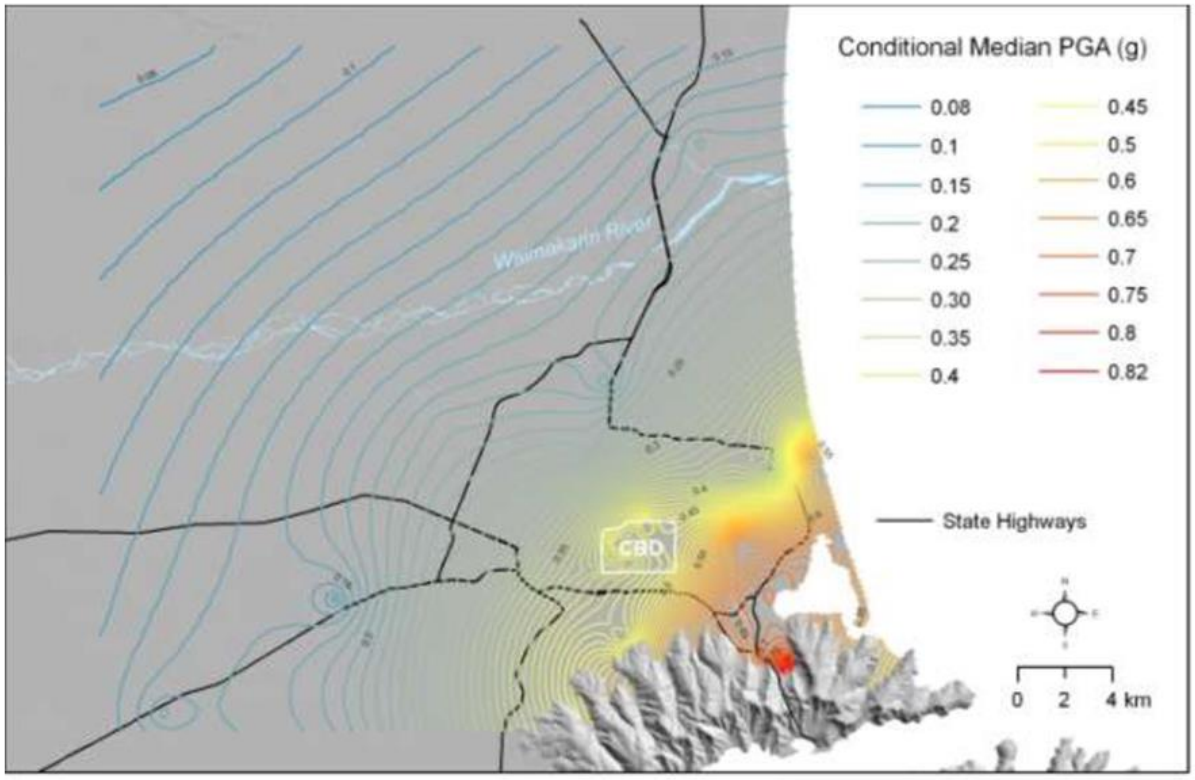

Figure 2-11. Conditional median PGA predicted from the February 2011 earthquake (Bradley & Hughes, 2012)

2.4.1.2 Permanent ground deformation – liquefaction and lateral spreading

Liquefaction is a phenomenon resulting from strong ground motions which causes substantial strength and stiffness loss in saturated, unconsolidated soils. During the CES it was demonstrated that liquefaction had been particularly damaging to underground brittle assets such as reinforced concrete pipes due to the associated lateral spreading and differential subsidence (New Zealand Lifelines Council, 2017).

The minimum PGA required to yield liquefaction manifestations and corresponding subsidence is 0.1-0.2 g and in Christchurch this has an estimated return period of between 40-170 years (Stirling, et al., 2008). However, in susceptible soils with high water table this could be as low as 0.08 g (Hughes et al., 2015).

Liquefaction and ground damage varied by suburb during the earthquake sequences; this is due to spatial variability of the shallow subsoil classification in different areas of the city (Cubrinovski et al., 2011). Some soil types are more susceptible to earthquake-induced ground motions than others. One way this can be quantified is through the use of a Liquefaction Resistance Index (LRI) developed by (Cubrinovski et al., 2011). The LRI is based on a factor of safety against triggering liquefaction, multiplied by a cyclic stress ratio. The factor of safety is assigned based on observed liquefaction and estimated ground settlement in liquefied areas in accordance to Table 2-7. In areas with no visible liquefaction, the water table depth was used to estimate the factor. The cyclic stress ratio is calculated from PGA recorded using strong motion sensors across the city and interpolated.

Table 2-7. Factor of safety against liquefaction (Cubrinovski et al., 2011)

Average Factor of Safety, $\overline{FS}$	Liquefaction Severity	Typical Manifestation and Damage to Structures	Estimated Ground Settlement
0.90	Traces of liquefaction	Some evidence of liquefaction, but limited both in extent and impacts, and judged non-damaging for structures	< 50 mm
0.75	Low to moderate	Clear evidence of liquefaction, with scattered sand boils (sand ejecta) and ground distortion; low damage to residential buildings and buried pipe networks.	50 – 200 mm
0.50	Moderate to severe	Very large, continuous and thick sand ejecta, severe ground distortion (undulations, fissures) and substantial total and differential settlements; moderate to severe damage to residential buildings and buried pipe networks.	200 – 400 mm
0.25	Very severe (extreme)	Extreme manifestation of liquefaction with excessive ground distortion including very large total and differential settlements, vertical offsets and ground fissures, often accompanied with severe effects of lateral spreading; excessive (most often beyond repair) damage to residential buildings and buried pipe networks.	> 400 mm

The LRI value were sorted into five different zones where the susceptibility is directly proportional between different zones. The higher the LRI value, the less the liquefaction susceptibility.

Figure 2-12 shows the LRI zones in Christchurch city with the locations of repaired waste water pipe midpoints superimposed. The worst affected liquefaction areas appear to be within close proximity to the Avon River, and affecting "alluvial and marine fine sediments in the eastern suburbs, in the region of late Holocene coastal progradation" (Hughes et al., 2015).

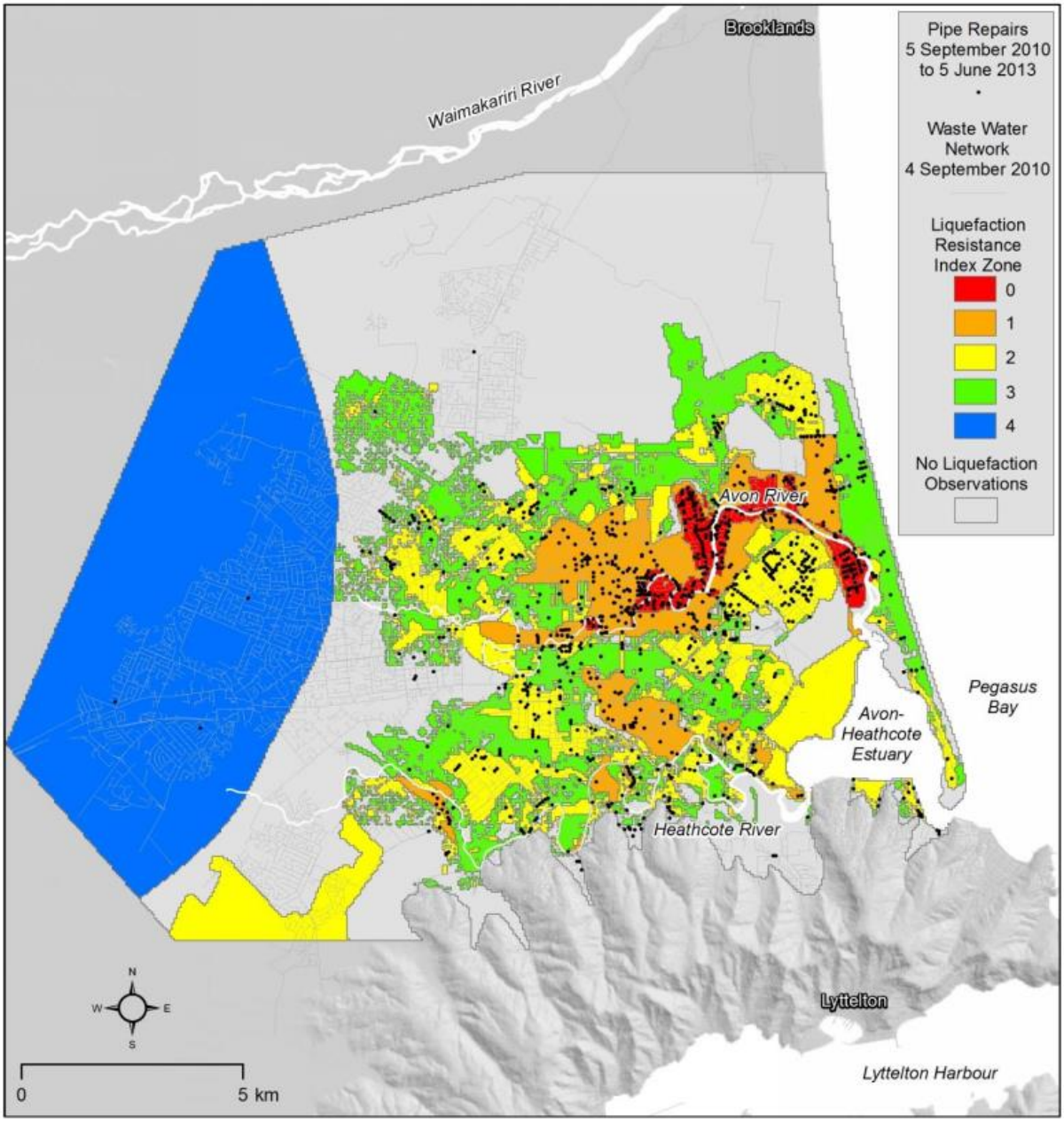

Figure 2-12. Locations of repaired waste water pipe midpoints within the LRI analysis area, and LRI zones (Cubrinovski et al., 2014)

Figure 2-13 below shows the summary repair data for the four most widespread materials (Concrete, Earthenware, Asbestos Cement and Plasticised Polyvinyl Chloride) within the LRI

zones. For the waste water network in Christchurch city, we can visually discern that the higher the LRI (less susceptible to liquefaction), the fewer repairs were generally required, and nearly 80% of the damaged water mains were in liquefied areas (Cubrinovski et al., 2014).

Observed damage type has also been reported to differ between pipes subjected to varying levels of liquefaction. For example, previous studies regarding the potable water network showed that in high liquefaction zones, liquefaction-based failures were more evident as breaks in the pipes and its fittings resulted from differential soil pressure. In non-liquefaction areas, ground shaking and Fluid Structure Interaction (FSI) effects were dominant, resulting in breakages and leaks due to excessive pressure surges (Rais et al., 2015).

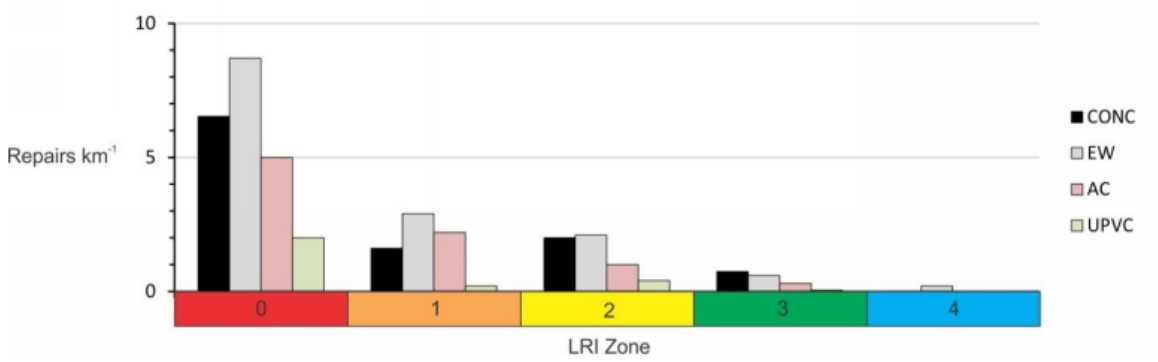

Figure 2-13. Summary repair data for the four most spatially extensive waste water pipe materials (Concrete, Earthenware, Asbestos Cement and Unplasticised Polyvinyl Chloride) within Liquefaction Resistance Index Zones. Data cover the period 5 September 2010 to 5 June 2013 (Cubrinovski et al., 2014)

2.4.2 Subsidence and lateral spreading

Ground surface subsidence and lateral spreading were the primary shallow ground movements during the CES. Ground tectonic uplifts were recorded up to 400 mm near the Avon/Heathcote estuary and the central and northern suburbs experienced tectonic subsidence up to 150 mm. Overall, however, widespread subsidence was caused predominantly by liquefaction-induced settlement. Permanent lateral ground displacements were recorded in the order of 2.0 – 3.0 m along the Avon and Kaiapoi River, but were usually constrained to narrow corridors near bodies of water (Cubrinovski et al., 2011).

LiDAR surveys were used to measure the extent of ground movement before and after each main CES event. Millions of position data points were collected from sweeping lasers mounted on aircraft as a LiDAR (Light Detection and Ranging) survey point cloud. The data points may be categorised as ground or non-ground, e.g. for survey points reflecting off vegetation and other structures. The ground data points were averaged and reported as a single value within a square cell (usually 5m × 5m) and used to generate a suite of Digital Elevation Models (DEMs) due to the large quantity of data available (Canterbury Geotechnical Database, 2014) (Canterbury Geotechnical Database, 2014). The DEMs can be compared to a baseline DEM taken between 2003-2008 to identify overall changes to ground movement, and compared before and after each event to indicate the change in ground level during each event. Most LiDAR surveys were taken one month after each event to allow time for the removal of liquefaction ejecta (Canterbury Geotechnical Database, 2014).

LiDAR surveys have limitations on accuracy, including measurement errors, error due to interpolation in areas with a low density of ground data points, and limitations due to capture resolution known as granularity. These are depicted graphically in Figure 2-14 below:

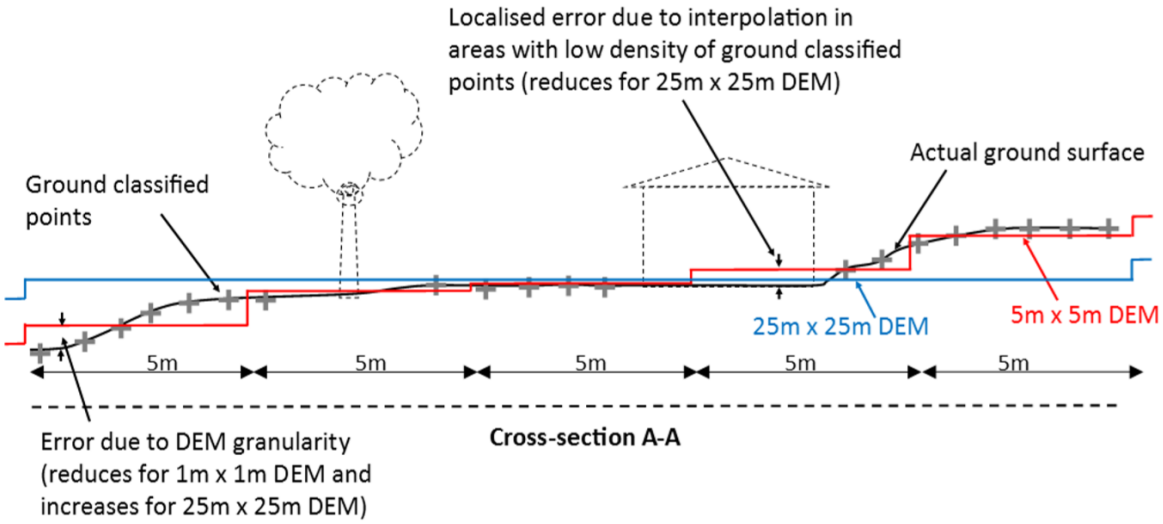

Figure 2-14. Cross section showing DEM accuracy errors of an area with vegetation and buildings (Canterbury Geotechnical Database, 2014)

The horizontal accuracy is ± 0.55 m and the vertical accuracy is ± 0.15 m for the 2003 baseline survey, and ± 0.07 m for the CES surveys. The accuracy limitations are due to the data collection process, where some ground data is scanned twice or more on repeat

flyovers, and due to dynamic corrections, which were applied to account for aircraft movement such as side-to-side rolling (Canterbury Geotechnical Database, 2014). Additional sources of error include Global Positioning Survey (GPS) errors and approximations within the New Zealand Quasigeoid reference surface. The point clouds were verified by comparing them to surveyed benchmarks, which themselves have a vertical accuracy of ± 0.03 m (Canterbury Geotechnical Database, 2014).

The overall accuracy is calculated as cumulative frequency distributions by the Canterbury Geotechnical Database (2014) and provided below in Figure 2-15. The median error is mostly similar for the different DEM sets collected throughout the various events and the 2003 data set had the largest standard deviation due to older equipment being used, which had greater accuracy limitations.

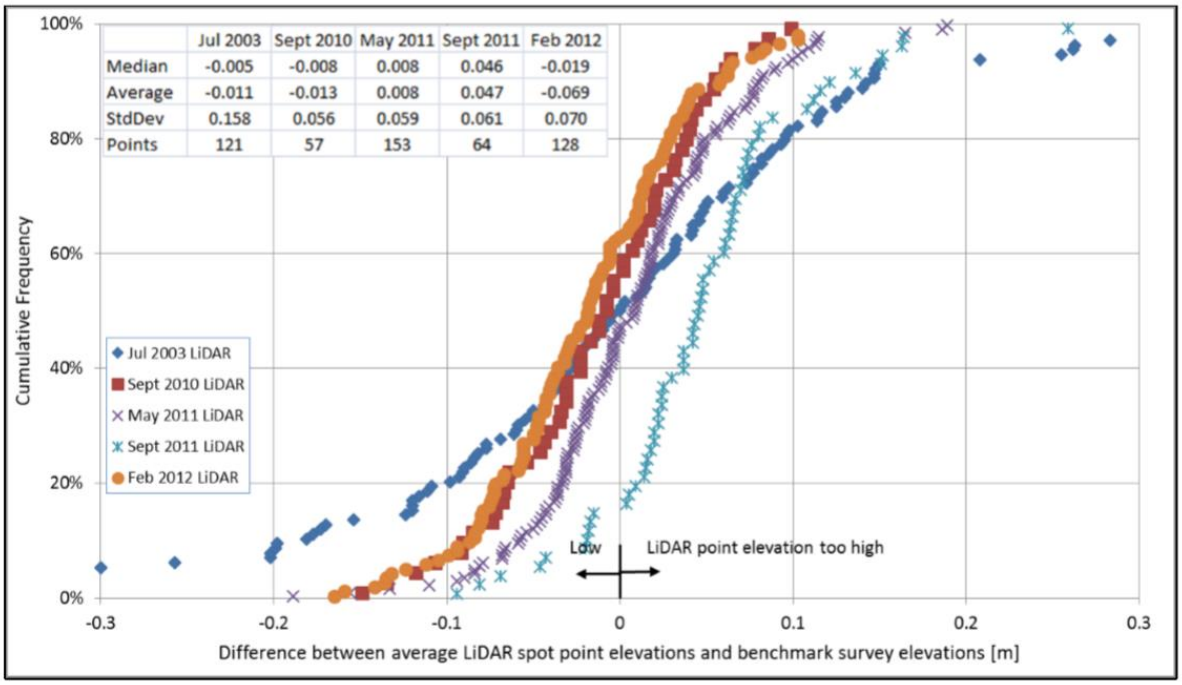

Figure 2-15. Cross section showing DEM accuracy errors of an area with vegetation and buildings (Canterbury Geotechnical Database, 2014).

Angular distortion was often used as an indication of the deformation of the ground between two points. It is a dimensionless parameter obtained from the differential vertical movement between two adjacent LiDAR measurements divided by the distance between them (O'Rourke et al., 2014). The parameter is widely used together with horizontal soil strain to estimate the effects of subsidence and lateral spreading on foundations, and a

reference chart was developed by (Boscardin & Cording, 1989) from field observations and analytical models to relate these parameters with damage severity.

2.4.3 Impacts on the built environment and infrastructure lifelines

The CES resulted in 185 fatalities and triggered widespread damage to buildings and city infrastructures, especially in the Central Business District (CBD). The events created the largest lifeline disruption in 80 years in New Zealand, with severe liquefaction, lateral spreading, sand boils, and ejected material ponding on the soil surface in the Christchurch urban area. The total economic loss resulting from the CES has been estimated at approximately 30 billion New Zealand dollars, which is equivalent to 15% of national GDP (O'Rourke et al., 2014). Liquefaction was estimated to have affected over 51,000 residential properties, where 15,000 were damaged beyond repair. The CCC received and addressed over 36,000 water supply and waste water service requests within the five months following the earthquake (Giovinazzi et al., 2011).

The Christchurch water and waste networks were extensively damaged as a result of the CES. Lateral ground movements and vertical settlement resulted in differential movement of pipes relative to each other and the surrounding ground or structures. This was demonstrated through the loss of grade in gravity pipes and inconsistencies in the invert level, resulting in blockage and reducing the network carrying capacity (Cubrinovski et al., 2011). Structural cracking was evident as leakages at interfaces with rigid structures, and joint dislocations resulted in silt and groundwater infiltration. In total, approximately 100 sewer pump stations and 528 kilometres of sewer pipes were damaged in the city, which constituted approximately 31% of the total waste water pipe network length (Liu et al., 2014). Damage was observed to be more frequent in smaller pipes than larger ones, most likely due to thinner pipe walls and a high occurrence of potentially lower-quality fittings in pipes with smaller diameters (Cubrinovski et al., 2014).

The liquefaction-induced angular distortion and horizontal strains from lateral spreading during the earthquakes resulted in a complex combination of forces being imposed on buried pipes. O'Rourke et al. (2014) found statistically significant relationships between pipe repair rates in buried waste water pipes with angular distortion and lateral ground

strain, which they stated would be useful to approximate damage in response to measured ground displacements in the future. This is shown in Figure 2-16 below.

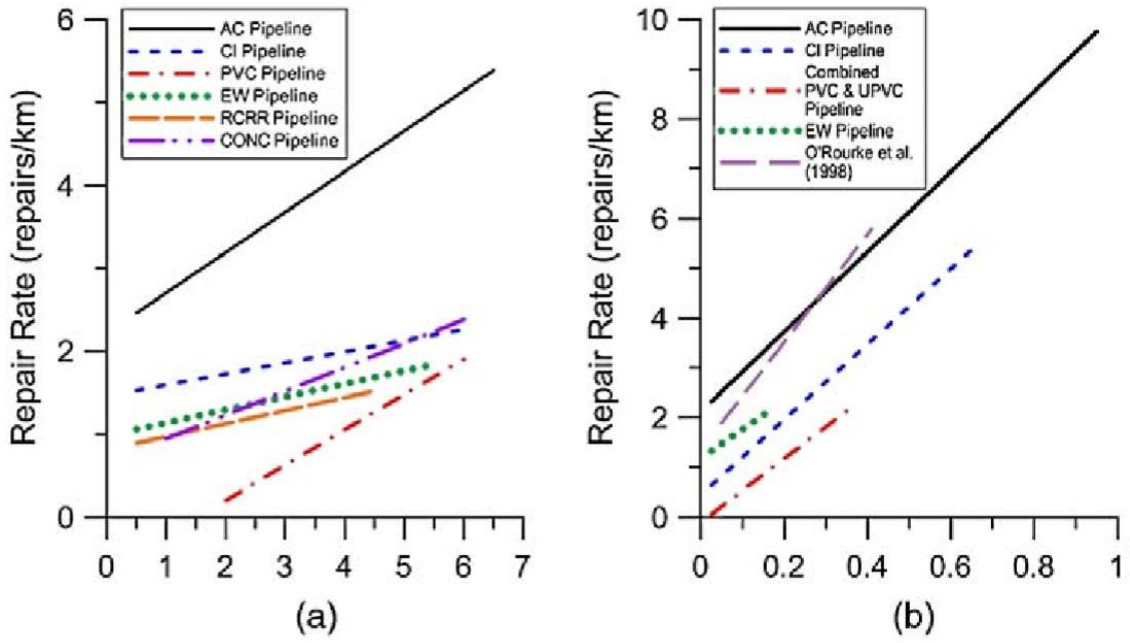

Figure 2-16. Comparison of repair rate vs. angular distortion and lateral strain for different pipe types: (a) Angular distortion, β (10−3) and (b) lateral ground strain, εHP (%) (O'Rourke et al., 2014).

In a subsequent study, (Bouziou & O'Rourke, 2017) incorporated LiDAR data with ground motion information to study the effects of transient and permanent ground deformations on the Christchurch water distribution system. They concluded that the higher resolution of data compared to their 2014 study resulting from the LiDAR data inclusion significantly influenced the repair rate to lateral ground strain relationships, and that repair regressions and are highly sensitive to the degree of data resolution available.

In a ground rupture experiment featuring a scaled-down reinforced concrete pipeline by Kim et al. (2012), "bending at the pipeline joints closest to the fault plane" was identified as one of the highest occurring defect types in conjunction with compression failure associated with telescoping-type deformation. This was indicated by tensile cracking on the tension face and possible joint spalling at the compression face. Bending and shear forces resulted from differential uplift or settlement of the ground along different lengths of the pipe, where the magnitude was largely dependent on bedding material and installation (Edkins et al., 2016).

Edkins et al. (2016) found that the two most common types of shear acting on the pipe are barrel transverse shear and barrel longitudinal shear. Barrel transverse shear is the most common kind of shear and occurs when the force is at or near 90 degrees to the pipeline axis, and is commonly observed as a transverse break in the middle third of the pipe. Barrel longitudinal shear occurs in pipes with insufficient tensile strength when the superimposed soil load results in a failure plane close to the spring line. It appears as a longitudinal crack orientated horizontally along the pipe barrel adjacent to the joint.

Figure 2-17. Tension cracks occurring at the top wall of the pipe only, indicating bending actions due to subsidence of adjacent pipe segments (this study).

Connecting structures such as the presence of lateral adjoining pipes influenced the damage observed, and for pipes entering rigid vertical structures, joint pull-out was the most frequently observed failure mechanism (Edkins et al., 2016). An example of this is the connections between pipelines and manholes or pump stations. Joint failure prevalence increased when rubber gaskets mounted on tapered spigots displaced due to large hoop stresses being generated. Embedded concrete pipes connecting to a rigid end structure such as a manhole also experienced torsional forces when the manhole rotated on a lean.

Damage was more frequent on spigot and collar joints of segmented reinforced concrete pipelines than on the pipe itself (Edkins et al., 2016). These were observed as opened joints,

or the thrusting of the spigot of one pipe into the collar of the neighbouring segment, resulting in spalling damage. The joint failures are due to axial forces which occur when the soil strata changes characteristics, and where the earthquake forces propagating through the soils encounter a local change of density and therefore in acceleration.

Axial forces also occur when forces interact with a pipeline at an angle, when pipes exit vertical rigid structures such as pump stations due to different oscillation frequencies, or at the junction between underground/above ground pipes (Edkins et al., 2016).

Figure 2-18. Compression forces acting on a joint causing rupture (Edkins et al., 2016)

About 50 days after the earthquake, a steady state repair rate of four times the pre-quake average was reached (O'Rourke et al., 2014). Repairs to the waste water network immediately after the initial February 2011 event were delayed to focus of resources on the repair of the water supply, and the process was also more complicated than the water supply network due to larger installation depths requiring trench support and dewatering (Cubrinovski et al., 2011). The daily waste water pipe repairs and cumulative frequency of repairs between the February 2011 event and the June 2011 event are shown in Figure 2-19.

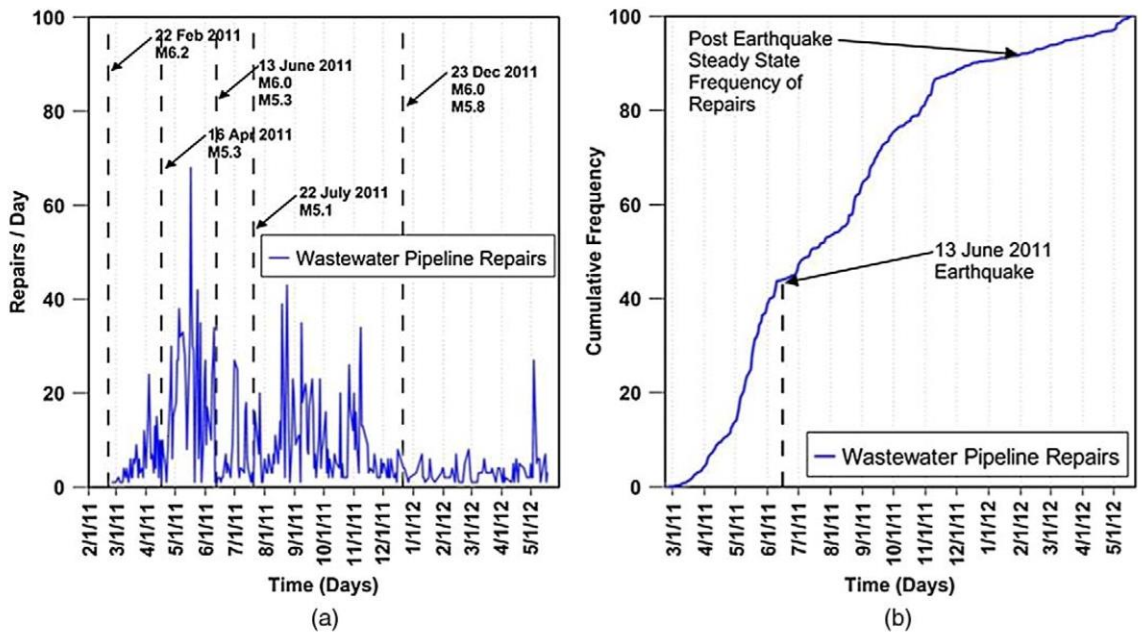

Figure 2-19. Daily repair rate (left) and cumulative repair frequency (right) of waste water pipes following the CES (O'Rourke et al., 2014)

2.5 Post-CES waste water system assessment

This section reviews how the waste water system impacts from the CES were assessed and managed.

Following the CES, the CCC and New Zealand government were confronted with "an almost-crippled underground waste water system" amidst a significantly damaged horizontal infrastructure network. It was determined that a repair programme based on the alliance model would result in the greatest efficiency and least risk to undertake the 2.2 billion dollar, 5.5 year civil construction programme to follow (SCIRT Learning Legacy, 2019).

This resulted in the formation of the Stronger Christchurch Infrastructure Rebuilt Team (SCIRT), specifically to address the horizontal infrastructure repairs. As mentioned in Section 1.3, SCIRT consisted of the Christchurch City Council (CCC), New Zealand Transport Agency (NZTA) and Canterbury Earthquake Recovery Authority (CERA), which were three funding organisations where two were asset owners. The other five members were previously-rival construction companies (City Care, Downer, Fletcher Construction, Fulton Hogan and McConnell Dowell) who undertook the repairs (SCIRT Learning Legacy, 2019).

SCIRT followed the Infrastructure Recovery Technical Standards and Guidelines (IRTSG) in order to undertake repairs. The document was prepared by CCC engineers to manage the technical aspects of the repairs to ensure that the different member companies had a unified repair method.

The IRTSG required the use of the New Zealand Pipe Inspection Manual (NZPIM) for assessment of gravity waste water pipes (Heiler et al., 2012). This manual covered the inspection of pipelines exclusively using CCTV surveys. The process involves inserting a camera mounted rover into a pipe from an access manhole and capturing and transferring video recordings to an operator with a screen at the ground surface. A jetting/suction truck was often required to clean the pipe of debris and silt infiltration, as shown in Figure 2-20.

CCTV data have been chosen to represent damage to the waste water network in this study, as they are readily available from local territorial authorities that manage waste water systems, CCTV surveys are the predominant tool for condition assessment in New Zealand, and are fast becoming the primary method to determine the structural and service condition of pipes across the world. It is also quick and relatively cheap in comparison to alternative survey methods (ProjectMax Ltd, 2006).

Figure 2-20. Typical example of CCTV operation showing jetting/suction truck with CCTV van, retrieved from "Asset Assessment using GIS and InfoNet" by Heiler et al. (2012)

CCTV surveys in Christchurch following the CES utilised up to 150 full-time equivalent staff separated into 20 teams, which was equivalent to half of the national CCTV field resource (SCIRT Learning Legacy, 2019). CCTV surveys were often combined with other investigation methods such as manhole level surveys, pole cameras and pipe profile assessments. As the process was slow and expensive, it was viewed by territorial authorities as a poor return in asset assessment in low-damage areas. The physical camera itself also posed some access limitations due to pipe size and flow issues (SCIRT Learning Legacy, 2019).

CCTV survey limitations include any information beyond the interior pipe surface, such as thickness or condition of the pipe wall or any cavities outside the pipe. The inspections also cannot confirm if a pipe is leaking during dry inspection conditions. Detailed information such as dip and pipe grade also could not be reported in older models of CCTV equipment (ProjectMax Ltd, 2006).

The assessment of gravity waste water and storm water pipes contributed over 50% of the total cost of the rebuild of horizontal infrastructure in Christchurch, and needed to be completed in advance of other infrastructure as they are typically the deepest asset (Heiler et al., 2012).

2.5.1 Geographic Information Systems and InfoNet

Geographic Information Systems (GIS) and associated databases allow disaster researchers and stakeholders to manage large quantities of heterogenous data, and facilitate post-disaster response and situational awareness. GIS began being adopted in Christchurch prior to the amalgamation of the CCC in 1990. The earliest such database for waste water pipes was affected by three primary issues (Cubrinovski et al., 2014):

1. Data entry from paper-based records was regarded as a non-specialist task. When datasets were merged together in 1990 there was considerable variability in the quality of the data produced among the different local boroughs.
2. After the amalgamation of the CCC, two databases were used, one for managing physical infrastructure and one for financial management, When updates were made to one, edits did not carry over to the other.
3. Data capture methods prior to the CES were inefficient and not detailed, therefore CCC repair decisions were overwhelmingly based on contractor personal knowledge and anecdotal evidence.

Following the 4 September 2010 earthquake, the CCTV contractors recorded inspections on computer-based programs, Cleanflow / WinCan or paper-based log sheets (Christoffersen, 2012). In order to manage this, a Microsoft Excel spreadsheet was used by the CCC to manage the data and determine whether repairs were required. The original videos and CCTV inspection catalogue were stored at the CCC on a network drive. Some of the video disks could not be copied to the network drive due to errors (Christoffersen, 2012).

Following the 22 February 2011 earthquake, significantly more damage occurred and the CCC began regarding the CCTV surveys as not only for repair purposes, but for “as-yet-unknown future requirements” which necessitated a change in the data collection process (Christoffersen, 2012). The CCC transferred the pipe inspection priorities and instructions to the newly formed SCIRT, and the management responsibility to City Care. All video footage assessments began to be catalogued in a database known as InfoNet. The platform was used by SCIRT to store both current and historical assessment information by pipe ID, and allowed data analysis to compare surveys taken at different times, identify damage trends, and compare damage against IRTSG thresholds to determine whether the pipe required

renewal, repair or no action (Heiler et al., 2012). The assessment data were also able to be presented in an easily accessible form for sharing between project teams, and viewable using an in-house online GIS viewer, which was accessed by over 920 users from 20 different organisations in 2012 (Heiler et al., 2012). Many of these users developed their own spreadsheets that automatically retrieved data from the SCIRT GIS viewer on a daily basis to ensure that the latest information was available.

Following the CES, the CCC GIS database still featured inconsistencies and errors from earlier merging efforts. A data validation process called the Feature Manipulation Engine (FME) by Safe Software was developed to check that survey details and pipe IDs matched between the CCTV catalogue and GIS system. As a result of this process, the percentage match of records increased from 75% to 99.6% for the wastewater network, and could be used to verify data in SCIRT's InfoNet (Christoffersen, 2012). The CCC catalogue was later migrated from the Excel spreadsheet format to a "SQL database with a web-based front end" which allowed easier access, version control and administration (Christoffersen, 2012). This database was used to access the CCTV footage used in the survey.

2.5.2 Standardised Damage Coding in accordance to the New Zealand Pipe Inspection Manual

The New Zealand Pipe Inspection Manual (NZPIM) was first developed in 1989 to provide a universal terminology system in New Zealand to assess gravity pipes using CCTV surveys, and allows trained assessors to distinguish and assign severity to the damage types identified. It is the only document of its type in New Zealand and was originally based on the UK Water Research Centre "Manual of Sewer Condition Classification" which was published in 1980, and similar inspection documents based on the UK manual have been developed around the world from Europe to the USA (ProjectMax Ltd, 2016). The second edition of the manual was published in March 1999, and the current edition (third) was produced in 2006 by ProjectMax Ltd (ProjectMax Ltd, 2006). The damage observed in this thesis was coded in accordance with the NZPIM.

The NZPIM separates the classification of pipe observations into 25 Defect Codes and 14 Feature Codes (ProjectMax Ltd, 2006). The defect and feature codes are presented in Table 2-8 and Table 2-9, respectively.

Table 2-8. Defect codes in accordance to the NZPIM (ProjectMax Ltd, 2006)

Code	Defect	Description
CC	Crack, Circumferential	Cracking occurring at right angles to the pipeline axis. Maximum longitudinal length 100mm. If cracking occurs only within a joint zone, then it is allocated a Joint Faulty "JF" code.
CL	Crack, Longitudinal	Cracking parallel to the axis of the pipe, which may occur anywhere around the circumference.
CM	Crack, Multiple	Cracks both circumferential and longitudinal at the same longitudinal location in the pipe. The cracks join, but do not for "pieces" pipe.
DE	Debris, Silty	Silt and gravel deposited within the pipe.
DF	Deformed Pipe	Usually applies to a rigid pipe, such as earthenware, asbestos cement of concrete pipe deformed by external forces.
DG	Debris, Greasy	Refers to grease, fat, scale and all adhering material, except encrustation deposits ("ED").
DP	Dipped Pipe	Sagging of the pipeline across more than one pipe section, and will have a continuity. Dipped pipes are commonly identified by water level changes.
ED	Encrustation Deposits	Encrustation deposits on a pipe wall result from infiltration seepage transporting dissolved solids from the surrounding soil that are precipitated and deposited on the pipe wall, building up over time. Encrustation is often orange due to the prevalence of iron oxide in many soils.
IP	Infiltration Present	Visible ground water infiltration from defects either in the pipe wall, or at pipe joints. Encrustation Deposits ("ED") may be present, but infiltration appears as wetness or water flowing at various rates from seeping, dripping, running,

		jetting or gushing.
JD	Joint, Displaced	Horizontal (left or right) or vertical displacement at a pipe joint. The pipe diameter can be used as a guide to the percentage of displacement.
JF	Joint, Faulty	Joint sealing defects or physical damage at joints within the joint zone, excluding open and displaced joints. The joint zone is a length of pipe 200mm long, 100mm either side of the joint centre.
JO	Joint, Open	Pipe sections that are longitudinally displaced and separated at joint. Joint width tolerances vary between pipe materials and diameter. Open joints do not necessarily equate to faulty joint seals.
LF	Lateral, Sealing Faulty	LF applies to any sealing or physical damage occurring within the lateral connection zone; an area encompassing the main pipe wall thickness and a 50mm area around the lateral connection.
LP	Lateral, Protruding	Part of the lateral pipe is protruding into the mainline.
LX	Lateral, Problem	Defects identified inside a lateral pipe.
OP	Obstruction, Permanent	An obstruction in the pipeline caused by embedded objects in the pipe wall or an object that is not able to be removed using standard cleaning equipment and specialist machinery or methods are required for its removal.
OT	Obstruction, Temporary	An obstruction in the pipeline, which does not require specialist machinery to remove and is not attached nor embedded in the pipe wall.

PB	Pipe, Broken	The pipe is still functional as a free-flowing conduit but parts of it may have broken out or are displaced from one another or could become displaced. More severe than "CM" as cracking has extended such that they formed "blocks" of pipe that can displace and fall out or lead to a collapsed pipe.
PF	Deformed Plastic Pipe	Plastic pipe, such as PVC, PE or GRP is deformed due to pressure or loading, which can include ovality or bulging.
PH	Pipe, Holed	A hole which has been intentionally or unintentionally cut or punched into the pipe, for example to either gain access or during installation of nearby underground services.
PL	Protective Lining Defective	Defect such as bulges, weld failures in the pipe liner which has been installed during rehabilitation works.
PX	Pipe, Collapsed	The pipe has collapsed and is no longer functional, although water may still flow through the rubble of the collapsed pipe.
RI	Root Intrusion	Roots growing into the pipe through penetrations or openings.
SD	Surface Damage	Damage to the interior surface which includes spalling, abrasive erosion or chemical and biological corrosion.
RM	Tomo	A cavity which exists beyond the pipe wall. The backfill surrounding the pipe has been eroded or slumped. Tomos are generally caused by a pipe break or hole allowing the material into the pipe and running water either inside or outside the pipe removing it.

Table 2-9. Feature codes in accordance to the NZPIM (ProjectMax Ltd, 2006)

Code	Defect	Description
CF	Construction Feature	Construction features are typically drainage fittings (other than manholes) installed or constructed as part of, or for the purpose of, servicing the pipeline.
DC	Dimension Change	A change in the pipes cross-sectional dimensions. Typically, this is the pipe diameter, but could equally relate to the shape of the pipe.
GC	General Comment	This code is used to provide any relevant information about the inspection at a particular distance in the pipe that is not provided for elsewhere, or covered satisfactorily by a defect or feature code.
IA	Inspection Abandoned	The finishing code for inspections abandoned prior to reaching the end node from a single direction. The reason for the abandonment is noted under the “remarks” field.
IE	Inspection Ends	The general finishing code for all inspections unless abandoned prematurely, in which case the code to be used is “IA”.
IS	Inspection Start	The first entry for all pipeline inspections.
LB	Lateral Blank	A lateral is blank, e.g. an end cap is visible
LC	Lining Change	Documents any inserted lining in the original pipe.
LL	Line Deviates Left	Documents significant changes in the direction of the pipeline towards the left. This can include fittings such as bends or changes in alignment through joints or breaks in the pipe.
LR	Line Deviates	Documents significant changes in the direction of the

	Right	pipeline towards the right. This can include fittings such as bends or changes in alignment through joints or breaks in the pipe.
LD	Line Deviates Down	Documents significant changes in the grading of the pipeline downwards. This can include fittings such as bends or changes in alignment through joints or breaks in the pipe.
LU	Line Deviates Up	Documents significant changes in the grading of the pipeline upwards. This can include fittings such as bends or changes in alignment through joints or breaks in the pipe.
LO	Lateral OK	Satisfactory lateral connection with no defects is open (ie. Not Blank) and would not otherwise attract a condition code of LB, LF, LP or LX.
MC	Material Change	A change of pipe material. This is typically due to a section of the original pipe that has been excavated and replaced as part of a repair.

2.6 Summary

This Chapter has reviewed the various risk components that need to be considered to determine the performance of reinforced concrete waste water pipes through the CES.

- Sections 2.1 and 2.2 focused on the risk component of “exposure”, which in this study is defined as the reinforced concrete waste water pipe network in Christchurch. The former section presented the history of reinforced concrete pipe design and showed that the modern design standard in New Zealand was periodically updated in the past century based on design innovations overseas. The latter section focused on the Christchurch waste water system and revealed that the geotechnical challenges of the region required the formation of a specific organisation in the form of the Christchurch Drainage Board in order to construct and expand the network.

- Section 2.3 explored the risk component of “vulnerability”, which are multiple factors considered to affect the durability and performance of the reinforced concrete pipe. The factors explored include chemical and biological deterioration, fabrication and installation methods, above ground and surrounding soil conditions, pipe age and dimensions. The extent of existing literature and their findings varied depending on the factor under consideration.
- Section 2.4 presented a general discussion of the risk component of “hazard”, which is defined as the CES. The CES caused damage on an unprecedented scale due to ground motions, deformations, subsidence and lateral spreading.
- Section 2.5 explored the tools and methods that enable impact assessment for the buried concrete pipes following the “hazard”. The section highlighted the importance of databases for managing infrastructural assessments. CCTV surveys were the most common choice of assessment, with a clearly defined and standardised coding system available in the form of the NZPIM to assess the gravity pipe networks.

The following chapter introduces a method to assess reinforced concrete waste water pipes using the assessment tools discussed. The pipe selection process is explained, followed by the damage assessment procedure and geospatial analysis.

Chapter 3 - Method

3.1 Pipe subset selection

As of 2014, Christchurch City had a total of 43,273 waste water pipes with varying materials diameters and installation dates; these pipes also spanned a range of mapped liquefaction zones of varying severity. For this study, 55 pipes were chosen for assessment based on a selection process, with guidance from the CCC. The selection process is illustrated in Figure 3-1.

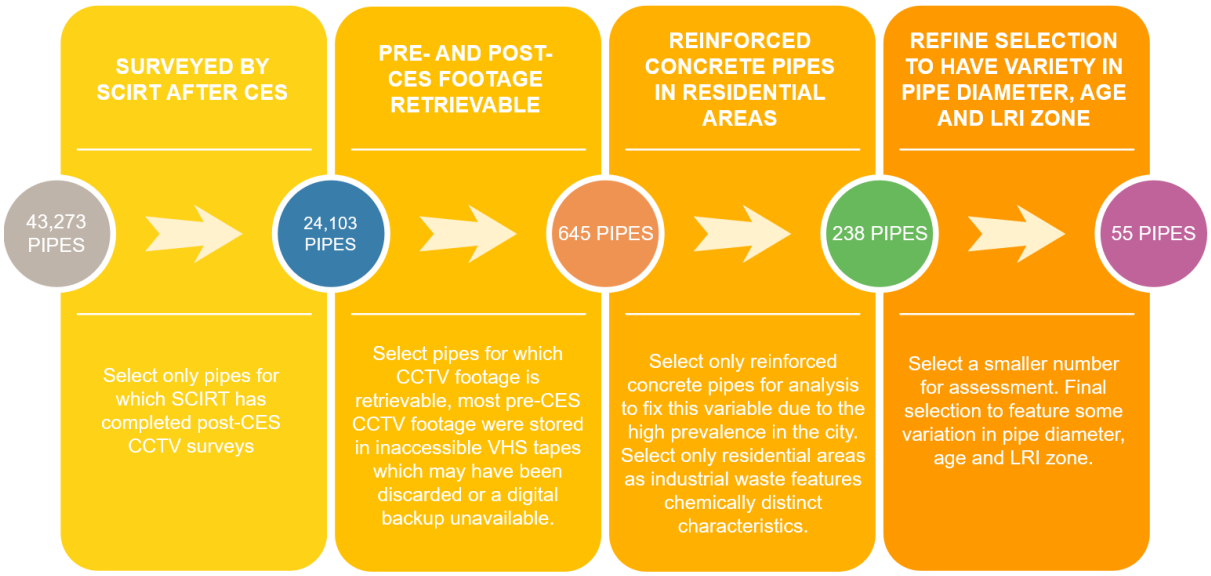

Figure 3-1. The pipe selection process used in this study.

As discussed in section 2.5.1, CCC currently keeps track of CCTV data in a database. At the time of data retrieval, the total number of pipes for which SCIRT conducted post-CES CCTV analysis was 24,103 pipes (approximately 46% of the total network). The total number of pipes for which pre-CES CCTV surveys had been conducted was 12,475 pipes, with most of the surveys having been conducted between 1990-2010.

The post-CES CCTV recordings were entirely available in digital format and a backup was kept in the CCC archives, readily accessible for viewing. However, for the pre-CES recordings, due to older technologies being used at the time, these were stored either digitally in an archived folder (referred by CCC as 'DVD') or on physical video tapes (referred by CCC as

'VHS') where a digital backup was not kept. The 'VHS' tapes were not accessible as their physical locations were not known and thus all CCTV records which referred to the 'VHS' format were unable to be used. Therefore, despite the large number of pipes surveyed, most of the pre-CES CCTV footage were lost, corrupted or otherwise inaccessible.

In order to confirm the availability of matching pre-CES and post-CES 'DVD' footage, the InfoNet and current CCC databases were merged. Once the databases were compared, the total number of waste water pipes that had matching and retrievable pre-CES inspections and post-CES CCTV footage was only 645 pipes (approximately 1.5% of the total network).

Discussions were held with the CCC to discuss how to further refine the selection of pipes. It was agreed to limit the scope of the research to study parameters such as pipe diameter and installation date by keeping the material constant. Therefore, it was agreed to focus on reinforced concrete (CONC or RCRR depending on reference) as it was considered to provide the widest variations in diameter, wall thickness, installation age and distribution. In addition, the material is still widely used in Christchurch for trunk mains, and is also the predominant material used in cities elsewhere in New Zealand and throughout the world.

After discussions with the CCC, it was also decided to limit the research to pipes in Christchurch residential areas. This was to exclude pipes in industrial areas, where contaminated and corrosive discharges may over time have led to encrustations and degradation that would obscure pre-CES and post-CES damage. Spatial data of the CCC land use zones were used to exclude all pipes in industrial areas. Following this procedure, 238 reinforced concrete pipes remained for residential land use areas with readily retrievable pre- and post-CES CCTV footage.

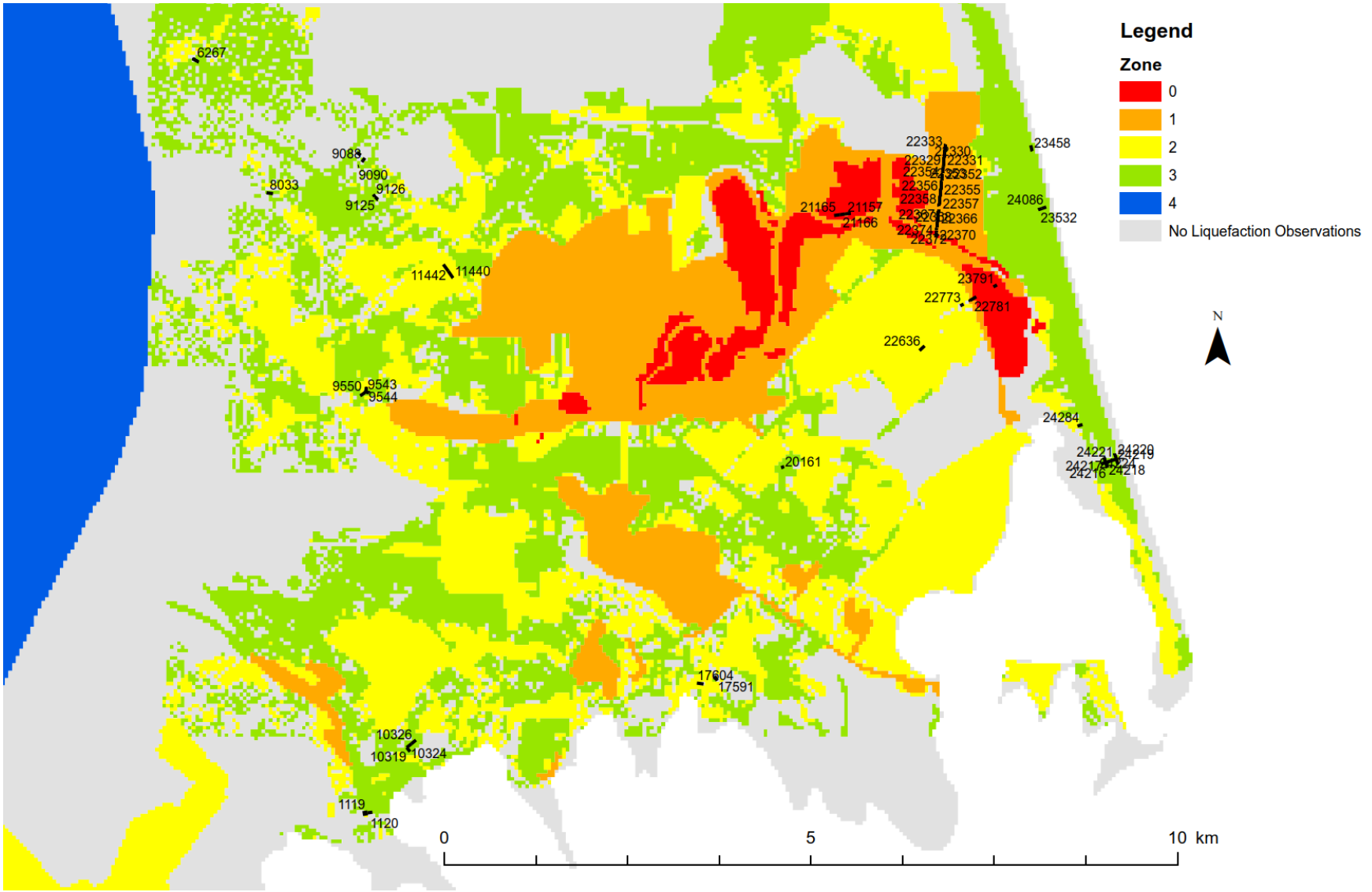

Figure 3-2. Pipe selection in and around Christchurch City overlaid with LRI zones, LRI map by (Cubrinovski et al., 2014)

Table 3-1. Pipe selection and specifications listed in increasing diameter of pipe. LRI Zone information from Cubrinovski et al. (2014)

Pipe ID.	Diameter (mm)	Year of Installation	LRI Zone	Est. Vertical Settlement (mm)	Est. Lateral Displacement (mm)	Pipe ID.	Diameter (mm)	Year of Installation	LRI Zone	Est. Vertical Settlement (mm)	Est. Lateral Displacement (mm)
23532	150	1954	3	20-50	20-40	**22355**	225	1950	1	250-500	200-400
8033	150	1955	3	20-50	20-40	**22356**	225	1950	1	250-500	200-400
9082	150	1955	3	20-50	20-40	**22357**	225	1950	1	250-500	200-400
9088	150	1955	3	20-50	20-40	**22358**	225	1950	1	250-500	200-400
9090	150	1955	3	20-50	20-40	**22366**	225	1950	1	250-500	200-400
9543	150	1955	3	20-50	20-40	**22367**	225	1950	1	250-500	200-400
9544	150	1955	3	20-50	20-40	**22368**	225	1950	1	250-500	200-400
9550	150	1955	2	50-250	40-200	**22370**	225	1950	1	250-500	200-400
22636	150	1955	2	50-250	40-200	**22374**	225	1951	0	>500	>400
17591	150	1956	3	20-50	20-40	**24086**	225	1954	3	20-50	20-40
17604	150	1956	2	50-250	40-200	**23458**	225	1958	3	20-50	20-40
24216	150	1958	3	20-50	20-40	**20161**	225	1960	3	20-50	20-40
24217	150	1958	3	20-50	20-40	**22372**	250	1951	1	250-500	200-400
24218	150	1958	3	20-50	20-40	**24284**	375	1956	3	20-50	20-40
24219	150	1958	3	20-50	20-40	**22773**	450	1952	2	50-250	40-200
24220	150	1958	3	20-50	20-40	**22781**	450	1952	0	>500	>400
24221	150	1958	3	20-50	20-40	**23791**	450	1952	0	>500	>400
24224	150	1958	3	20-50	20-40	**10319**	450	1956	3	20-50	20-40
9125	150	1958	3	20-50	20-40	**10324**	450	1956	3	20-50	20-40
9126	150	1958	3	20-50	20-40	**10326**	450	1956	3	20-50	20-40
6267	150	1959	3	20-50	20-40	**1119**	450	1960	3	20-50	20-40
22329	225	1950	1	250-500	200-400	**1120**	450	1960	3	20-50	20-40
22330	225	1950	1	250-500	200-400	**21157**	450	1991	0	>500	>400
22331	225	1950	1	250-500	200-400	**21165**	450	1991	0	>500	>400
22333	225	1950	1	250-500	200-400	**21166**	450	1991	0	>500	>400
22352	225	1950	1	250-500	200-400	**11440**	900	1955	2	50-250	40-200
22353	225	1950	1	250-500	200-400	**11442**	900	1955	2	50-250	40-200
22354	225	1950	1	250-500	200-400						

Finally, 55 pipes were selected to include variation in pipe diameter, age of installation and LRI. Figure 3-2 shows the spatial distribution of the final pipes selected for analysis, and the pipe specifications are presented in Table 3-1.

CCTV data were chosen to represent damage to the waste water pipes under investigation, as is the data are territorial authorities that manage waste water systems, CCTV surveys are the predominant tool for condition assessment in New Zealand, and are fast becoming the primary method to determine the structural and service condition of pipes across the world. CCTV surveys are also quick and relatively cheap in comparison to alternative survey methods (ProjectMax Ltd, 2006).

3.2 Damage analysis

I received official CCTV training with Project Max on 26 July 2017, with the professionally registered role being CCTV Reviewer. The training was based on the NZPIM, and covered the CCTV inspection procedure of gravity pipes and the identification, grading and reporting of pipe features and defects. Familiarity with the NZPIM is considered to be essential for professionals involved in CCTV operation, contract administration or pipe condition assessment.

First the pre-CES footage was reviewed, and the starting and finish manholes were recorded and the inspection date was noted. The manhole IDs are the access points and are used to check whether the inspection direction was upstream or downstream.

The recorded footage was viewed as the camera travelled from the starting manhole to the finishing manhole. When a construction feature, anomaly or damage item was observed by the original CCTV operator at the time of survey, they paused the camera and oriented it towards the target for a clearer view, and proceeded to rotate the camera to identify the extent of the damage. For example, if a faulty joint was suspected, the camera would rotate from where the damage was most visible and proceed slowly around the entire pipe joint to identify if the whole joint was damaged or whether the damage was localised.

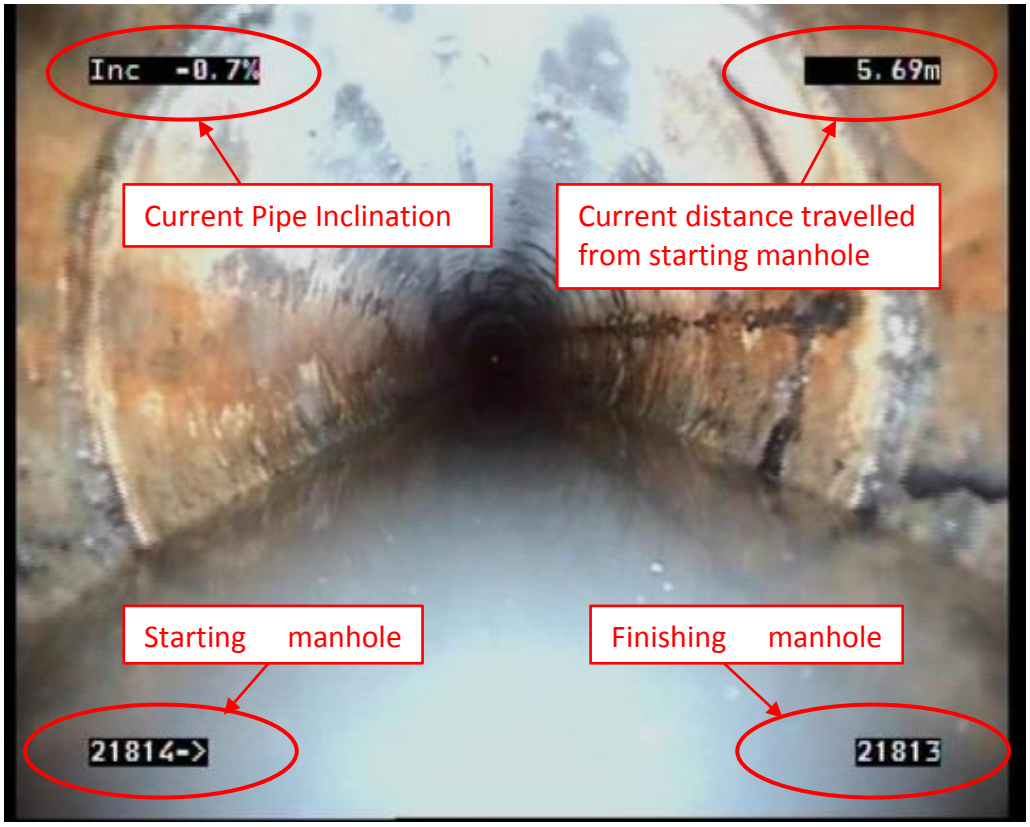

Figure 3-3. Typical screenshot of CCTV footage with on-screen information explained. The format and extent of the on-screen information varied between different contractors and often differed between pre-CES and post-CES footage.

For this research, the damage items were coded with two-letter abbreviations depending on damage type and assigned a severity code (refer to Table 2-8 and Table 2-9 for further information regarding the codes). The distance along the pipe where the damage was observed was written down, along with the standard 'clock' position from the 12 o'clock point.

The footage was inspected until either the finish manhole was reached, or no more footage was available due to the presence of water or other obstructions; the length of the final available footage was noted. The post-CES footage of the same pipe was then reviewed. If for any reason only partially complete footage was available due to a technical issue, the damage observations were only considered for analysis if footage existed at this location in both the pre- and post-CES CCTV footage. Damage observations in areas of incomplete footage were discarded from the analysis, but were included in the damage logs for completeness and reference purposes.

After the pipe footage was reviewed, the damage codes were classified as being structurally significant or insignificant. This was achieved using an evaluation table provided by the CCC (Table 3-2). The damage codes that are structurally significant are located at the top of the table. Depending on the nature of damage and its assigned severity (Small, Medium or Large), a score from 1 to 5 was assigned; the higher the score, the more urgency existed to address the damage item from an asset management perspective. For example, an IP score of either Medium or Large is given a score of 5, as it indicates the presence of a crack extending through the wall of the pipe. The colours in the table cells provide a quick visual indication of the score. The codes that are structurally or operationally insignificant are located near the bottom of the table and shaded in grey.

A pipe summary score was calculated for each pre- and post-CES CCTV inspection for each pipe. This value enabled ease of comparison between pre-CES and post-CES footage, where a high score following the CES indicates that the pipe has experienced damage. The summary score is given by the total sum of each damage item multiplied by its corresponding the severity score from Table 3-2.

Table 3-2. Damage code severity table (provided by the CCC)

Code	Definition	S	M	L	Code	Definition	S	M	L
IP	Infiltration Present	4	5	5	DE	Debris, Silty	NA	NA	NA
JD	Joint, Displaced	2	3	5	DG	Debris, Greasy	NA	NA	NA
PB	Pipe, Broken	3	4	5	PF	Deformed Plastic Pipe	NA	NA	NA
PH	Pipe, Holed	2	3	5	ED	Encrustation Deposits	NA	NA	NA
PL	Protective Lining Defective	2	3	5	OT	Obstruction, Temporary	NA	NA	NA
PX	Pipe, Collapsed	NA	NA	5	CF	Construction Feature	NA	NA	NA
RI	Root Intrusion	4	4	5	DC	Dimension Change	NA	NA	NA
TM	Tomo	NA	NA	5	GC	General Comment	NA	NA	NA
CM	Crack, Multiple	2	3	3	IA	Inspection Abandoned	NA	NA	NA
CC	Crack, Circumferential	1	3	3	IE	Inspection Ends	NA	NA	NA
CL	Crack, Longitudinal	1	3	3	IS	Inspection Start	NA	NA	NA
JF	Joint, Faulty	2	3	3	LB	Lateral Blank	NA	NA	NA
JO	Joint, Open	2	2	3	LC	Lining Change	NA	NA	NA
LF	Lateral, Sealing Faulty	2	3	3	LL	Line Deviates Left	NA	NA	NA
LX	Lateral, Problem	2	3	3	LR	Line Deviates Right	NA	NA	NA
LP	Lateral, Protruding	2	3	3	LD	Line Deviates Down	NA	NA	NA
DF	Deformed Pipe	NA	3	5	LU	Line Deviates Up	NA	NA	NA
PF	Deformed Plastic Pipe	2	3	3	LO	Lateral OK	NA	NA	NA
SD	Surface Damage	2	2	4	MC	Material Change	NA	NA	NA
OP	Obstruction, Permanent	2	2	4	DP	Dipped Pipe	NA	NA	NA

3.3 Assigning geospatial information to pipes

The following geospatial data were assigned to each pipe to enable interpretation of pipe damage:

- Pipe Locations (from CCC);
- Manhole locations (from CCC);
- Pipe damage locations and failure modes (this analysis);
- LiDAR-derived differential ground movements (New Zealand Geotechnical Database, 2012);
- Peak Ground Accelerations and Peak Ground Velocities (Bradley & Hughes, 2012).

The pipes were discretised into one metre segments along their length, where the distance along the pipe featuring a damage observation was rounded to the nearest metre. This was done in order to adjust for some minor discrepancies between the starting distances of the footage before and after the earthquakes so that the damage items could be spatially compared. The reason for the discrepancies was that the distance counter on the CCTV footage was not calibrated to a specific datum to represent the 0.0 m starting measurement, and the reported distances of repeat CCTV footage are often out of sync from one another by up to 1 metre in the worst observed cases. Therefore, to ensure that fixed location construction features, such as laterals, were aligned when comparing the pre- and post-CES footages, some distance rounding and adjustment was necessary.

The starting and finishing manholes for each pipe were chosen based on gradient and hence flow direction by gravity. For instances when the different CCTV surveys before and after the earthquake started from opposite manholes, the reporting distance was always chosen to be that from the starting manhole of the flow direction, so that both pre- and post-CES CCTV observations were spatially comparable when visually plotted. The manholes were also used to ensure consistency in starting and ending observations between pre- and post-CES records.

In order to distinguish between the pre- and post-CES observations, the pre-CES footage was plotted as squares while the post-CES footage was plotted as circles. The circles were chosen to be slightly smaller (size 5) than the squares (size 12) in order to allow both sets of observations to be visible when overlaid. Damage codes were also plotted adjacent to the location along the pipe for identification. The severity-based colour coding in Table 3-2 was adopted in the GIS software.

When more than one damage item existed at a single location, the damage item with the highest severity rating was plotted as only one item was visible at a time. This occurred frequently for certain damage codes such as IP (Infiltration Present) or ED (Encrustation Deposit), which are always accompanied by crack codes or joint damage codes due to the nature of the damage itself, as these items indicate complete penetrations in the pipe walls allowing external water to enter and cause gushing (IP) or rusting (ED).

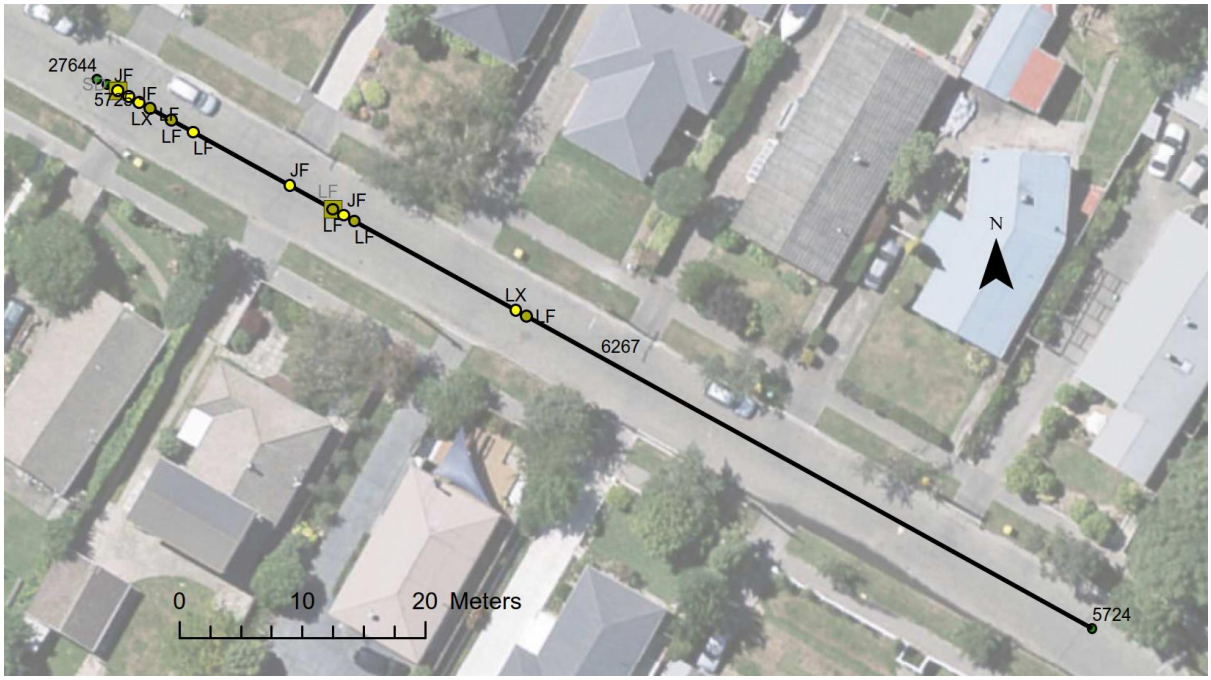

Figure 3-4. Typical pipe (Pipe ID 6267 shown) with damage observations mapped along the length of the pipe. World imagery map layer retrieved from Esri (2018). See Table 3-2 for explanation of damage codes.

Figure 3-4 shows an example pipe (ID 6267) with the pre- and post-CES damage observations colour-coded, labelled with NZPIM damage codes and distributed spatially along the length of the pipe between the manholes.

Because it is not possible to attribute specific damage observations to individual earthquakes within the 2010-2011 CES, and all post-CES CCTV observations were in any case conducted from early 2012, any CCTV damage observations attributable to earthquakes are impacts integrated over the entire CES period. Therefore the primary LiDAR ground deformation (vertical movement) data used here were for the period pre-4th September 2010 (2003) to post-23rd December 2011 (New Zealand Geotechnical Database, 2012). However, the spatial extent of these data does not cover all of Christchurch City. Where these vertical movement data were not available for particular pipes because they were located outside the spatial extent of combined LiDAR flight campaigns for the entire CES period, a second database was used that covered the period post-4th September 2010 (5th September 2010) to post-23rd December 2011 (New Zealand Geotechnical Database, 2012). Figure 3-5 and Figure 3-6 show the spatial extent of these databases.

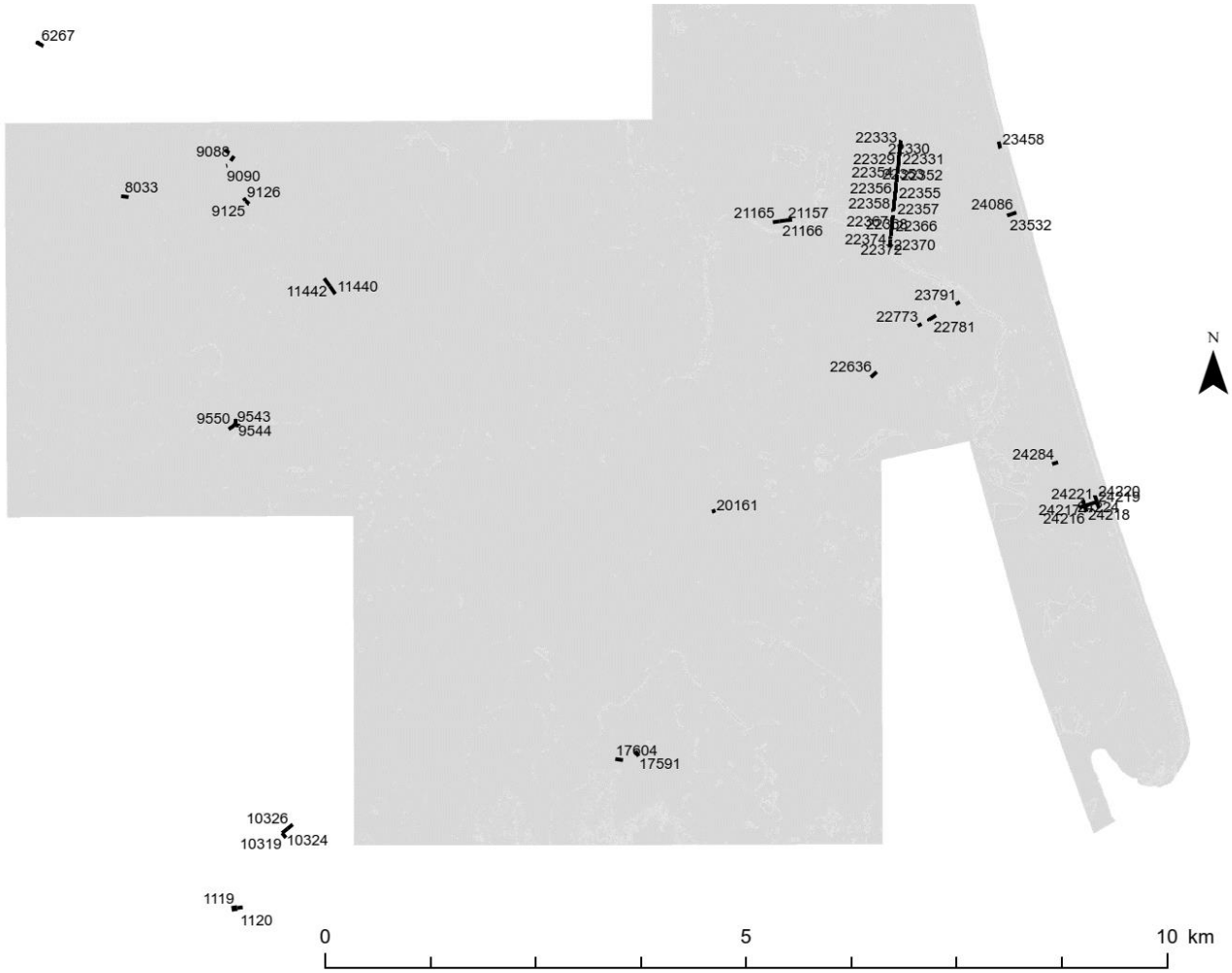

Figure 3-5. Pipe selection showing extent of Pre-2010 to Post Dec 2011 LiDAR data availability. LiDAR data retrieved from (New Zealand Geotechnical Database, 2012) "Vertical Ground Surface Movements", Map Layer CGD0600 - 23 July 2012, from https://www.nzgd.org.nz/

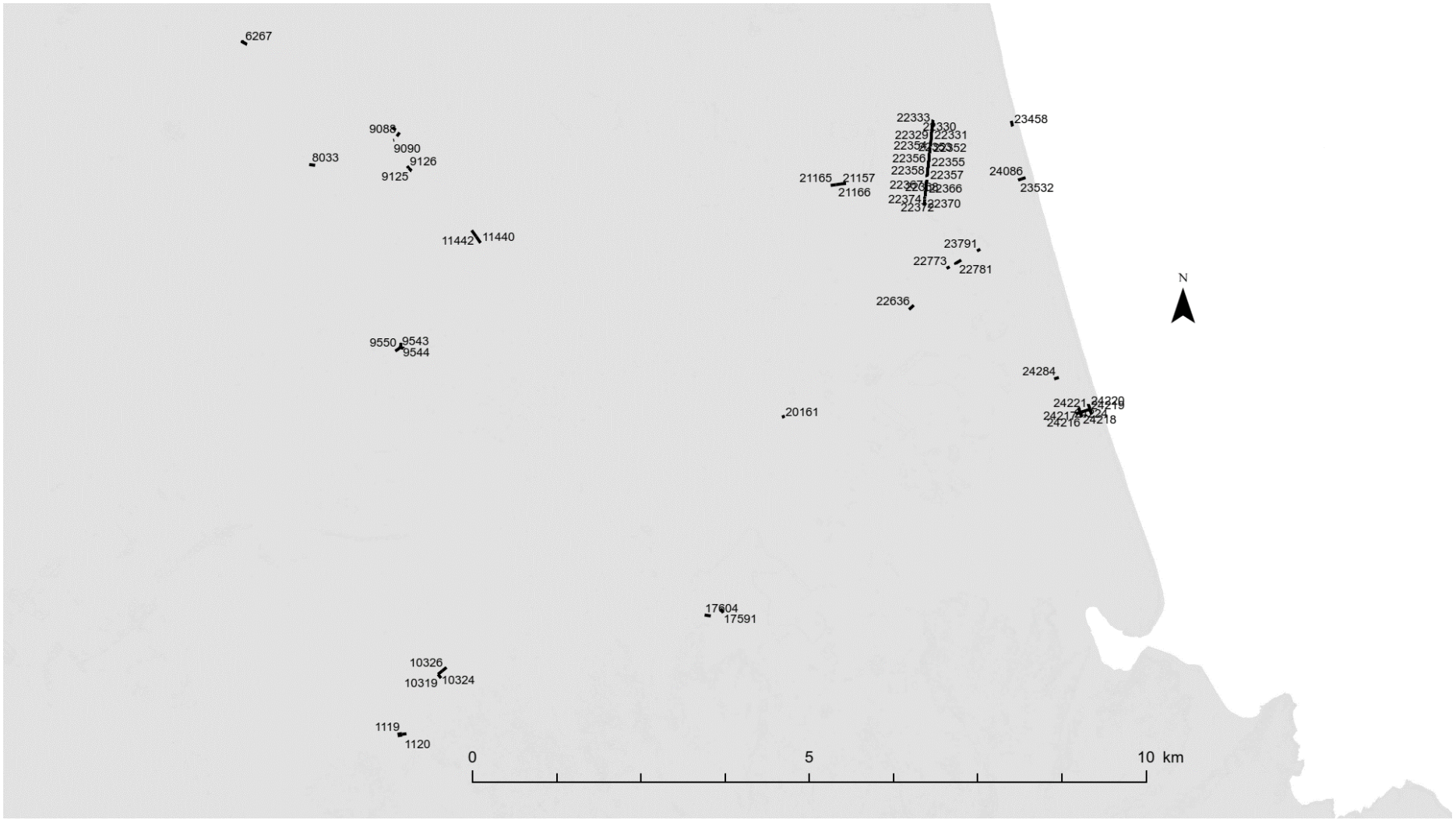

Figure 3-6. Final Pipe selection showing extent of Post-2010 to Post Feb 2011 LiDAR data availability. LiDAR data retrieved from (New Zealand Geotechnical Database, 2012) "Vertical Ground Surface Movements", Map Layer CGD0600 - 23 July 2012, from https://www.nzgd.org.nz

Using spatial analyst tools in GIS, differential ground movements were extracted to points at 1 metre intervals along the length of the pipe. In this instance, negative raster values indicate ground subsidence and positive raster values indicate uplift. The differential ground settlements were plotted along the axis of the pipe along with both pre and post-CES damage observations.

A summary of the analysis results using the method discussed in this section is presented in the following Chapter. Pipe damage observations are analysed and summaries compared regarding various pipe parameters.

Chapter 4 - Results and Discussion

This chapter presents the assessment results from the method outlined in Chapter 3. Working backwards from available evidence observed, relationships and insights were drawn regarding the broader topics discussed in the literature review in Chapter 2.

4.1 Pipe summary score

For each pipe, the number of observations were counted in both pre- and post-CES footage. Each individual observation was given a severity in accordance to Table 3-2 and the severities were tallied for all observations for both sets of footage to give a resultant score. The tallies are given below in Table 4-1, and the differences in number of observations and total score is also given. Positive changes indicate an increase in the number of damage observations and greater damage score level, which consequently means the overall severity of damage in the pipe has increased; the number represents the corresponding magnitude of increase.

Table 4-1 shows that for all but three of the pipes, the number of observations either increased or stayed the same following the CES. Also, all but one pipe resulted in an increase in the total damage score. This is a clear indication that the CES resulted in increased cumulative damage to the concrete gravity waste water pipelines. It is considered that the pipes with a decrease in the total damage score was a result of repairs which were undertaken between the pre-CES and post-CES surveys.

Table 4-1. Differences in number of damage observations and score between pre- and post- earthquake footage, listed in increasing diameter of pipe

Pipe No.	Diameter (mm)	No. of observations (pre-EQ)	Pre-EQ Score	No. of observations (post-EQ)	Post-EQ Score	Change in No. of observations	Change in Score
23532	150	1	3	4	9	3	6
8033	150	6	13	17	42	11	29
9082	150	5	12	7	17	2	5
9088	150	4	10	7	17	3	7
9090	150	3	7	4	9	1	2
9543	150	4	9	5	12	1	3
9544	150	9	24	9	24	0	0
9550	150	2	7	3	7	1	0
22636	150	2	4	32	109	30	105
17591	150	0	0	1	2	1	2
17604	150	4	10	11	27	7	17
24216	150	3	6	10	20	7	14
24217	150	4	8	12	30	8	22
24218	150	4	8	17	42	13	34
24219	150	0	0	3	6	3	6
24220	150	1	2	4	8	3	6
24221	150	3	6	7	15	4	9
24224	150	1	2	9	17	8	15
9125	150	3	7	19	52	16	45
9126	150	0	0	7	15	7	15
6267	150	2	4	15	39	13	35
22329	225	9	18	23	75	14	57
22330	225	9	19	9	23	0	4
22331	225	2	7	9	21	7	14
22333	225	5	10	12	29	7	19
22352	225	4	11	4	11	0	0
22353	225	3	6	7	17	4	11
22354	225	5	8	12	28	7	20
22355	225	3	5	7	21	4	16
22356	225	4	8	5	10	1	2
22357	225	3	7	4	11	1	4
22358	225	5	9	6	15	1	6
22366	225	6	11	4	12	-2	1
22367	225	3	6	7	19	4	13
22368	225	4	8	8	29	4	21
22370	225	10	19	9	25	-1	6
22374	225	5	13	9	25	4	12
24086	225	0	0	2	7	2	7
23458	225	0	0	2	4	2	4
20161	225	1	2	5	10	4	8
22372	250	5	14	11	25	6	11
24284	375	1	2	2	5	1	3
22773	450	2	4	12	26	10	22
22781	450	9	31	13	41	4	10
23791	450	0	0	0	0	0	0
10319	450	5	10	8	14	3	4
10324	450	1	2	6	12	5	10
10326	450	4	8	6	11	2	3
1119	450	2	4	6	15	4	11
1120	450	3	6	3	7	0	1
21157	450	1	2	13	34	12	32
21165	450	0	0	8	21	8	21
21166	450	3	7	8	20	5	13
11440	900	1	3	4	12	3	9
11442	900	5	15	3	11	-2	-4

4.2 Damage type observations

The most common types of damage observed are presented in this section. For definitions of the defect codes refer to Table 2-8.

Figure 4-1 presents the pre-CES defect codes in order of observation frequency. Surface Damage (SD) was the most common observation, and was more than three times the frequency of the next most frequent damage type observed (defect in the lateral pipes). Surface damage is one of the most obvious examples of chemical and biological deterioration discussed in section 2.3.1 in accordance with the NZPIM (ProjectMax Ltd, 2006), and therefore this result is in line with expectations as most pre-CES damage is considered to be the result of deterioration. The pre-CES damage may also be attributed to disturbances from above ground construction and traffic over the years as presented in section 2.3.4.

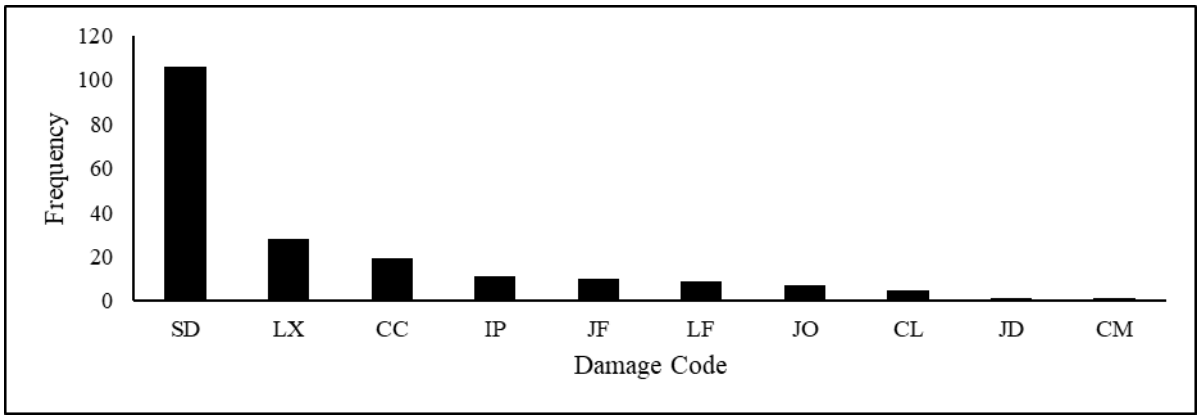

Figure 4-1. Pre-CES damage code in order of observation frequency

Figure 4-2 presents the post-CES defect codes in order of observation frequency. Surface Damage (SD) was again the most common type of observation, however all other damage types are much more frequent, especially damage to the main pipe joints and lateral joints such as LX, JF and LF. This agrees with assessment outcomes by O'Reilly et al. (1989; Section 2.3.2) in which joints were generally more vulnerable to damage than the pipe body.

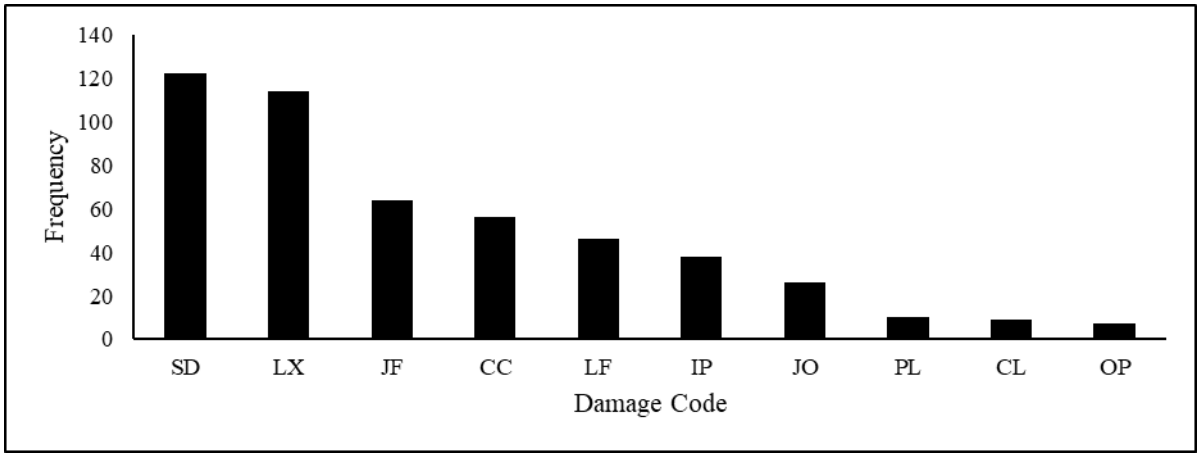

Figure 4-2. Post-CES damage code in order of observation frequency

4.3 Potential influence of ground deformation on pipe damage

For each of the 55 pipes included in Table 4-1, a detailed pipe damage map was produced that included the damage along the distance of the pipe both pre- and post-CES, compared against the LiDAR-derived vertical ground movements obtained from the New Zealand Geotechnical Database (2012).

For the damage observations, the X-axis indicates the distance along the pipe from the designated "starting" manhole to the "finish" manhole. The Y-axis of the upper chart indicates the magnitude of differential ground movement recorded in metres. For each observation the corresponding NZPIM damage code is shown at the same distance along the pipe in the lower chart. The colour coding indicates damage severity in accordance with Table 3 2. Pre-CES results are shown as squares and post-CES results are shown as circles, as previously mentioned. Where applicable the vertical black line shows the distance along the pipe up to which footage was available for both the pre- and post-CES CCTV footage; no observations were recorded after the vertical black line.

The full results for pipe damage maps and transects are presented in Appendix B. Certain damage observations frequently occurred at locations of obvious differential settlement, as highlighted by the yellow bars in Figure 4-3 below. Multiple points of differential ground movement (up to 0.2 m) were recorded to the ground surface for this pipe. At many of

these locations damage items such as lateral pipe failures, infiltrations and broken segments were identified.

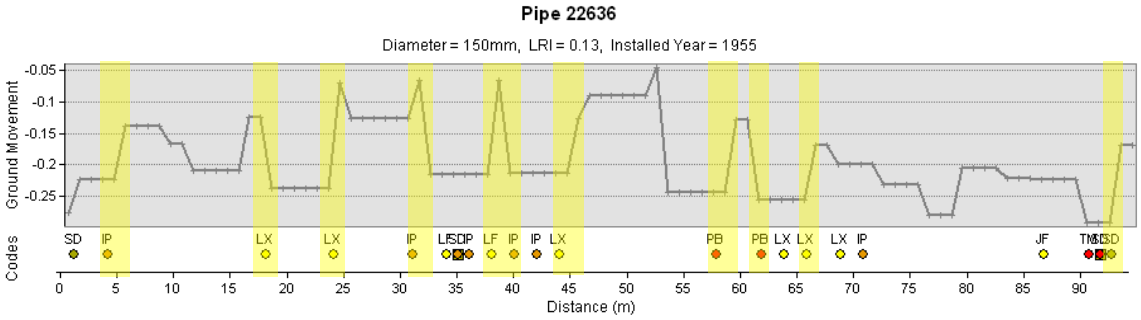

Figure 4-3. Damage observations for pipe 22636

To further illustrate this the apparent coincidence of differential ground movement and damage locations, another example (pipe 6267) is presented in Figure 4-4. Similar to the previous example, damage corresponded to areas of high differential ground movement. In this case the observations were lateral pipe failures and joint failures.

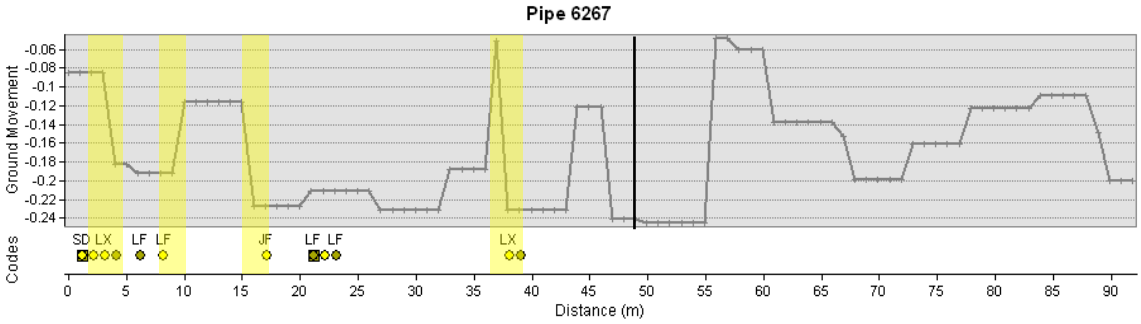

Figure 4-4. Damage observation for pipe 6267

Qualitatively, the differential ground deformations align with a high frequency of post-CES damage in certain pipes. However, for the whole sample set the differential ground deformation did not necessarily predict increased damage occurring at these points. It is suggested that damage frequency in relation to ground deformation could be more pronounced with a larger sample set, and a more systematic and rigorous method of associating damage with ground deformation should be developed.

Due to this approach of visually plotting ground deformation inflection points to corresponding damage at a particular location, continuous damage (such as continuous surface damage of the pipe walls) could not be effectively represented, and therefore the

extent and severity of certain damage types such as continuous CL (longitudinal cracking) or SD (surface damage) may be currently under-represented.

The LiDAR survey also features multiple sources of error resulting from data collection to interpolation as discussed in 2.4.2. This is also likely to have an impact on ground deformation measurement accuracy.

4.4 Influence of Pipe Dimensions

Figure 4-5 and Figure 4-6, respectively, show the change in number of observations and total damage score when compared with pipe diameter. The results are also averaged and summarised in Table 4-2 for the major pipe diameter groups.

Table 4-2. Damage observation summary with respect to diameter

Diameter (mm)	Number of pipes	Average pre-EQ no. of damage observations	Average pre-EQ score	Average change in number of damage observations	Average change in score
150	21	2.9	6.8	6.8	18.0
225	19	4.3	8.8	8.8	11.8
250	1	5.0	14.0	6.0	11.0
375	1	1.0	2.0	1.0	3.0
450	11	2.7	6.7	4.8	11.5
900	2	3.0	9.0	0.5	2.5

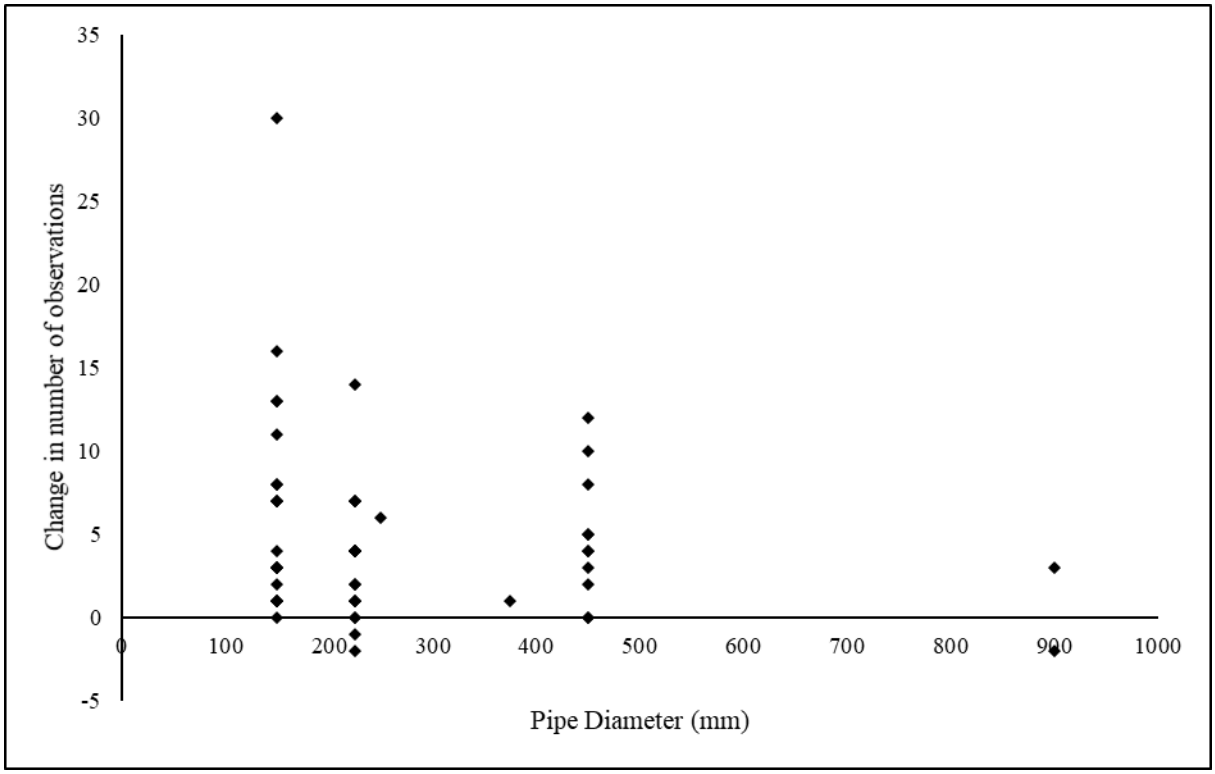

Figure 4-5. Change in the number of observations post-CES, plotted according to diameter

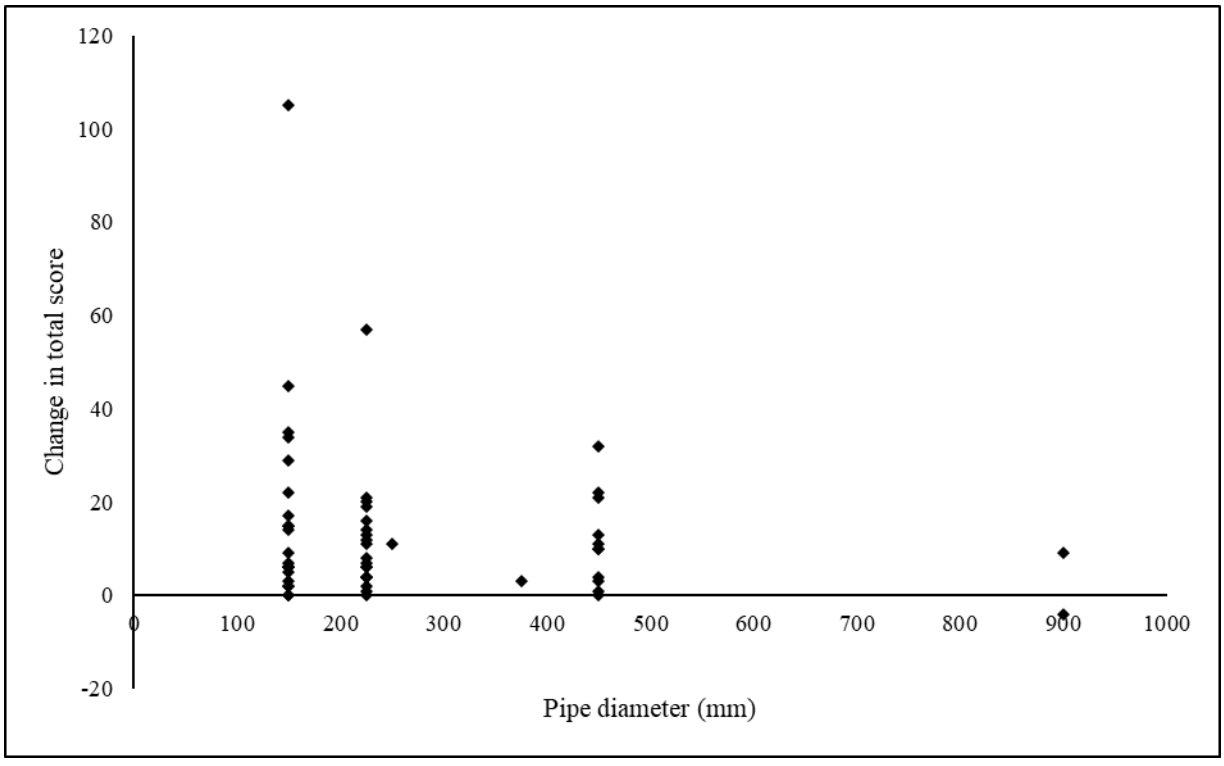

Figure 4-6. Change in total score post-CES, plotted according to diameter

From the results, smaller pipes appeared to exhibit more earthquake-related damage compared to larger ones. This is likely due to increased wall thickness and quantity of steel

reinforcing in larger-diameter pipes, which increases flexural and shear strength as mentioned by Wong and Nehdi (2018) as presented in section 2.3.6.

The pipe diameter range available for this study covers all three pipe fabrication methods mentioned in section 2.3.2, and it cannot be confirmed with certainty which fabrication method was used for any given pipe. However, one can infer that the Vibration Technology method was probably not represented in this study, as it was introduced very recently and primarily reserved for diameters larger than 675 mm. The other two methods (centrifugal spun and roller suspension) have overlapping diameter ranges and timeframes, and thus were equally likely to have been implemented and cannot be compared with regards to pipe performance.

Some diameter classes in this study could not be properly represented. For example, there is only one pipe in each of the 225 mm and 375 mm diameter classes, and two pipes in total in the 900 mm diameter class. Therefore, further research is recommended using a larger sample set so that each diameter class is properly represented in order to understand the relationship between pipe dimensions and earthquake performance.

4.5 Influence of deterioration

For many pipes, a significant level of damage existed prior to the CES. This is likely attributable to chemical and biological deterioration processes discussed in Section 2.3.1.

To determine if damage due to deterioration prior to the CES had any effect on the damage attributed to the CES, existing damage prior to the CES was compared with the total change in number of observations and scores. These are presented in the following tables.

Table 4-3. Change in the number of damage observations post-CES with respect to number of damage observations pre-CES

Average pre-EQ no. of damage observations	Number of pipes	Average change in number of damage observations
0 to 1	15	4.1
2 to 3	16	6.9
4 to 5	17	3.9
6 to 7	2	4.5
8 to 9	4	4.5
10+	1	-1.0*

*This suggests that repair works were undertaken

Table 4-4. Change in total score post-CES, with respect to pre-CES total score

Average pre-EQ score	Number of pipes	Average change in score
0 to 4	19	16.7
5 to 9	20	12.7
10 to 14	10	10.5
15 to 19	4	15.8
20 to 24	1	0.0
25+	1	10.0

No relationships were identified between the level of damage due to deterioration with damage increase following the CES. This may that the level of pre-CES deterioration in reinforced concrete pipes had no effect on earthquake performance. However, a larger sample set will need to be assessed before any firm conclusions can be drawn.

4.6 Influence of year of installation

The year of installation is a potential influence on the damage observations. Figure 4-7 and Figure 4-8 show the total pre-CES number of observations and damage score, respectively, plotted against the original year of installation. The net change in number of observations and damage score through the earthquake sequences are also plotted in Figure 4-9 and Figure 4-10 respectively. The figures show that most pipes were constructed between 1950 and 1960, and only three other pipes were constructed outside this category in 1991, which is 31 years later.

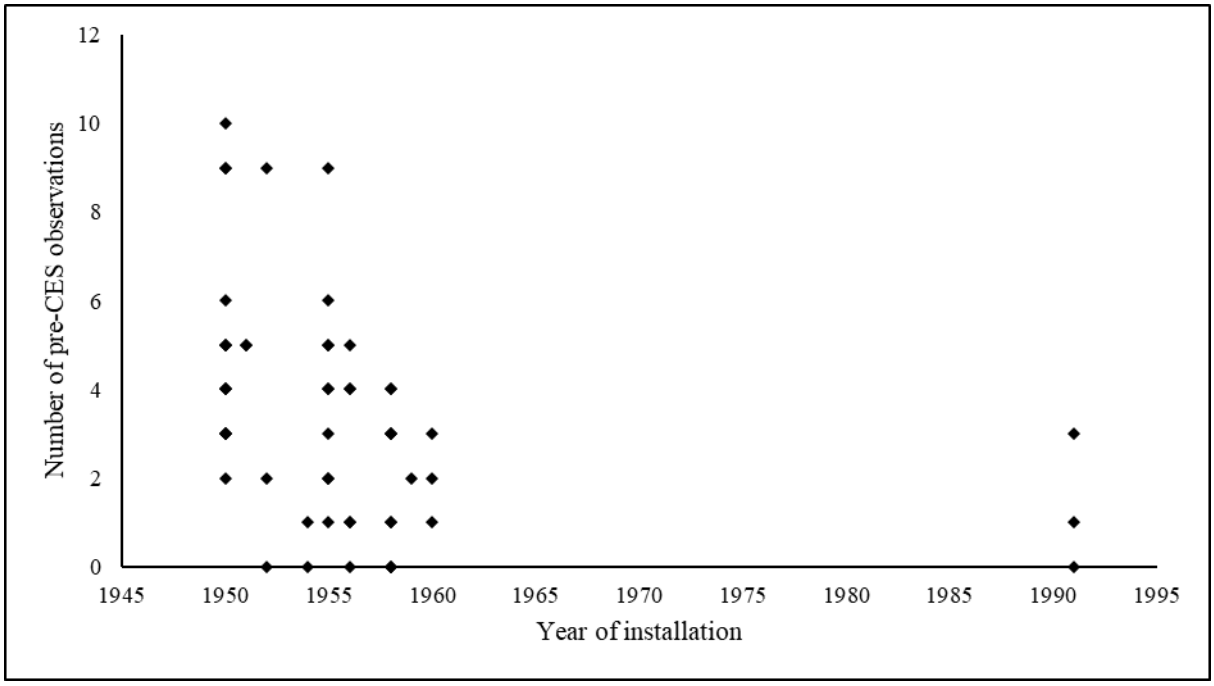

Figure 4-7. No. of pre-CES observations and year of installation

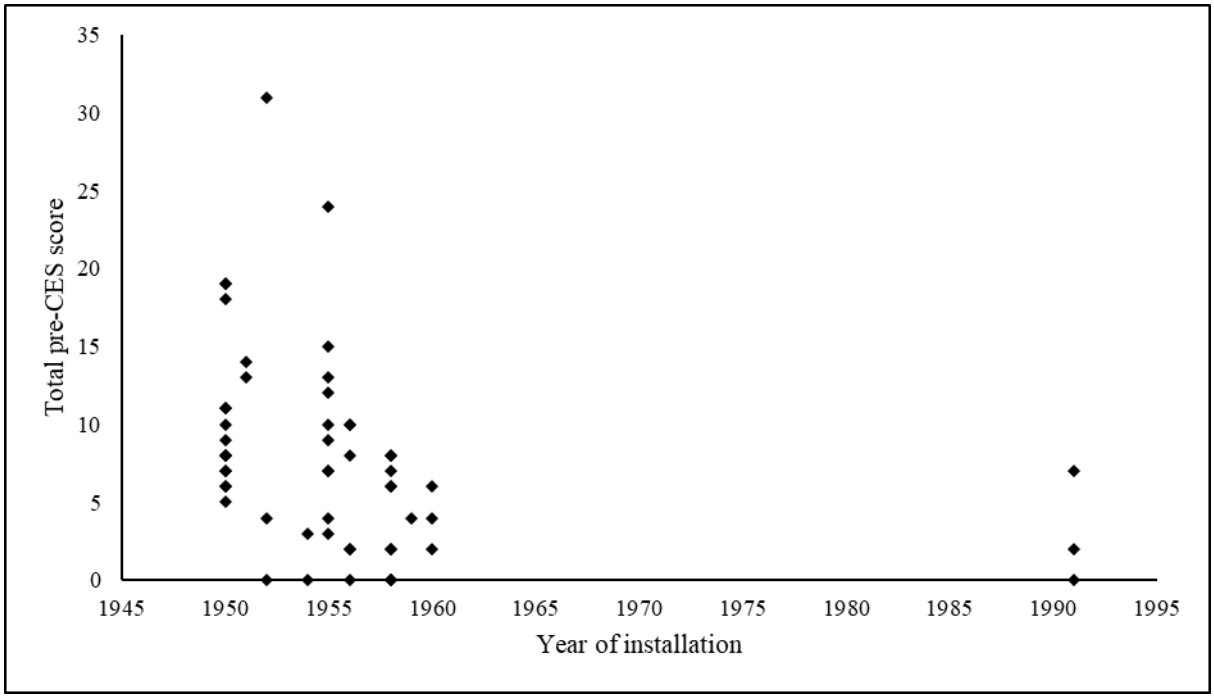

Figure 4-8. Total pre-CES score and year of installation

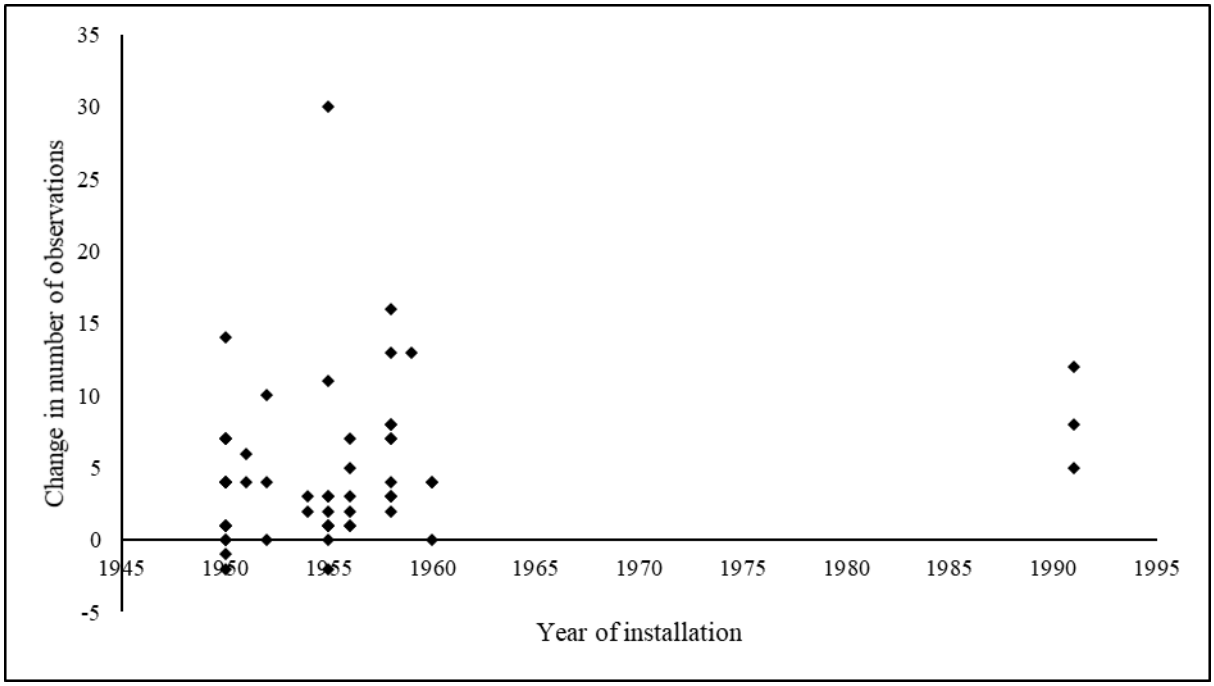

Figure 4-9. Change in the number of observations post-CES, plotted according to year of installation

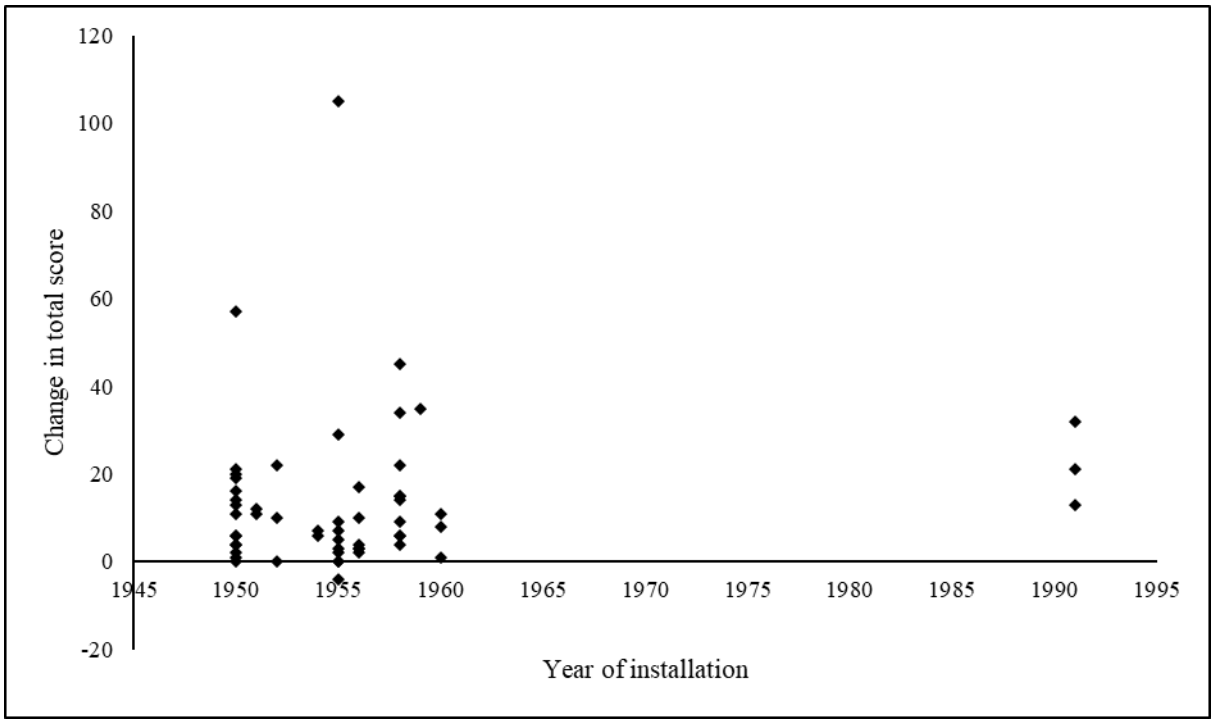

Figure 4-10. Change in total score post-CES, plotted according to year of installation

Design standards governing pipe specifications varied depending on year of installation, as discussed in Section 2.1.1, therefore the pipes have been classified in accordance with the

applicable buried pipe standard and concrete pipe standard. The applicable buried pipe standards are presented in Table 4-5.

Table 4-5. Damage observation summary with respect to applicable buried pipe standard

Applicable buried pipe Standard	Year Installed	Number of pipes	Average pre-EQ no. of damage observations	Average pre-EQ score	Average change in number of damage observations	Average change in score
Australian Standard A35:1937	1937-1956	38	3.8	8.3	4.2	12.2
Australian Standard A35:1957	1957-1974	14	2.6	6.6	6.8	18.5
NZS 4451:1974	1974-1989	0	NA	NA	NA	NA
AS/NZS 3725:1989	1989-2007	3	1.7	3.3	4.3	9.0
AS/NZS 3725:2007	2007-Present	0	N/A	N/A	N/A	N/A

It appears that all but three of the pipes were designed to A35:1937 and A35:1957. Therefore, most pipes in the study were expected to have been designed using the 'indirect method', which is based on Spangler's (1933) bedding configurations and described in Section 2.1.1. The pipes installed prior to 1957 were all assumed to be designed to strength Class X, however there is a probability that some of the pipes constructed after 1957 were designed to the stronger Classes Y and Z, which were additions to A35:1957. This cannot be confirmed and therefore its effect cannot be gauged in this study.

The other three pipes selected which were constructed in 1991 were assumed to be designed to AS/NZS 3725:1989, which has incorporated the findings from SPIDA and the 'direct method'. This could indicate that these pipes were designed using a different methodology than the others, however this is not necessarily the case because Spangler's bedding configurations were widely used until the 1990s. Nevertheless, the three newer pipes show a smaller average change in score through the CES compared to the earliest pipes, which may indicate the advantages of the 'direct method' compared to the 'indirect method' for earthquake performance. Given the regional differences in backfill method as per Table 2-6 it is also likely that the three newest pipes were specified with AP20 or AP40

backfills while the older pipes were backfilled with native soils, however this could not be confirmed.

The pipes have also been classified in accordance with the applicable concrete pipe standard. This is presented in Table 4-6 below.

Table 4-6. Damage observation summary with respect to applicable concrete pipe standard

Applicable Concrete Pipe Standard	Year Installed	Number of pipes	Average pre-EQ no. of damage observations	Average pre-EQ score	Average change in number of damage observations	Average change in score
Australian Standard A35:1937	1937-1956	38	3.8	8.3	4.2	12.2
Australian Standard A35:1957	1957-1977	14	2.6	6.6	6.8	18.5
NZS 3107:1978	1978-1991	3	1.7	3.3	4.3	9.0
AS/NZS 4058:1992	1992-2006	0	N/A	N/A	N/A	N/A
AS/NZS 4058:2007	2007-Present	0	N/A	N/A	N/A	N/A

For most pipes, the concrete pipe standard was synonymous with the buried pipe standard, with the exception of the three pipes constructed in 1991, which were most likely designed to NZS3107:1978. The water tightness specification changed for NZS3107:1978 which affected the three 1991 pipes, therefore their water tightness performance is considered to be marginally improved compared to the older pipes (10 m compared to 9.1 m for the latter).

Table 4-5 and Table 4-6 show that pipes installed to older standards have a higher average number of pre-CES damage observations and scores compared to newer pipes, suggesting more deterioration has occurred, which is in line with expectations and existing literature on deterioration, such as the research from O'Reilly et al. (1989) presented in section 2.3.5. Newer pipes have also been subject to less time for the chemical and biological processes outlined in Section 2.3.1 to occur, while also benefitting from improved concrete mix designs in later design standards due to overseas innovations discussed in Section 2.1.1.

As the concrete mix specification for each pipe was not available, the mix parameters, such as chloride and sulphate content, aggregate type and size, cannot be associated with pipe performance as these parameters have overlapping acceptable ranges between the standards.

As with other performance interpretations presented above, it is expected that with a larger sample pool these results would become more pronounced and the relationships more evident.

4.7 Influence of liquefaction

The susceptibility of soils to liquefaction-induced ground deformation has been demonstrated to influence broader network performance, as reported by O'Rourke et al. (2014) and Cubrinovski et al. (2014).

Detailed soil or backfill descriptions for each pipe were not obtainable. However, the backfill specifications are assumed to have been specified in accordance to Table 2-6. The best indication of surrounding soil response conditions in this study is considered to be the liquefaction zone as defined in Section 2.4.1.2.

The following figures show the change in number of observations and total score when compared against the LRI zone in which the pipe is located. The results are also averaged and summarised in Table 4-7 for the major LRI zone groups.

Table 4-7. Damage observation summary with respect to liquefaction zone

Liquefaction Zone	Number of pipes	Average pre-EQ no. of damage observations	Average pre-EQ score	Average change in number of damage observations	Average change in score
0	6	3.0	8.8	5.5	14.7
1	16	5.0	10.4	3.6	12.8
2	6	2.7	7.2	8.2	24.8
3	27	2.6	5.7	4.7	11.3

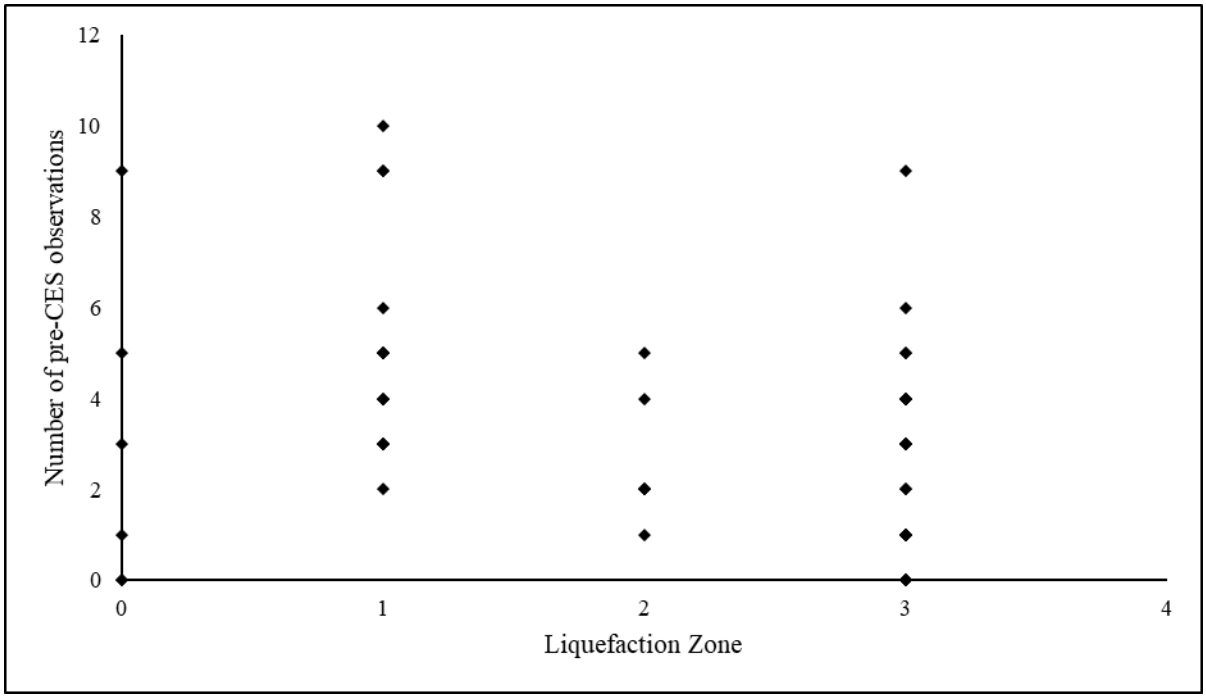

Figure 4-11. Number of pre-CES observations and LRI Zone

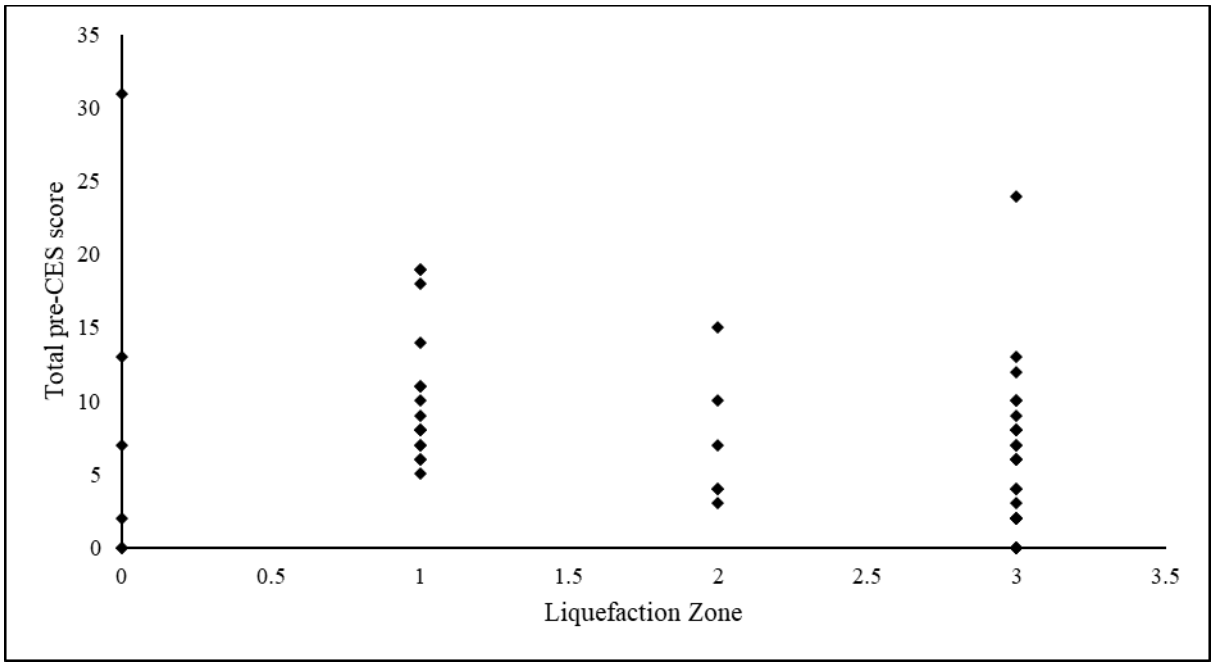

Figure 4-12. Total pre-CES score and year of installation

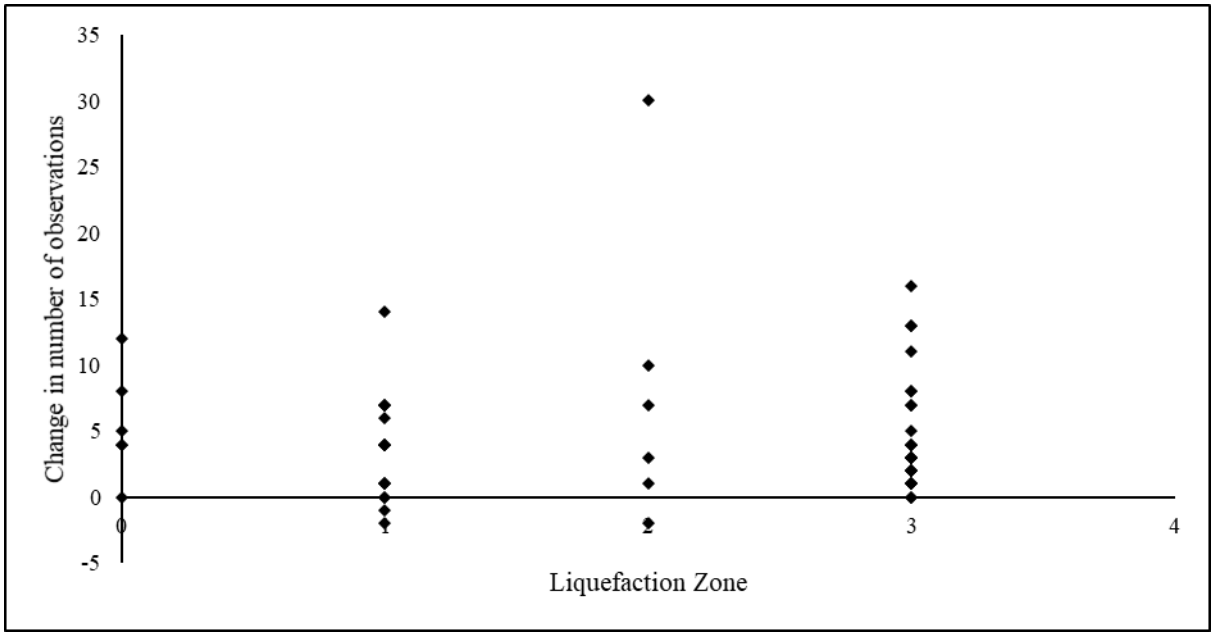

Figure 4-13. Change in the number of observations post-CES, plotted according to liquefaction zone

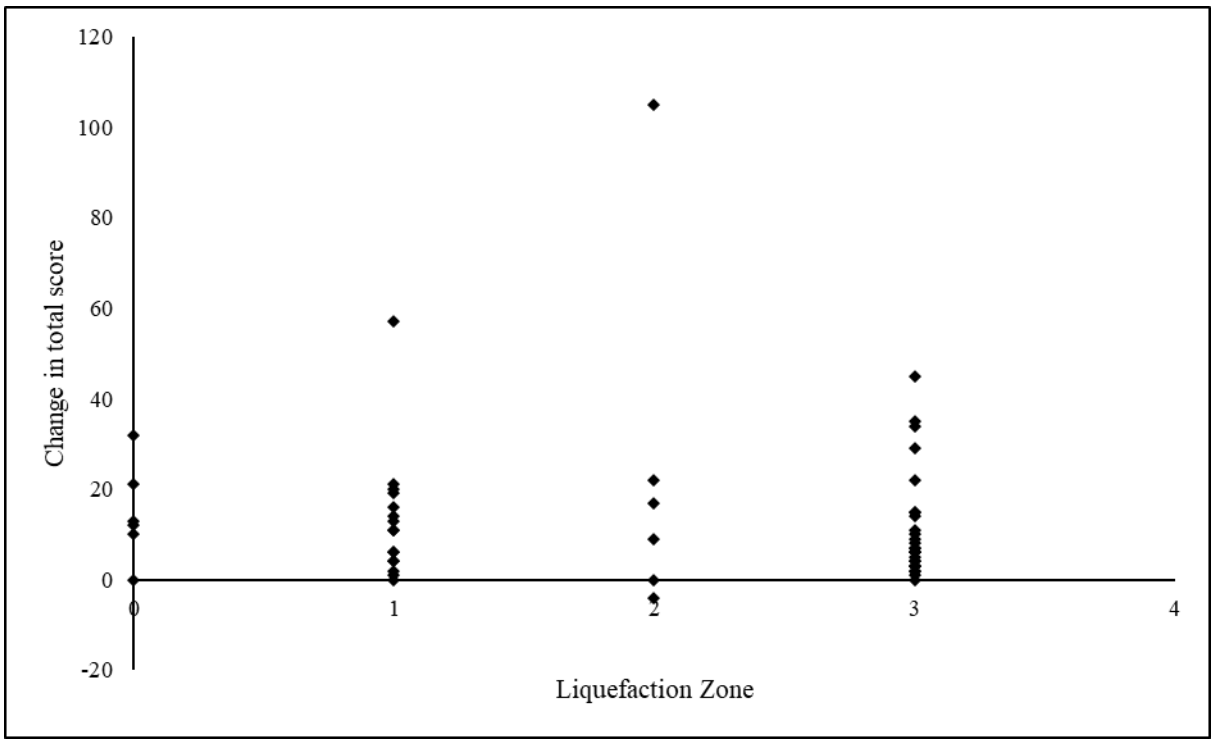

Figure 4-14. Change in total score post-CES, plotted according to liquefaction zone

From the results, there is no clear trend in damage with LRI zone; all LRI zones have overlapping ranges of increase in scores. This does not align with previous studies by Cubrinovski et al. (2014). However, LRI zones are only general categories developed during the CES itself to guide designers in their thinking on more resilient system design, and were

not intended to capture or predict high-resolution ground movements. As evidenced by the limitations of LiDAR data discussed in section 2.4.2, there is significant spatial heterogeneity on ground deformation within each LRI zone. The sample size for certain liquefaction zones such as 0 and 2 are also very low (6 pipes in each zone), therefore it is expected that a larger sample size would result in clearer relationships for liquefaction zone.

4.8 Influence of seismic ground motions

Seismic ground motions are considered to affect the performance of the pipes directly, as discussed in Section 2.4.1.1. This section presents the estimated PGA and PGV values from Bradley and Hughes (2012) with the change in number of damage observations and damage scores.

As no CCTV observations were undertaken immediately subsequent to each major CES event, specific damage observations were unable to be associated with specific earthquakes. However, if we assume that the maximum estimated PGA and PGV values across the major earthquake events are the primary causative factor influencing observed damage in the post-CES CCTV inspections, then we can check for relationships between pipe performance and ground motions. The maximum estimated PGA and PGV values are summarised below in Table 4-8 and Table 4-9, respectively, and compared with the average change in damage observation number and score.

Table 4-8. Damage observation summary with respect to maximum probable peak ground accelerations

Maximum PGA (g)	Number of datapoints	Average change in number of damage observations	Average change in score
0.0-0.2	0	N/A	N/A
0.2-0.4	15	5.4	14.1
0.4-0.6	29	4.3	13.8
>0.6	11	5.4	12.4

Table 4-9. Damage observation summary with respect to maximum probable peak ground velocity

Maximum PGV (cm s^{-1})	Number of datapoints	Average change in number of damage observations	Average change in score
0-20	0	NA	NA
20-40	7	7.6	19.7
40-60	33	3.5	10.7
>60	15	6.4	17.1

Figure 4-15 and Figure 4-16 show the maximum estimated PGA plotted against change in number of observations and damage score, respectively, for each individual pipe. *Figure* 4-17 and Figure 4-18 show equivalent plots for maximum estimated PGV.

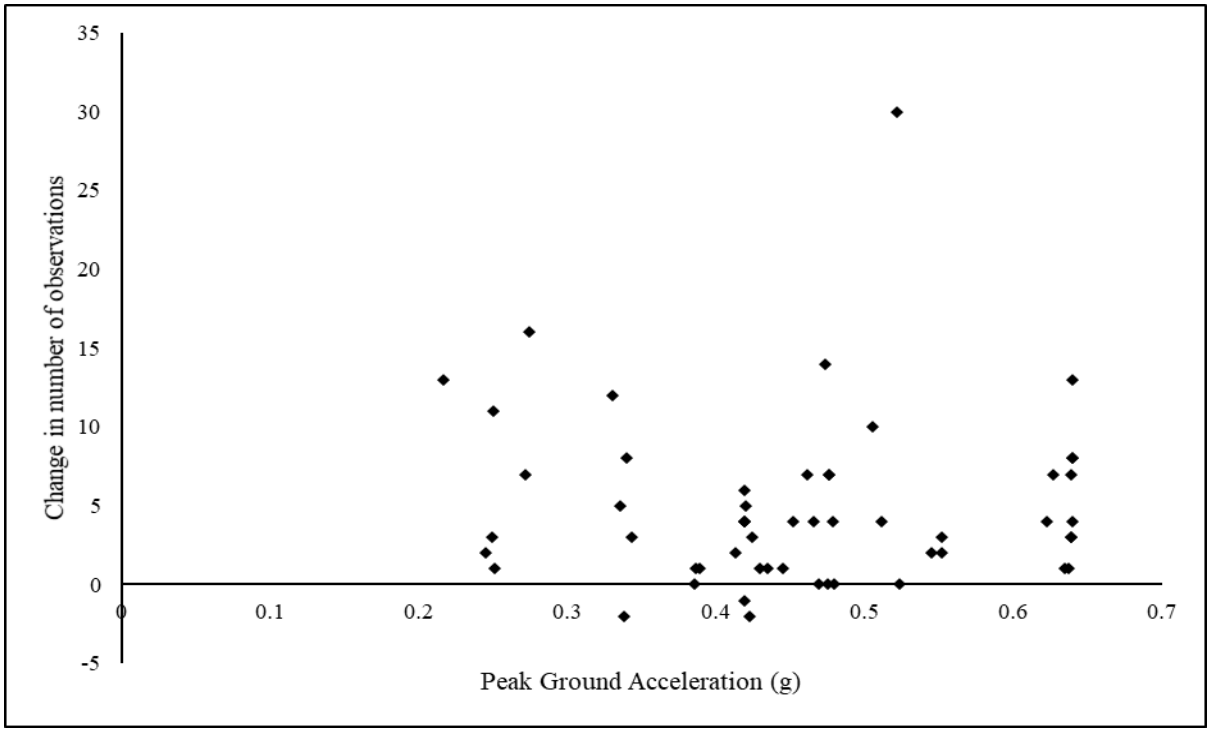

Figure 4-15. Change in number of observations and max PGA through the CES

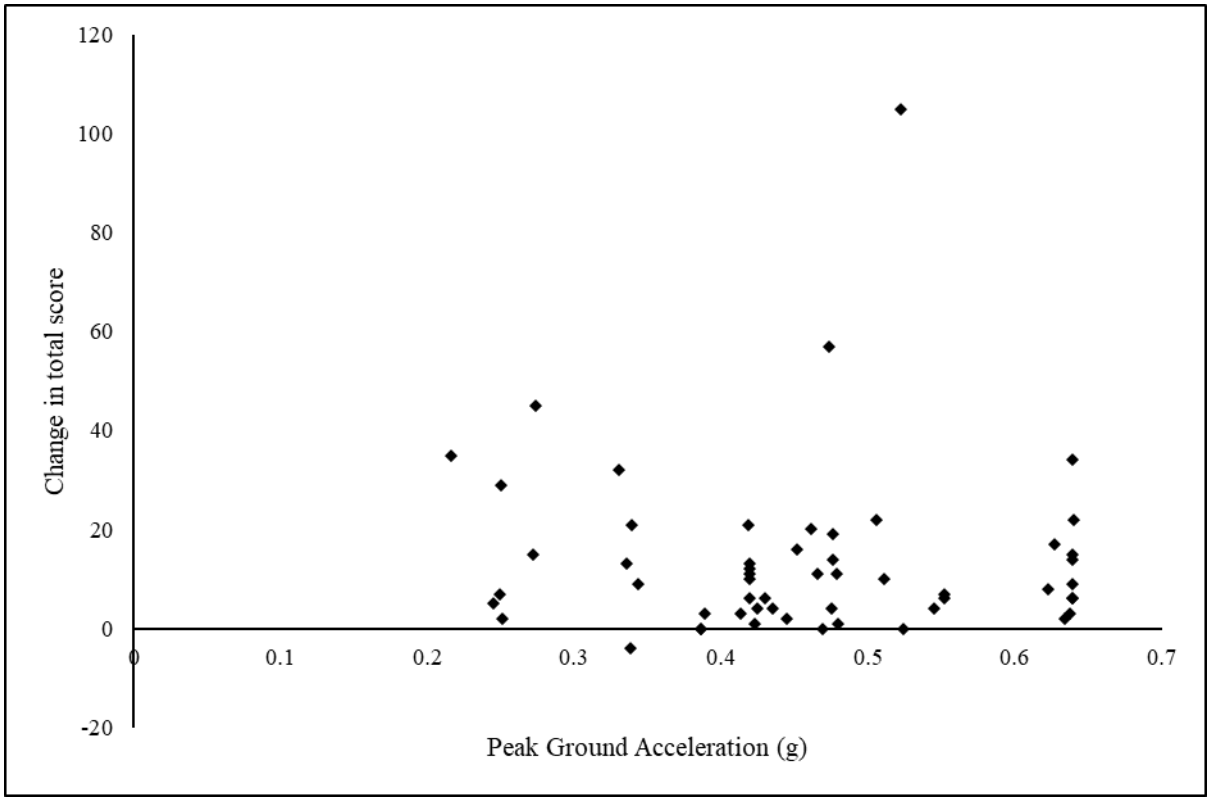

Figure 4-16. Change in total score and Peak Ground Acceleration through the CES

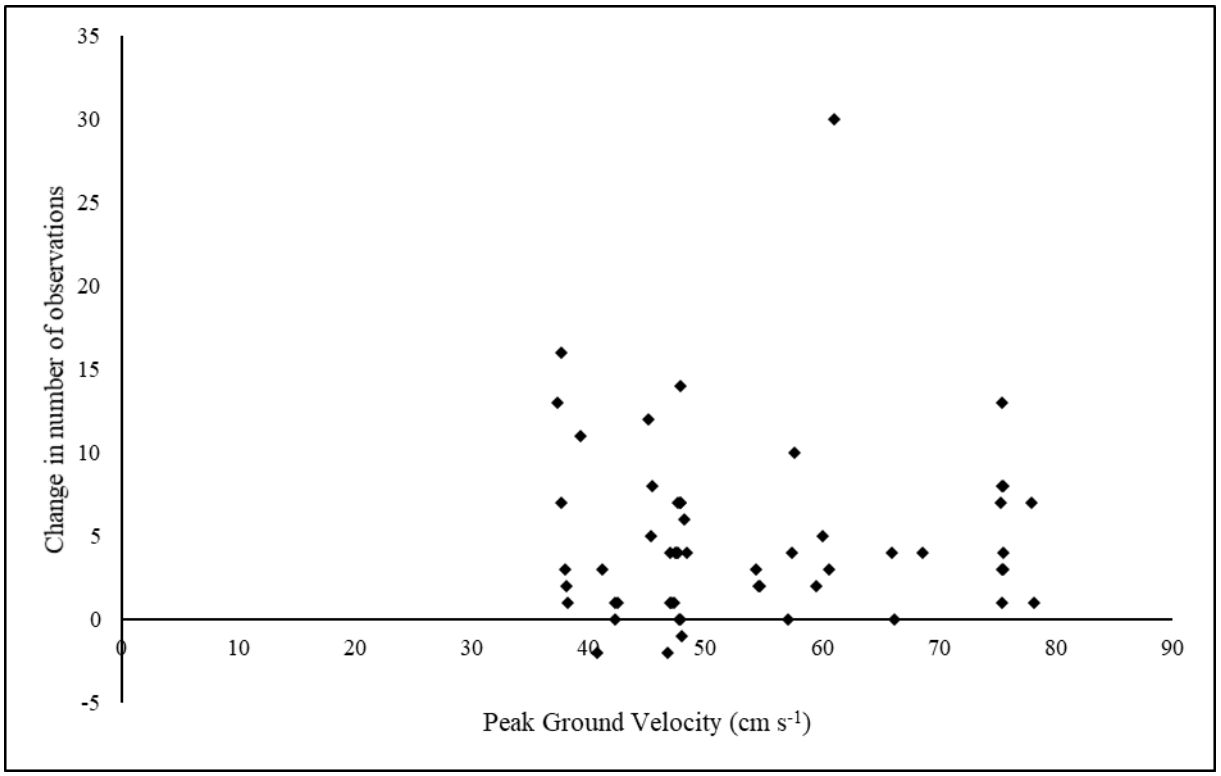

Figure 4-17. Change in number of observations and Maximum PGV through the CES

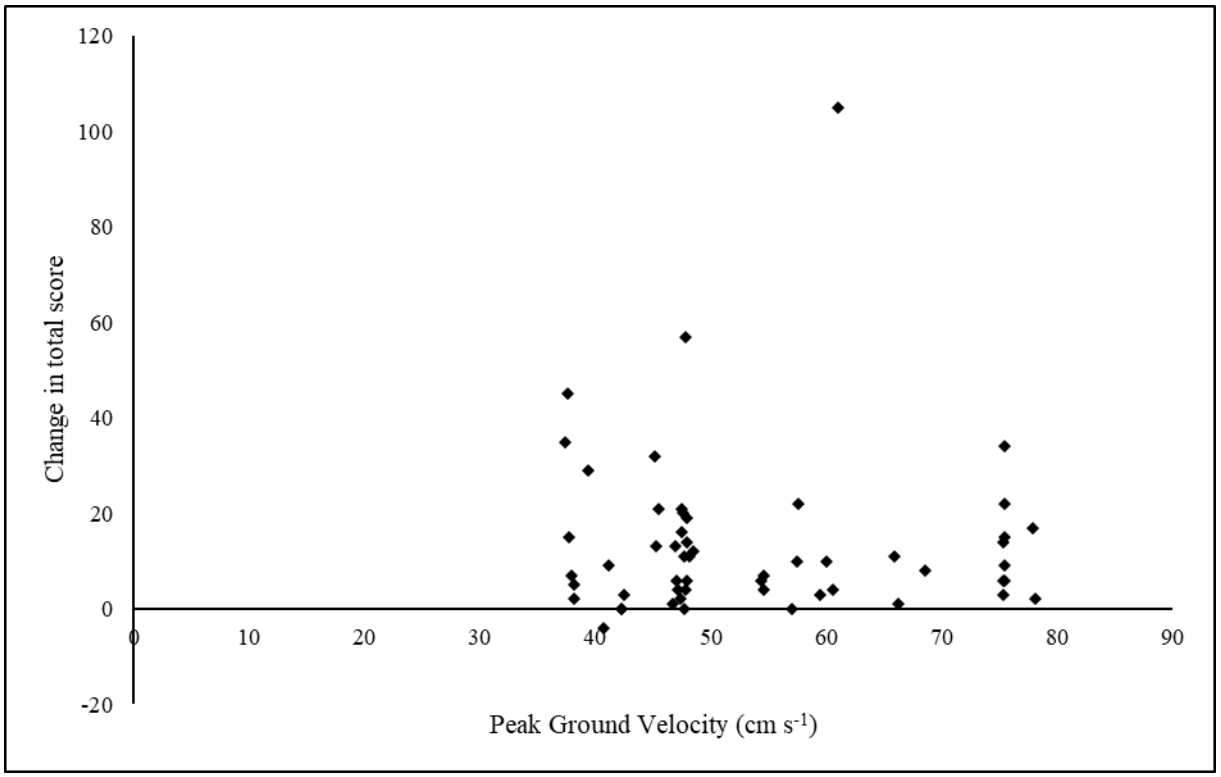

Figure 4-18. Change in total damage score and PGV through the CES

From the results, there is no clear trend in damage with PGA or PGV. For a given value of PGA or PGV, pipes can undergo either very small or large increases in damage score. An explanation for this may be that these parameters are calculated as probability distributions constrained by the actual measurements from accelerometers and strong motion stations, as outlined in Section 2.4.1.1, hence the accuracy of prediction is reduced with increasing distance from these instruments as stated by Bradley and Hughes (2012). With a sample size of only 55 pipes, where many are located at a considerable distance from instruments shown in GeoNet's continuous GNSS network in Figure 2-10, the accuracy may be limited in this case. In addition, seismic force exerted on the pipe is not only a function of the ground motion, but also the transient local soil characteristics and displacements, which have their own inherent uncertainties (Refer to Section 2.4.1). Further research is recommended using a larger sample set to understand the relationship between ground motions and earthquake performance of pipes.

4.9 Method Limitations

4.9.1 CCTV Limitations

The CCTV damage assessment method has inherent limitations in the scope and accuracy of data which it is able to collect. These limitations were outlined in Section 2.5.1. The intention of the CCTV survey is for qualitative decision-making purposes for local councils; hence defects observed this way are not readily amenable to being quantified nor measured. Likewise, the NZPIM rating system of Small (S), Medium (M) and Large (L) to indicate severity is mainly intended for high-level repair pricing purposes (ProjectMax Ltd, 2006).

In this research one observer (Y. Tang) was responsible for interpretation of all CCTV footage. In this way all footage would have been interpreted equivalently, avoiding the error resulting from differences in subjective opinion from multiple assessors. However, until an assessment method exists which can more rigorously quantify the damage observed, CCTV footage interpretation is relatively subjective regarding the classification and severity of a damage item, as the sole method to determine this is visually on screen. Further, the footage was recorded by a variety of other camera operators, and there was no quality

control in the rigour with which the original footage was captured (see Section 4.9.2 below). For some sections of the pipes inspected, the quality of the video footage was questionable at best. Some of the older CCTV inspections were also more prone to motion blur and had reduced clarity at low light levels. The cleanliness of the pipe was also influential in the interpretation of the results, as well as the level of flow during the inspection. Pipes which were covered with silty debris or fat deposits may hide cracks underneath.

As all CCTV footage is retrieved from the pipe interior, it is not possible to determine information beyond the inside wall of the pipe, such as whether a crack extends through the thickness of the wall. Therefore, the actual severity of cracks and joint damage could not be directly observed, but needed to be inferred from secondary effects such as the presence of infiltration or staining.

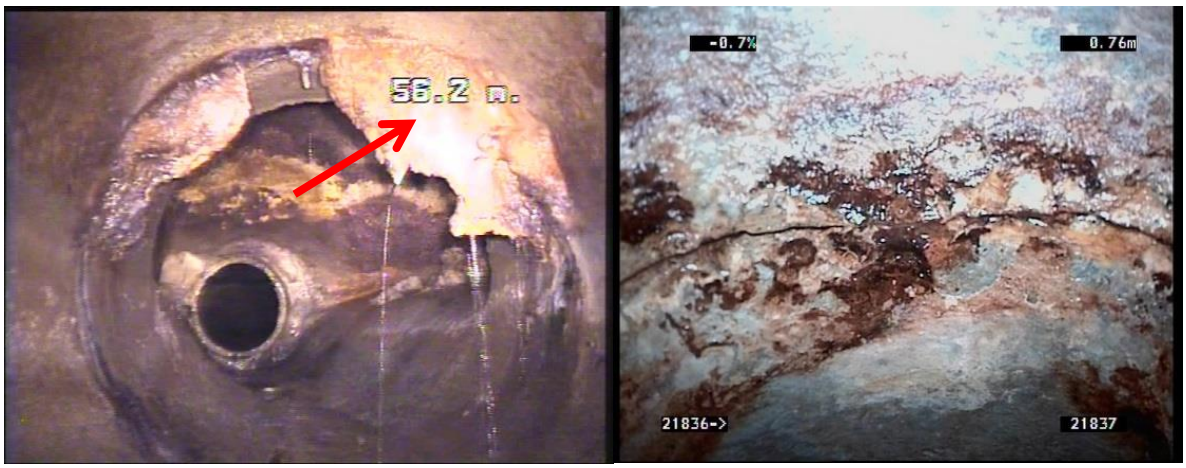

Figure 4-19(a) Encrustation and running flow from opened joint, (b) groundwater infiltration from significant circumferential cracking

The above photos show evidence of secondary effects, which are associated with damage that has penetrated the thickness of the pipe walls. Figure 4-19(a) shows an opened joint where encrustation deposits could be observed, which results from infiltration seepage from the surrounding soil. The precipitated salts present in the seepage build up over time in large orange deposits as moisture evaporates. Figure 4-19(b) shows groundwater has permeated the pipe walls to enter the pipe interior. When secondary effects are not obvious, such as when the ground water table is below the depth of the pipe so no leaking occurs, the severity of pipe cracking is not able to be inferred from secondary effects and is again dependent on the video quality.

As the distance counter on the CCTV footage was not calibrated to a specific datum to represent the 0.0 m starting measurement, the reported distances of repeat CCTV footage are often out of sync from one another by up to 1 metre in the worst observed cases. This was identified when comparing the distances of laterals along the pipe between inspections, which do not change, but had margins of error of up to 1.0 metre. To ensure that the distance along the pipe of damage items are interpreted correctly, the pre-CES and post-CES footage needed to be aligned such that the laterals match across the footage. In this study, the reported distance from each CCTV inspection was rounded to the nearest metre as discussed in section 3.3, but some manual adjustments were still required to ensure that the reported distances at laterals were aligned.

Pipe dip was unable to be considered in this study and compared with LiDAR-derived ground deformations due to the inability of pre-CES cameras having the means of reporting this. Assessors typically observed the water line angle in the pipe as an indication of the dip angle prior to the availability of camera mounted tilt sensors, however this is cannot be quantified and was therefore excluded from the study.

To improve reliability of CCTV footage, technological advances in video resolution and distance calibration are will be important for achieving better results for comparing pre- and post-earthquake performance. However, given that older footage will always be compared with newer footage following an earthquake, this limitation is difficult to account for.

4.9.2 Operator inconsistencies

As the CCTV procedure is entirely manually operated, there exists considerable differences in the habits between different operators. Multiple pipes in the study were surveyed by different organisations at different points in time, with different hardware and software setups that capture varying levels of information. This can have an adverse effect on the reliability of comparing data.

In CCTV surveys, the operator upon discovering a damage item typically pauses at the location to pan the camera for a high-resolution view of the item with respect to the surrounding environment. Some pre-CES operators were more thorough in their inspections compared to post-CES operators, possibility due to the increased pressure and demand for CCTV services within a short timeframe following the CES. This may result in the illusion of

more frequent pre-CES damage being reported than post-CES, and the reason why some damage items are shown to “disappear” when comparing pre-CES and post-CES footage, despite no records of repairs being undertaken. At least 10% of the post-CES surveys are considered to be affected in this study.

It was inferred that some operators conducting post-CES damage surveys did not have access to pre-CES observation results, and hence were unaware of the pre-CES damage extent. On multiple occasions an existing damage observation was bypassed, which may not be obvious at the time due to lighting conditions, flow or other factors. Therefore, it is recommended that operators conducting CCTV reports be briefed on the existing damage condition of pipes before undertaking a survey.

Chapter 5 - Conclusions

The waste water network is considered to be crucial lifeline infrastructure fundamental to public health and safety, economic functioning, and the basic operation of any society. Improving the resilience of the waste water networks by reducing disaster impacts and hence disruption to basic services is a major component of the UNISDR Sendai targets. In New Zealand this is reflected by the overarching intent for increased resilience of infrastructure as a part of the 2018 Natural Disaster Resilience Strategy.

In order to contribute towards increased resilience of waste water networks, this thesis has outlined a method for assessing the seismic performance of buried gravity waste water pipes using existing CCTV data and ground motion information. The aim of the method was to develop a systematic approach to compare the pre-existing condition of the pipes with additional damage following seismic activity at a high-resolution detail, with the aim of attributing local damage observations to external factors from the environment. The need for such a method was identified as previous seismic assessments for buried pipework overlook pre-existing damage conditions and local effects that may vary along the pipe length.

The method development was feasible due to the extensive, high-resolution geospatial databases, and detailed CCTV damage records available in Christchurch, which is regarded as the one of the most comprehensive in the world. This was a result of intensive surveys conducted by contractors following the CES to reinstate the city's horizontal infrastructure, an event which caused widespread damage to the waste water network on an unprecedented scale.

55 pipes were chosen to demonstrate the potential findings and limitations of the method. The selection criteria focused on pipes in residential land use areas and included a diverse sample set in terms of pipe installation age, size and ground conditions. The final selection was governed by pre-CES and post-CES CCTV inspection records availability at the CCC. The pre-CES and post-CES CCTV footage was assessed in accordance with the NZPIM, the standardised guidelines for conducting CCTV inspections in New Zealand. The damage items identified this way were plotted in GIS software to the nearest metre and compared with

geospatial data including ground movements, accelerations, and liquefaction information for the identification of relationships and patterns.

The following results were identified:

- Main pipe joints and lateral connections were more vulnerable than the pipe body during a seismic event.
- Obvious differential ground movement resulted in increased local damage observations in many cases, however this was not obvious for all pipes.
- Smaller diameter pipes may be more vulnerable than larger pipes during a seismic event.
- Pipes with older installation ages exhibited more overall damage prior to a seismic event, which is likely attributable to increased chemical and biological deterioration. However, no evidence was found relating pipe age to performance during a seismic event.
- No evidence was found linking levels of pre-CES damage in a pipe with subsequent seismic performance.
- No evidence was found linking seismic performance with liquefaction resistance or magnitude of seismic ground motion.

Due to the small sample size used for method development in this study, trends are not clearly pronounced and certain pipe parameters such as age of installation and pipe diameter were not able to be effectively represented, so the results are expected to be of limited application. However, the advantages associated with the enhanced level of detail are evident compared with existing assessment methods, especially with regards to detailed pipe performance along the length of a pipe due to local ground deformation evidenced by LiDAR experienced through the CES.

Some study limitations have been discussed, including LiDAR and CCTV processes, the relatively subjective nature of defect coding, and reliance on manual operation. It is anticipated that developments in data acquisition technology such as AI powered image/pattern recognition software will improve accuracies and reduce inconsistencies, for example by providing a solution for quantifying defects measured with the CCTV camera.

In order to further develop the method presented here, the following areas of focus are recommended:

- A larger and more diverse sample set (i.e. featuring more pipes of various installation years and diameters) would better represent various pipe parameters in order to further understand associated seismic damage.
- An improved system to depict continuous effects along a pipe length will better reflect the extent of defect types such as surface damage and longitudinal cracking. For example, a coloured dashed line could be plotted between two damage points in parallel using GIS software.
- Pipe dips may be incorporated into the method. Dips are often assessed qualitatively by observing the angle of the water line in the pipe; however, this was not considered in this study due to pre-CES cameras not having the means of measuring this, so could not be compared to actual ground deformations and post-CES observations. However, it is considered that future CCTV surveys implementing the method in this thesis to build a CCTV database are able to take advantage of modern sensors and be able to record this information.
- A systematic and quantitative process for associating damage with above/nearby differential ground movement would allow results to be compared more easily than the current subjective and qualitative process. This process would account for pipe gradient, positional errors in defect locations, and errors in LiDAR-derived ground deformation data. An expanded analysis dataset may identify stronger relationships between pipe performance and ground deformation. This in turn may aid prioritisation of post-earthquake CCTV inspections, and/or inform analyses inferring damage to the network in the absence of inspection data.
- It is currently not possible to attribute specific damage items to individual CES events, as the pipe condition footage was captured following multiple earthquakes over the span of more than a year. Where CCTV records exist between events, they could be incorporated to observe differences in pipe condition between separate events.
- The current manual process is time-consuming to complete for a large number of pipes, and requires the assessor to be competent and trained. Where possible, steps

such as visual examination and data entry could be automated to improve completion times and reduce errors due to observation, subjectivity, and fatigue.

A key lesson from this research is the need for comprehensive, accurate and readily accessible CCTV footage of representative parts of the waste water network prior to earthquake events, against which post-event impacts can be compared. In addition, local territorial authorities should be prioritising LiDAR data capture across their areas, against which post-event LiDAR data can be compared.

The method proposed in this thesis will be useful for any territorial local authority needing to assess future earthquake impacts on gravity pipes, to support efforts to increase waste water network resilience. In countries other than New Zealand, the local CCTV guidelines may be used as a substitute for the NZPIM process described herein. It is able to be applied anywhere provided the region has a robust catalogue featuring the buried pipe assets and intrinsic parameters, the resources to undertake CCTV analysis of buried pipes, and a GIS database featuring soil information and earthquake records.

References

Al-Saleem, H. I., & Langdon, W. (2015). *Installation of Reinforced Concrete Pipes: Theory and Practice*.

Alexander, M. G., & Fourie, C. (2011). Performance of sewer pipe concrete mixtures with portland and calcium aluminate cements subject to mineral and biogenic acid attack. *Materials and Structures, 44*(1), 313-330.

Beliea, N. D., Monteny, J., Beeldens, A., Vincke, E., Gemert, D. V., & Verstraete, W. (2004). Experimental research and prediction of the effect of chemical and biogenic sulfuric acid on different types of commercially produced concrete sewer pipes. *Cement and Concrete Research, 34*(12), 2223-2236.

Boscardin, M. D., & Cording, E. J. (1989). Building response to excavation-induced settlement. *Journal of Geotechnical Engineering, 115*, 1-21.

Bouziou, D., & O'Rourke, T. D. (2017). *Response of the Christchurch water distribution system to the 22 February 2011 earthquake* (Vol. 97).

Bradley, B. (2014). *Site-specific and spatially-distributed ground-motion intensity estimation in the 2010–2011 Canterbury earthquakes* (Vol. s 61–62).

Bradley, B., & Hughes, M. (2012). *Conditional Peak Ground Accelerations in the Canterbury Earthquakes for Conventional Liquefaction Assessment*. Retrieved from Christchurch:

Broomfield, J. P. (2007). *Corrosion of Steel in Concrete, understanding, investigation and repair*. New York: Taylor and Francis Group.

Canterbury Geotechnical Database. (2014). *Technical Specification 03: Verification of LiDAR acquired before and after the Canterbury Earthquake Sequence* (52010.140.v1.0).

Carleton, E., Hiner, S., & Kurdziel, J. (2017). The History and Application of the Three-Edge Bearing Test for Concrete Pipe. In (pp. 18-27).

Christoffersen, G. A. (2012). *Information is Power – In Good Times and Bad*. Paper presented at the Water Nwe Zealand Annual Conference 2012.

Concrete Pipe Association of Australasia (Producer). (2018). Concrete Pipe Facts *Concrete Pipe Association of Australasia*. Retrieved from https://www.cpaa.asn.au/General/concrete-pipe-facts.html

Cubrinovski, M., Hughes, M., Bradley, B., McCahon, I., McDonald, Y., Simpson, H., . . . O'Rourke, T. (2011). *Liquefaction Impacts on Pipe Networks* (ISSN 1172-9511). Retrieved from

Cubrinovski, M., Hughes, M., Bradley, B., Noonan, J., Hopkins, R., McNeill, S., & English, G. (2014). *Performance of Horizontal Infrastructure in Christchurch City through the 2010-2011 Canterbury Earthquake Sequence* Retrieved from Department of Civil and Natural Resources Engineering, University of Canterbury

Davies, J. P., Clarke, B. A., Whiter, J. T., & Cunningham, R. J. (2001). Factors influencing the structural deterioration and collapse of rigid sewer pipes. *Urban Water, 3*, 73-89.

De Schutter, G. (2012). *Damage to Concrete Structures*.

Edkins, D., J., Orense, R., P., Henry, R., S., & Ingham, J., M. (2016). Signature Failure Modes of Pipelines Constructed of Different Materials When Subjected to Earthquakes. *Journal of Pipeline Systems Engineering and Practice, 7*(1), 04015014. doi:10.1061/(ASCE)PS.1949-1204.0000213

Erdogmus, E., Skourup, B. N., & Tadros, M. (2010). Recommendations for design of reinforced concrete pipe. *Journal of Pipelines Systems Engineering and Practice, 1*(1), 25-32.

Erdogmus, E., & Tadros, M. (2006). Behavior and Design of Buried Concrete Pipes. *Nebraska Department of Roads Research Reports*, Paper 54.

Esri (Producer). (2018, December 14). World Imagery Basemap. *ArcGIS*. Retrieved from https://www.arcgis.com/home/item.html?id=10df2279f9684e4a9f6a7f08febac2a9

Giovinazzi, S., Wilson, T., Davis, C., Bristow, D., Gallagher, M., Schofield, A., . . . Tang, A. (2011). *Lifelines performance and management following the 22 February 2011 Christchurch earthquake, New Zealand: Highlights of resilience* (Vol. 44).

GNS Science (Producer). (2018). Major Faults in New Zealand. Retrieved from https://www.gns.cri.nz/Home/Learning/Science-Topics/Earthquakes/Major-Faults-in-New-Zealand

Heger, F. (1963). Structural Behaviour of Circular Reinforced Concrete Pipe—Development of Theory. *J. Proc*, 1567-1614.

Heiler, D., Moore, J., & Gibson, A. (2012). *Asset Assessment using GIS and InfoNet.* Paper presented at the Water NZ conference and expo.

Hughes, M. W., Quigley, M. C., Ballegooy, S. v., Deam, B. L., & Brendon A. Bradley, R. M. (2015). The sinking city: Earthquakes increase flood hazard in Christchurch, New Zealand. *GSA Today, 25*, 4-10.

Institute of Public Works Engineering, A., Association of Local Government Engineers of New, Z., & National Asset Management Steering, G. (2015). *International infrastructure management manual*. [Sydney, NSW]; [Wellington, N.Z.]: IPWEA ; NAMS Group.

Kim, J., Nadukuru, S., Pour-Ghaz, M., Lynch, J., Michalowski, R., Bradshaw, A. S., . . . Weiss, W. (2012). *Assessment of the Behavior of Buried Concrete Pipelines Subjected to Ground Rupture: Experimental Study* (Vol. 3).

Lester, J., & Farrar, D. M. (1979). *An examination of the defects observed in 6 km of sewers*. Retrieved from Crowthorne, Berkshire.

Liu, M., Giovinazzi, S., MacGeorge, R., & Beukman, P. (2014). Wastewater Network Restoration Following the Canterbury NZ Earthquake Sequence: Turning Post-Earthquake Recovery into Resilience Enhancement. *International Efforts in Lifeline Earthquake Engineering*, 160-167.

Marston, A., & Anderson, A. O. (1913). *The Theory of Loads on Pipes in Ditches and Tests of Cement and Clay Drain Tile and Sewer Pipe*. Retrieved from Ames: Iowa Engineering Experiment Station.

Moradian, M., Shekarchi, M., Pargar, F., Bonakdar, A., & Valipour, M. (2012). Deterioration of Concrete Caused by Complex Attack in Sewage Treatment Plant Environment. *Journal of Performance of Constructed Facilities, 26*(1), 124-134. doi:10.1061/(ASCE)CF.1943-5509.0000189

Mori, T., Nonaka, T., KazueTazaki, Koga, M., Hikosaka, Y., & Noda, S. (1992). Interactions of nutrients, moisture and pH on microbial corrosion of concrete sewer pipes. *Water Research, 26*(1), 29-37.

Neville, A. (2004). The confused world of sulfate attack on concrete. *Cem Concr Res, 34*(8), 1275-1296.

New Zealand Geotechnical Database (Producer). (2012, July 23). Vertical Ground Surface Movements, Map Layer CGD0600. Retrieved from https://www.nzgd.org.nz/

New Zealand Lifelines Council (Producer). (2017, September 2018). New Zealand Lifelines Infrastructure Vulnerability Assessment: Stage 1. Retrieved from https://www.civildefence.govt.nz/assets/Uploads/lifelines/National-Vulnerability-Assessment-Stage-1-September-2017.pdf

New Zealand Ministry of Civil Defence and Emergency Management (Producer). (2018, October 11). Proposed National Disaster Resilience Strategy. *New Zealand Ministry of Civil Defence and Emergency Management*. Retrieved from https://www.civildefence.govt.nz/cdem-sector/plans-and-strategies/proposed-national-disaster-resilience-strategy/

New Zealand Parliamentary Counsel Office (Producer). (2018, June 1). Civil Defence Emergency Management Act 2002. *New Zealand Parliamentary Counsel Office / Te Tari Tohutohu Pāremata*. Retrieved from http://www.legislation.govt.nz/act/public/2002/0033/51.0/DLM149789.html

O'Reilly, M. P., Rosbrook, R. B., Cox, G. C., & McCloskey, A. (1989). *Analysis of defects in 180km of pipe sewers in southern water authority*. Retrieved from

O'Connell, M., McNally, C., & G. Richardson, M. (2010). *Biochemical attack on concrete in wastewater applications: A state of the art review* (Vol. 32).

O'Rourke, T. D., Jeon, S.-S., Toprak, S., Cubrinovski, M., Hughes, M., Ballegooy, S. v., & Bouziou, D. (2014). Earthquake Response of Underground Pipeline Networks in Christchurch, NZ. *Earthquake Spectra, 30*(1), 183-204.

Parande, A. K., Ramsamy, P. L., Ethirajan, S., Rao, C. R. K., & Palanisamy, N. (2006). Deterioration of reinforced concrete in sewer environments. *Municipal Engineer, 159*(ME1), 11-20.

ProjectMax Ltd. (2006). *New Zealand Pipe Inspection Manual 3rd Edition*. Retrieved from Wellington:

ProjectMax Ltd. (2016). *Recommendations for the Revision of the New Zealand Pipe Inspection Manual*.

Quigley, M. C., Hughes, M. W., Bradley, B. A., Ballegooy, S. v., Reid, C., Morgenroth, J., . . . Pettinga, J. R. (2016). The 2010-2011 Canterbury Earthquake Sequence: Environmental effects, seismic triggering thresholds and geologic legacy. *Tectonophysics, 672-673*, 228-274.

Rais, A., Giovinazzi, S., & Palermo, A. (2015). Pipelines at Bridge Crossings: Empirical-Based Seismic Vulnerability Index. *Pipelines 2015*, 1642-1654. doi:doi:10.1061/9780784479360.151

Romanova, A., Mahmoodian, D. M., & Alani, M. (2014). *Influence and Interaction of Temperature, H2S and pH on Concrete Sewer Pipe Corrosion* (Vol. 8).

Sampedro, I., & Hughes, M. W. (2018). *Underground Infrastructure and EQ events: how an advanced condition assessment and data collection process will assist in the planning for and recovery from an EQ event.* Paper presented at the Proceedings for Information Systems for Crisis Response and Management, Asia-Pacific Conference, Wellington.

Sampedro, I., & Hughes, M. W. (2018b). Data collection approaches for underground infrastructure condition assessment. *Engineering For Public Works*(12), 38-45.

Saricimen, H., Shameem, M., Barry, M. S., Ibrahim, M., & Abbasi, T. A. (2003). Durability of proprietary cementitious materials for use in wastewater transport systems. *Cem Concr Comp, 25*(4), 421-427.

SCIRT Learning Legacy (Producer). (2019, January 7). About SCIRT. Retrieved from https://scirtlearninglegacy.org.nz/

Seismology Research Centre (Producer). (2014, February 27). Strong Motion Accelerographs. Retrieved from https://www.src.com.au/strong-motion-accelerographs/

Song, Y., Jiang, G., Chen, Y., Zhao, P., & Tian, Y. (2017). Effects of chloride ions on corrosion of ductile iron and carbon steel in soil environments. *Scientific Reports, 7*, Article number: 6865.

Spangler, M. (1960). *Soil Engineering*. Scranton, PA, USA: International Textbook Company.

Standards Association of Australia. (1957). Australia Standard No. A35 - 1957. In: Standards Association of Australia,.

Standards New Zealand. (2007a). AS/NZS 3725:2007 Design for installation of buried concrete pipes. In: Standards New Zealand.

Standards New Zealand. (2007b). AS/NZS 4058:2007 Precast concrete pipes (pressure and non-pressure). In: Standards New Zealand.

Standards New Zealand. (2009). AS/NZS ISO 31000:2009 Risk Management - Principles and guidelines. In: Standards New Zealand.

U.S Geological Survey. (2011). ShakeMap Scientific Background. Rapid Instrumental Intensity Maps. *Earthquake Hazards Program*.

UNISDR (Producer). (2017). National Disaster Risk Assessment: Governance System, Methodologies, and Use of Results. *UNISDR Words into Action Guidelines*. Retrieved from https://www.unisdr.org/files/globalplatform/591f213cf2fbe52828_wordsintoactionguideline.nationaldi.pdf

UNISDR (Producer). (2018). Sendai Framework for Disaster Risk Reduction. *United Nations International Strategy for Disaster Reduction*. Retrieved from https://www.unisdr.org/we/coordinate/sendai-framework

UNISDR (Producer). (2019, January 5). Goal 6: Ensure access to water and sanitation for all. *United Nations*. Retrieved from https://www.un.org/sustainabledevelopment/water-and-sanitation/

Wilson, J. (1989). *Christchurch Swamp to City, A Short History of the Christchurch Drainage Board 1875-1989*. Christchurch: Te Waihora Press.

Wong, L. S., & Nehdi, M. L. (2018). *Critical Analysis of International Precast Concrete Pipe Standards*. Retrieved from Puslinch, ON N0B 2J0, Canada:

Appendix A - Pipe Selection Attribute List

Table A-1. Master pipe selection attributes

Pipe ID	Diameter (mm)	Year of Installation	Starting Manhole ID	Finish Manhole ID	Post-CES survey date	Pre-CES survey date	LRI Zone	Equivalent Cyclic Resistance Ratio (CRR)	Representative LRI (at water table)	Estimated Vertical Settlement (mm)	Estimated Lateral Displacement (mm)	Estimated Ground Strain	Median PGA of events between 4 Sep 2010-23 Dec 2011	Median PGV of events between 4 Sep 2010-23 Dec 2011
23532	150	1954	23017	23018	27/02/2014	17/04/2007	3	0.16–0.23	0.195	20-50	20-40	volumetric = 1%, shear = 1%	0.32	43.61
8033	150	1955	7439	7440	16/12/2013	10/07/2008	3	0.16–0.23	0.195	20-50	20-40	volumetric = 1%, shear = 1%	0.19	25.56
9082	150	1955	9082	9083	17/10/2012	12/01/2010	3	0.16–0.23	0.195	20-50	20-40	volumetric = 1%, shear = 1%	0.19	26.96
9088	150	1955	9084	9088	17/10/2012	13/01/2010	3	0.16–0.23	0.195	20-50	20-40	volumetric = 1%, shear = 1%	0.19	27.23
9090	150	1955	9089	9090	8/01/2014	13/01/2010	3	0.16–0.23	0.195	20-50	20-40	volumetric = 1%, shear = 1%	0.19	27.31
9543	150	1955	9499	9501	9/07/2011	14/09/2006	3	0.16–0.23	0.195	20-50	20-40	volumetric = 1%, shear = 1%	0.2	31.45
9544	150	1955	9498	9544	9/07/2011	14/09/2006	3	0.16–0.23	0.195	20-50	20-40	volumetric = 1%, shear = 1%	0.2	31.44
9550	150	1955	9501	9550	23/01/2016	15/09/2006	2	0.11–0.16	0.13	50-250	40-200	volumetric = 3%, shear = 2%	0.2	31.41
22636	150	1955	22102	22121	20/05/2011	1/05/2008	2	0.11–0.16	0.13	50-250	40-200	volumetric = 3%, shear = 2%	0.32	42.45
17591	150	1956	27234	17108	25/10/2016	11/04/2005	3	0.16–0.23	0.195	20-50	20-40	volumetric = 1%, shear = 1%	0.3	40.63
17604	150	1956	27487	17120	13/09/2012	30/06/2008	2	0.11–0.16	0.13	50-250	40-200	volumetric = 3%, shear = 2%	0.3	40.02
24216	150	1958	23677	23678	5/03/2015	7/12/2006	3	0.16–0.23	0.195	20-50	20-40	volumetric = 1%, shear = 1%	0.39	48.91
24217	150	1958	23706	23678	18/10/2012	7/12/2006	3	0.16–0.23	0.195	20-50	20-40	volumetric = 1%, shear = 1%	0.39	48.84
24218	150	1958	23680	23678	12/10/2012	4/12/2006	3	0.16–0.23	0.195	20-50	20-40	volumetric = 1%, shear = 1%	0.39	48.88
24219	150	1958	24043	23679	29/05/2015	5/12/2006	3	0.16–0.23	0.195	20-50	20-40	volumetric = 1%, shear = 1%	0.39	48.92
24220	150	1958	23704	23679	6/03/2015	7/12/2006	3	0.16–0.23	0.195	20-50	20-40	volumetric = 1%, shear = 1%	0.39	48.86
24221	150	1958	23679	23680	12/10/2012	4/12/2006	3	0.16–0.23	0.195	20-50	20-40	volumetric = 1%, shear = 1%	0.39	48.9
24224	150	1958	23678	23684	18/10/2012	4/12/2006	3	0.16–0.23	0.195	20-50	20-40	volumetric = 1%, shear = 1%	0.39	48.88
9125	150	1958	9116	9115	26/10/2016	14/03/2008	3	0.16–0.23	0.195	20-50	20-40	volumetric = 1%, shear = 1%	0.19	28.65
9126	150	1958	9114	9115	25/10/2013	14/03/2008	3	0.16–0.23	0.195	20-50	20-40	volumetric = 1%, shear = 1%	0.19	28.51
6267	150	1959	5725	5724	11/12/2013	28/12/2007	3	0.16–0.23	0.195	20-50	20-40	volumetric = 1%, shear = 1%	0.18	20.99
22329	225	1950	21813	21812	19/10/2017	9/08/2006	1	0.065-0.11	0.065	250-500	200-400	volumetric = 5%, shear = 4%	0.29	37.31
22330	225	1950	21814	21813	2/09/2011	7/08/2006	1	0.065-0.11	0.065	250-500	200-400	volumetric = 5%, shear = 4%	0.29	37.08
22331	225	1950	21815	21814	13/08/2011	7/08/2006	1	0.065-0.11	0.065	250-500	200-400	volumetric = 5%, shear = 4%	0.29	36.81
22333	225	1950	21733	21815	12/08/2011	7/08/2006	1	0.065-0.11	0.065	250-500	200-400	volumetric = 5%, shear = 4%	0.29	36.63
22352	225	1950	21812	21832	13/09/2011	9/08/2006	1	0.065-0.11	0.065	250-500	200-400	volumetric = 5%, shear = 4%	0.29	37.5
22353	225	1950	21832	21833	13/09/2011	15/08/2006	1	0.065-0.11	0.065	250-500	200-400	volumetric = 5%, shear = 4%	0.29	37.7
22354	225	1950	21833	21834	2/09/2011	16/08/2006	1	0.065-0.11	0.065	250-500	200-400	volumetric = 5%, shear = 4%	0.29	37.95
22355	225	1950	21834	21835	30/08/2011	16/08/2006	1	0.065-0.11	0.065	250-500	200-400	volumetric = 5%, shear = 4%	0.29	38.34
22356	225	1950	21835	21836	30/08/2011	18/08/2006	1	0.065-0.11	0.065	250-500	200-400	volumetric = 5%, shear = 4%	0.29	38.74
22357	225	1950	21836	21837	30/08/2011	18/08/2006	1	0.065-0.11	0.065	250-500	200-400	volumetric = 5%, shear = 4%	0.29	39.24
22358	225	1950	21837	21838	31/08/2011	21/08/2006	1	0.065-0.11	0.065	250-500	200-400	volumetric = 5%, shear = 4%	0.29	39.57
22366	225	1950	21845	21846	31/08/2011	23/08/2006	1	0.065-0.11	0.065	250-500	200-400	volumetric = 5%, shear = 4%	0.3	40.2
22367	225	1950	21846	21847	1/09/2011	23/08/2006	1	0.065-0.11	0.065	250-500	200-400	volumetric = 5%, shear = 4%	0.3	40.44
22368	225	1950	21847	21848	1/09/2011	23/08/2006	1	0.065-0.11	0.065	250-500	200-400	volumetric = 5%, shear = 4%	0.3	40.54
22370	225	1950	21848	22370	13/09/2011	28/08/2006	1	0.065-0.11	0.065	250-500	200-400	volumetric = 5%, shear = 4%	0.3	40.62
22374	225	1951	21851	21853	24/06/2016	28/08/2006	0	<0.065	-	>500	>400	volumetric > 5%, shear > 4%	0.3	40.7

24086	225	1954	23018	23560	4/10/2017	17/04/2007	3	0.16–0.23	0.195	20-50	20-40	volumetric = 1%, shear = 1%	0.32	43.69
23458	225	1958	23007	22943	30/03/2016	16/07/2008	3	0.16–0.23	0.195	20-50	20-40	volumetric = 1%, shear = 1%	0.32	39.4
20161	225	1960	19631	19616	10/08/2011	23/05/2006	3	0.16–0.23	0.195	20-50	20-40	volumetric = 1%, shear = 1%	0.32	40.99
22372	250	1951	21850	21851	29/01/2017	28/08/2006	1	0.065-0.11	0.065	250-500	200-400	volumetric = 5%, shear = 4%	0.3	40.65
24284	375	1956	23733	23735	5/01/2015	18/01/2007	3	0.16–0.23	0.195	20-50	20-40	volumetric = 1%, shear = 1%	0.38	48.1
22773	450	1952	22256	22250	15/12/2015	19/10/2007	2	0.11–0.16	0.13	50-250	40-200	volumetric = 3%, shear = 2%	0.32	43.06
22781	450	1952	23269	22258	5/10/2014	18/10/2007	0	<0.065	-	>500	>400	volumetric > 5%, shear > 4%	0.32	43.38
23791	450	1952	23274	23253	2/10/2014	7/07/2006	0	<0.065	-	>500	>400	volumetric > 5%, shear > 4%	0.32	44
10319	450	1956	10236	10238	5/03/2012	6/07/2006	3	0.16–0.23	0.195	20-50	20-40	volumetric = 1%, shear = 1%	0.22	31.83
10324	450	1956	10244	10324	10/11/2011	6/07/2006	3	0.16–0.23	0.195	20-50	20-40	volumetric = 1%, shear = 1%	0.22	31.8
10326	450	1956	10246	10244	10/11/2011	6/07/2006	3	0.16–0.23	0.195	20-50	20-40	volumetric = 1%, shear = 1%	0.21	31.76
1119	450	1960	8589	8591	15/03/2013	6/12/2006	3	0.16–0.23	0.195	20-50	20-40	volumetric = 1%, shear = 1%	0.22	31.87
1120	450	1960	8591	8592	15/03/2013	6/12/2006	3	0.16–0.23	0.195	20-50	20-40	volumetric = 1%, shear = 1%	0.22	31.89
21157	450	1991	20627	20617	28/01/2015	4/07/2006	0	<0.065	-	>500	>400	volumetric > 5%, shear > 4%	0.28	36.47
21165	450	1991	20583	20626	25/01/2015	4/07/2006	0	<0.065	-	>500	>400	volumetric > 5%, shear > 4%	0.27	36.12
21166	450	1991	20626	20627	26/01/2015	4/07/2006	0	<0.065	-	>500	>400	volumetric > 5%, shear > 4%	0.28	36.28
11440	900	1955	11345	11343	19/07/2011	10/02/2010	2	0.11–0.16	0.13	50-250	40-200	volumetric = 3%, shear = 2%	0.21	31.33
11442	900	1955	11348	11345	20/07/2012	10/02/2010	2	0.11–0.16	0.13	50-250	40-200	volumetric = 3%, shear = 2%	0.21	31.19

Figures A-1. Location of pipe selection in Christchurch City, World imagery map layer retrieved from Esri (2018)

Appendix B - Pipe Damage Observation List

The damage observations for the 55 pipes are shown in the following pages. The X-axis indicates the distance along the pipe from the designated “starting” manhole to the “finish” manhole. The Y-axis of the first chart indicates the magnitude of differential ground movement recorded in metres. For each observation the corresponding NZPIM damage code is shown at the same distance along the pipe below the chart. The colour coding indicates damage severity in accordance with Table 3-2. Pre-CES results are shown as squares and post-CESs results are shown as circles as previously mentioned.

Where applicable the vertical black line shows the distance along the pipe up to which footage was available for both the pre- and post-CES CCTV footage, no observations were recorded after the vertical black line (if applicable).

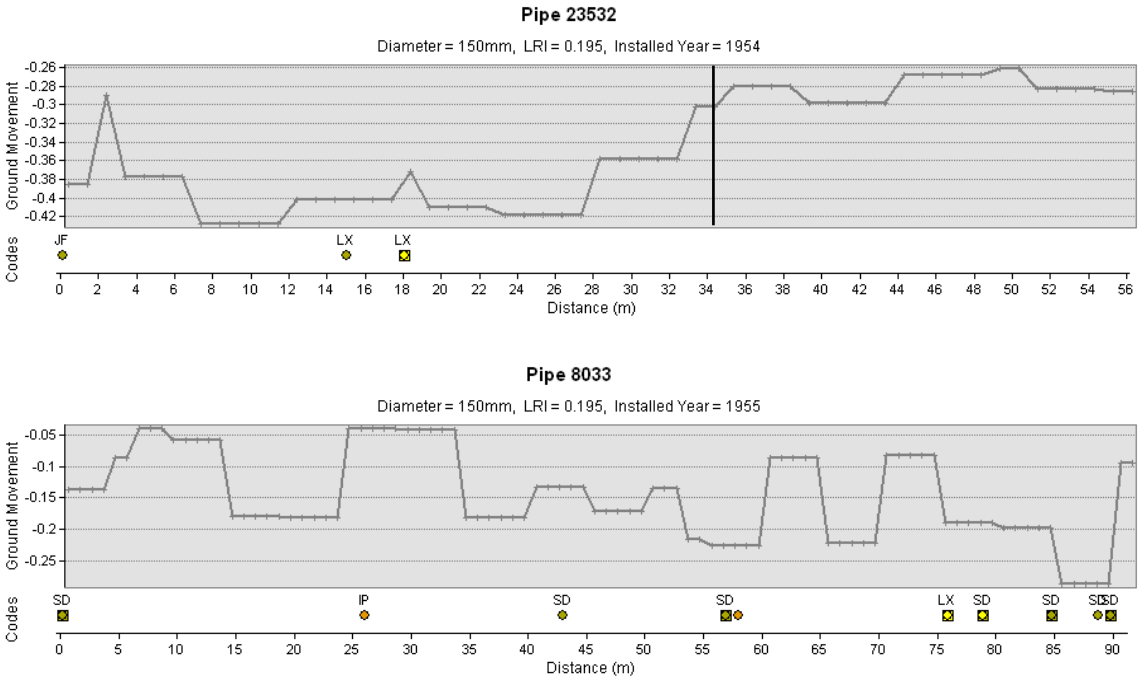

Figures B-1 to B-2. Individual pipe damage observation records

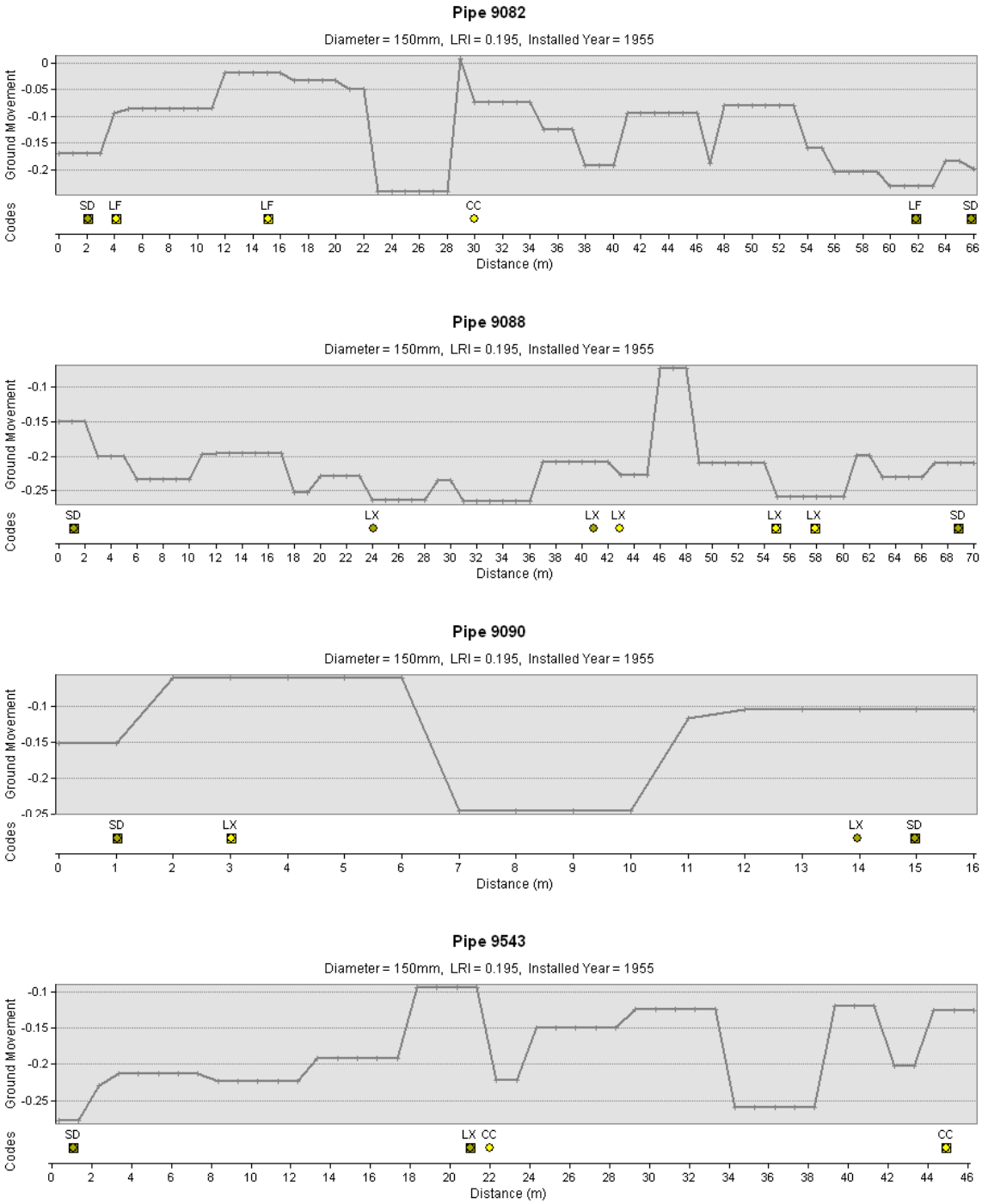

Figures B-3 to B-6. Individual pipe damage observation records

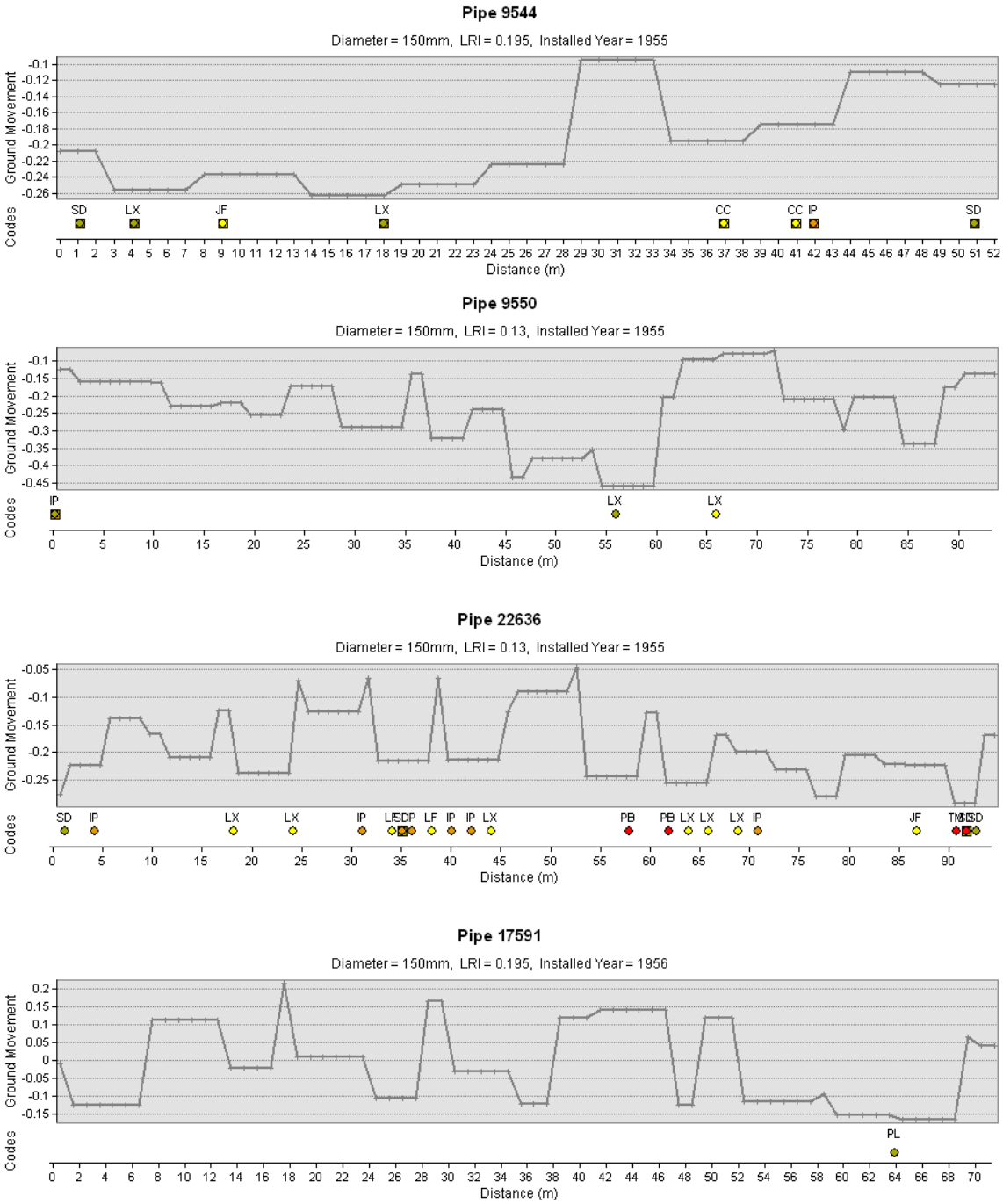

Figures B-7 to B-10. Individual pipe damage observation records

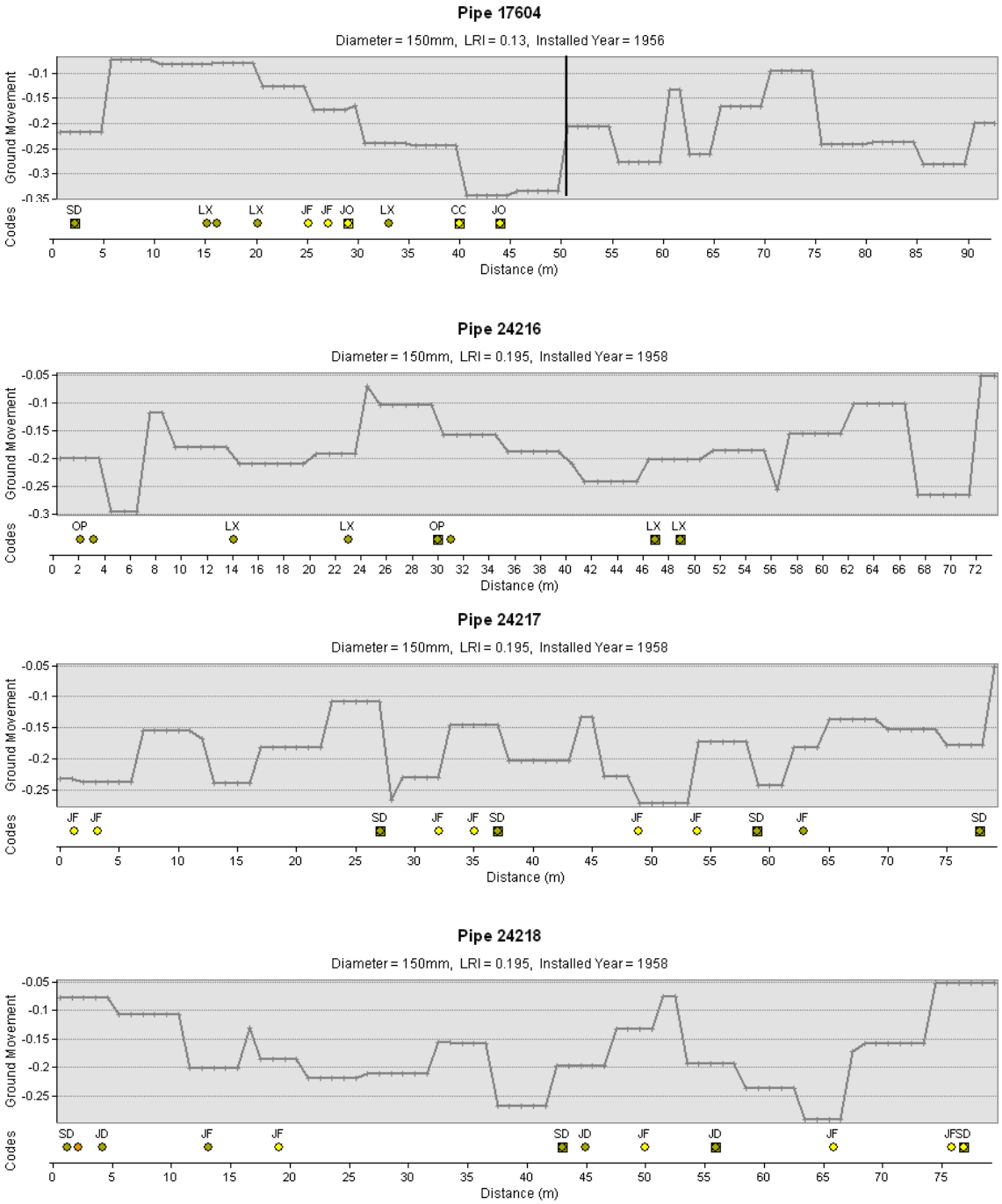

Figures B-11 to B-14. Individual pipe damage observation records

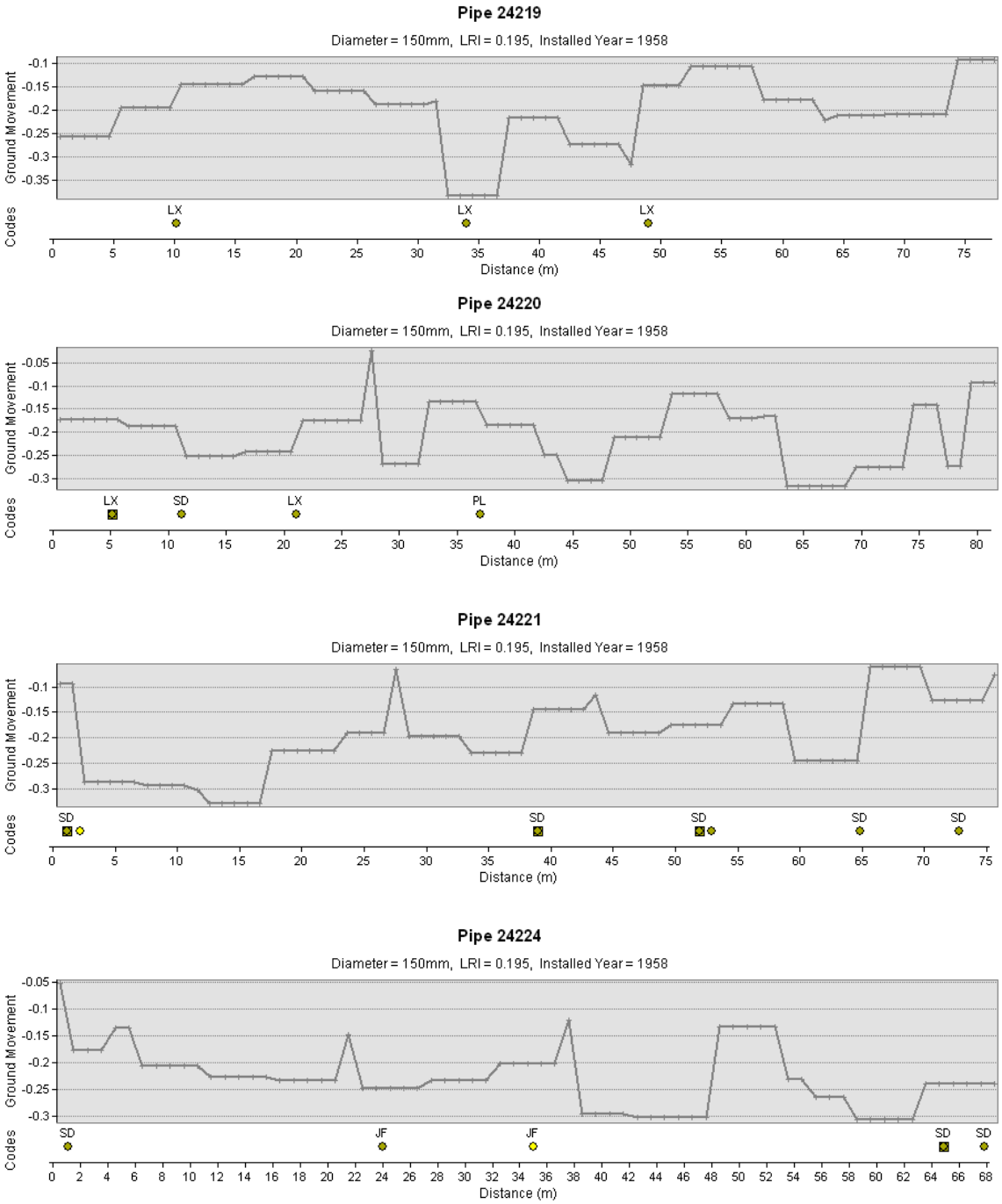

Figures B-15 to B-18. Individual pipe damage observation records

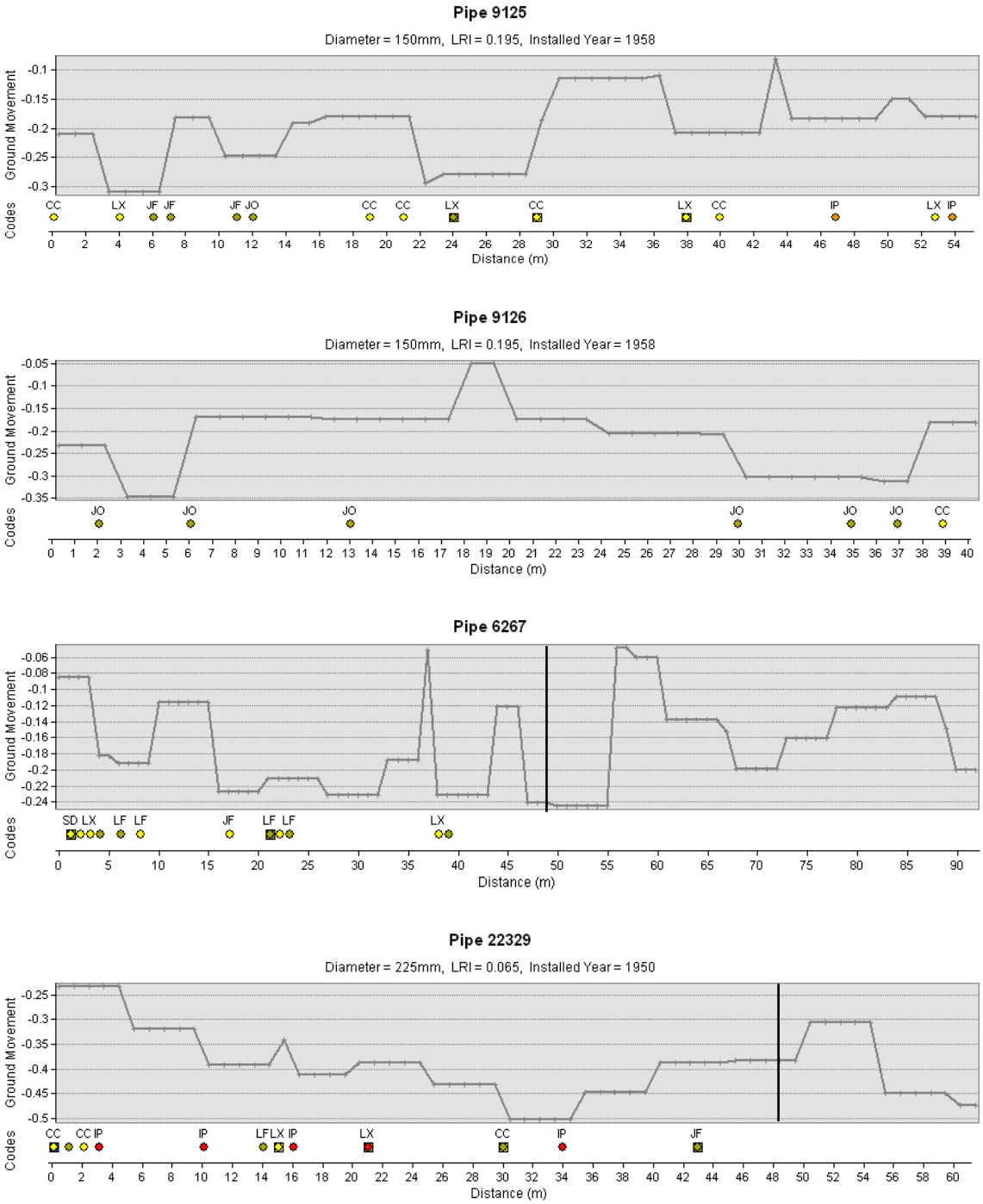

Figures B-19 to B-22. Individual pipe damage observation records

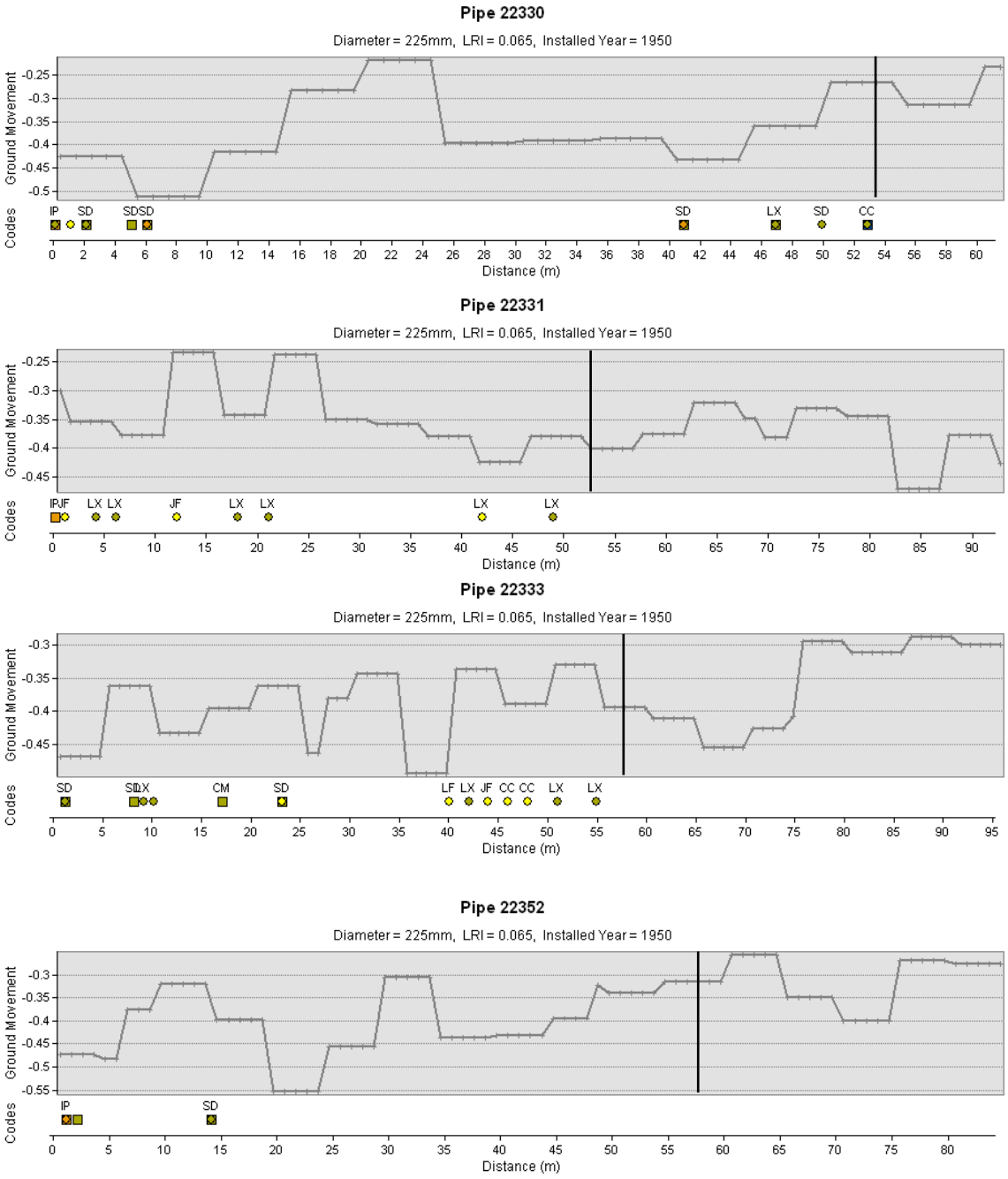

Figures B-23 to B-26. Individual pipe damage observation records

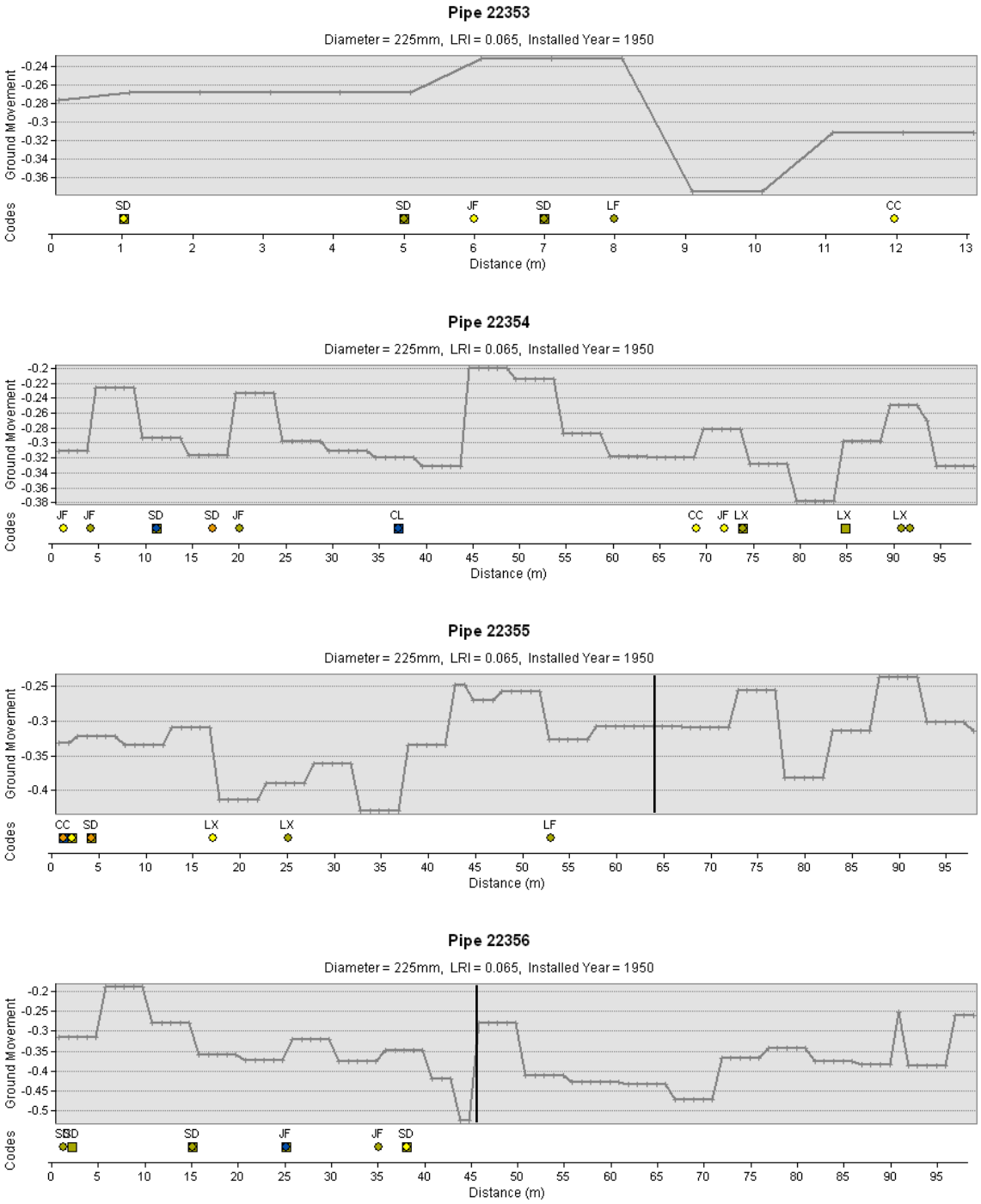

Figures B-27 to B-30. Individual pipe damage observation records

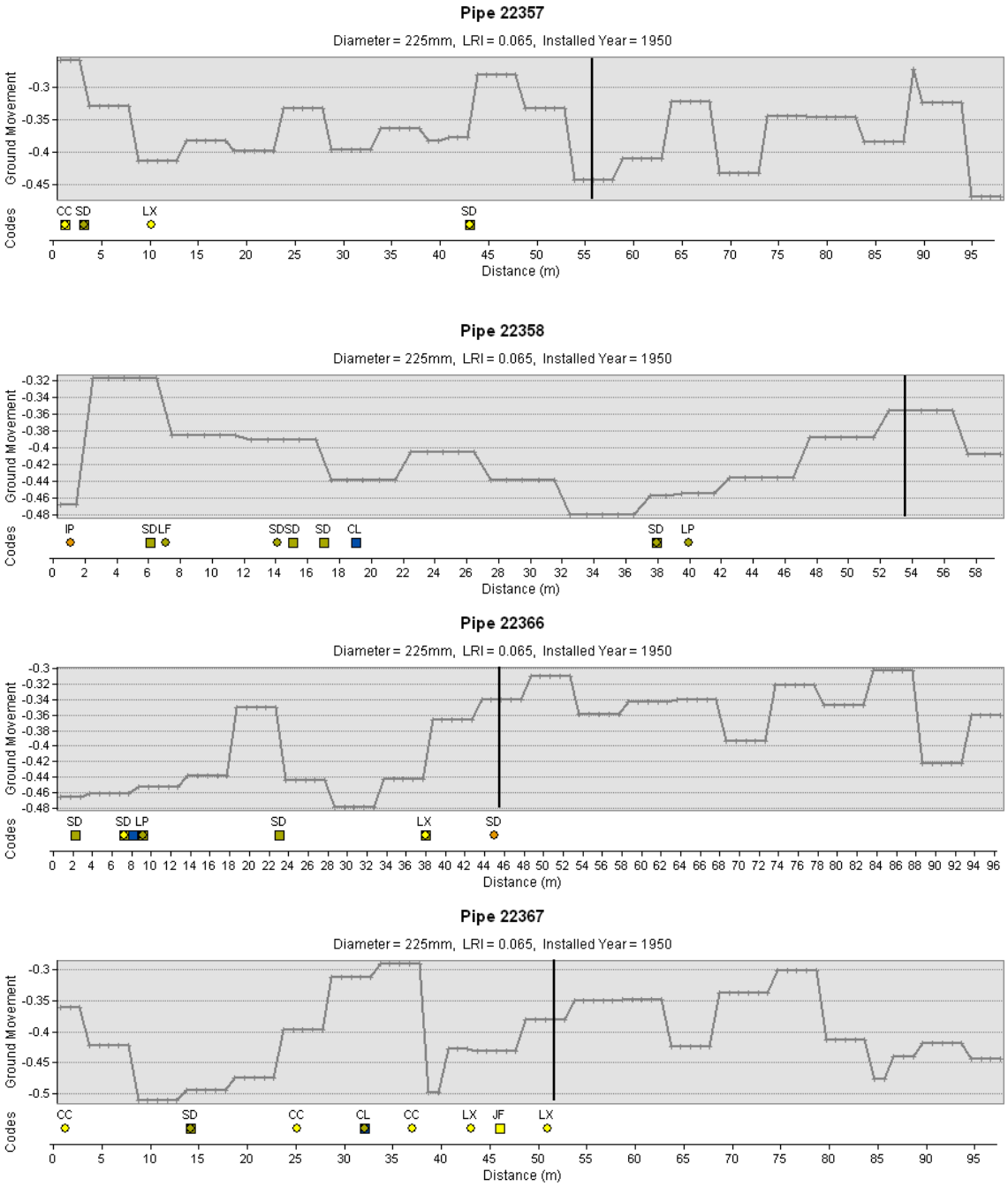

Figures B-31 to B-34. Individual pipe damage observation records

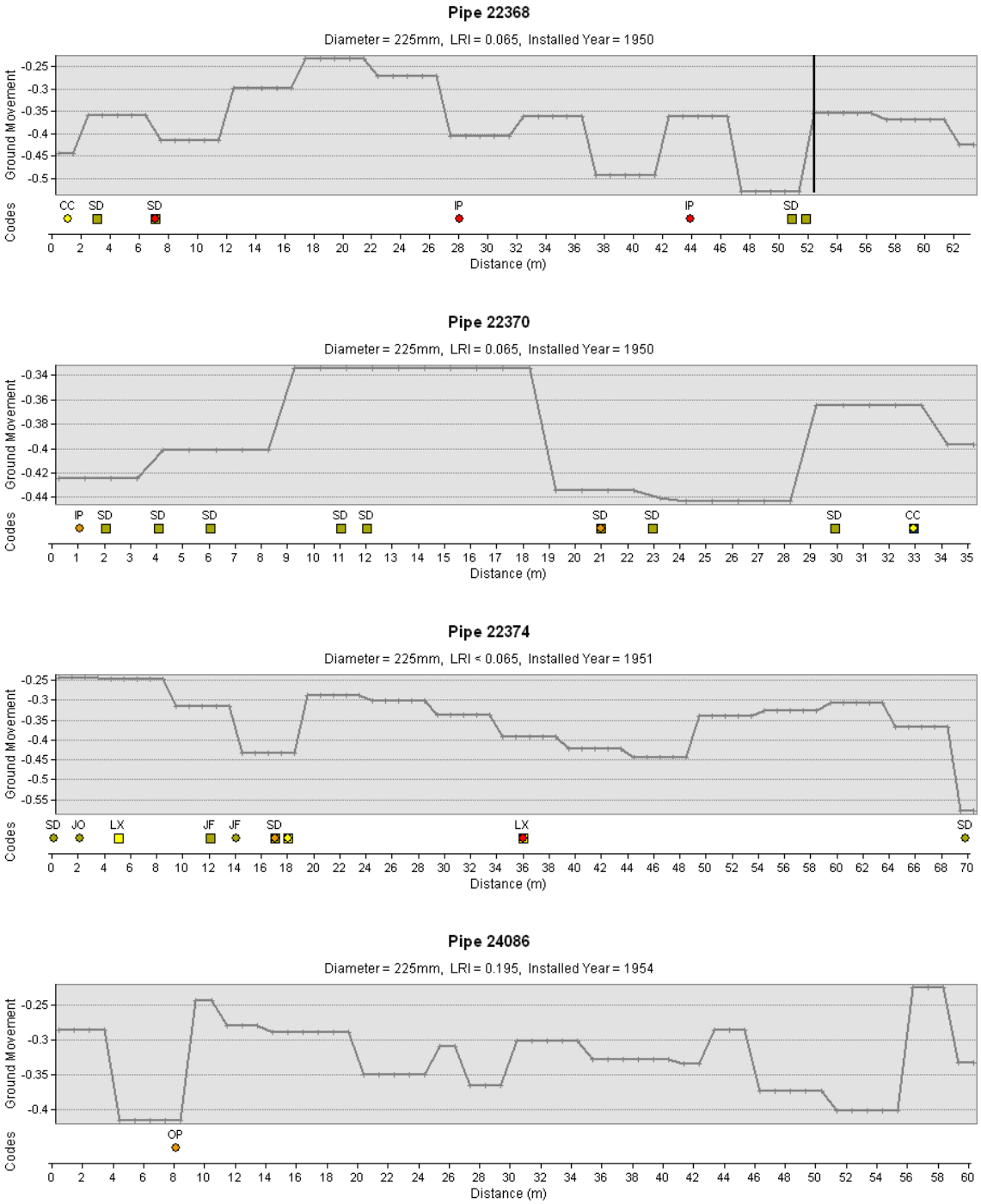

Figures B-35 to B-38. Individual pipe damage observation records

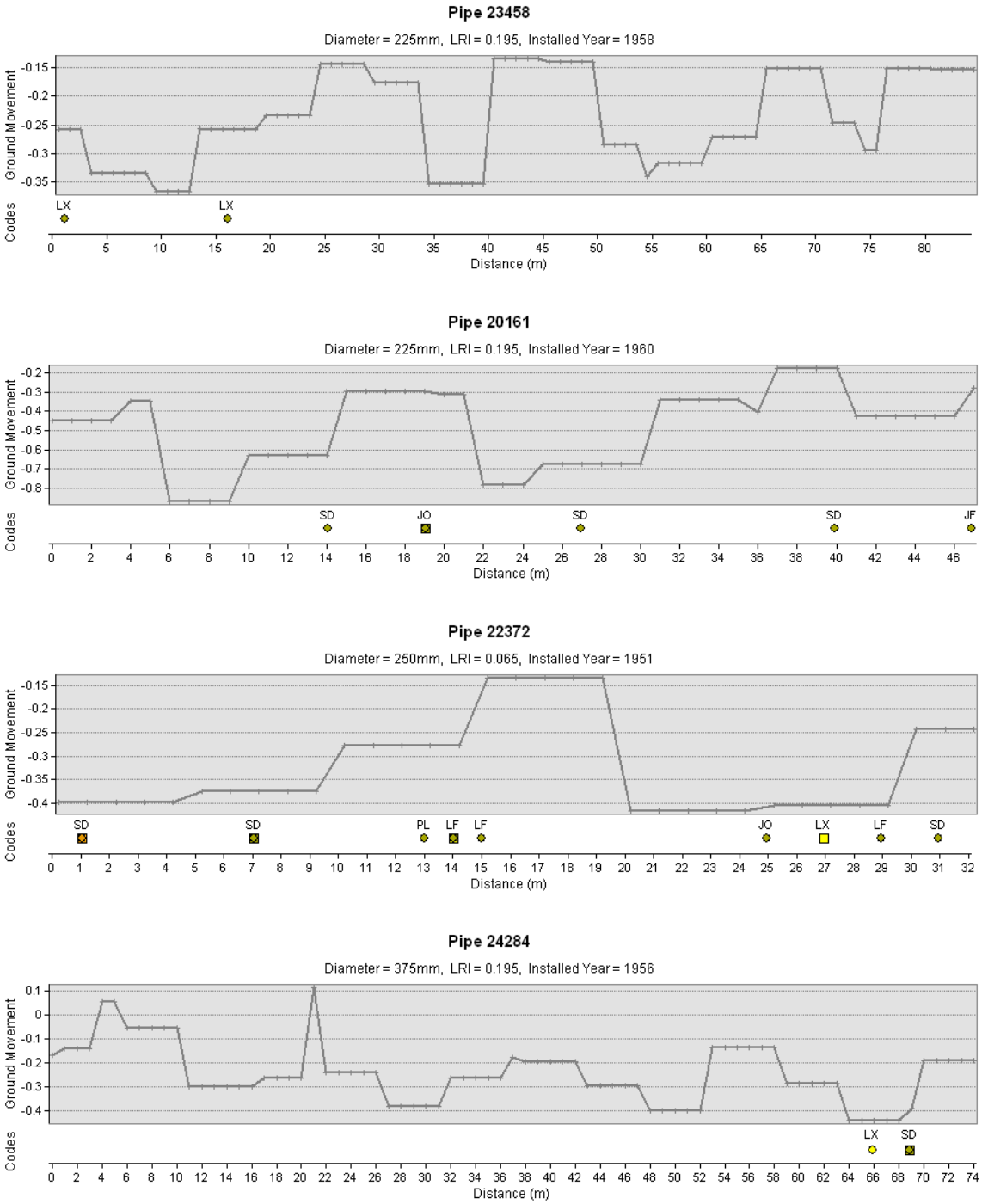

Figures B-39 to B-42. Individual pipe damage observation records

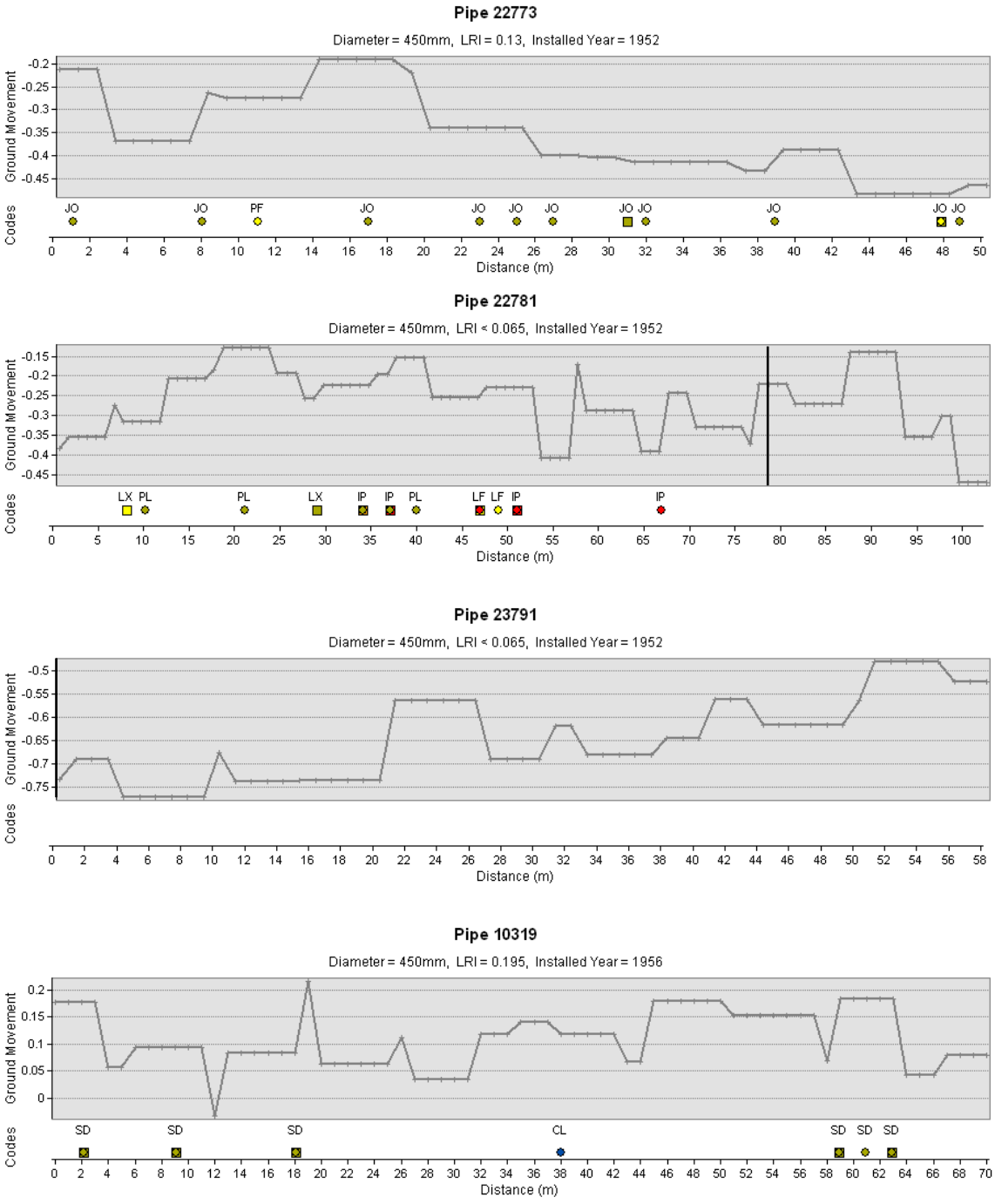

Figures B-43 to B-46. Individual pipe damage observation records

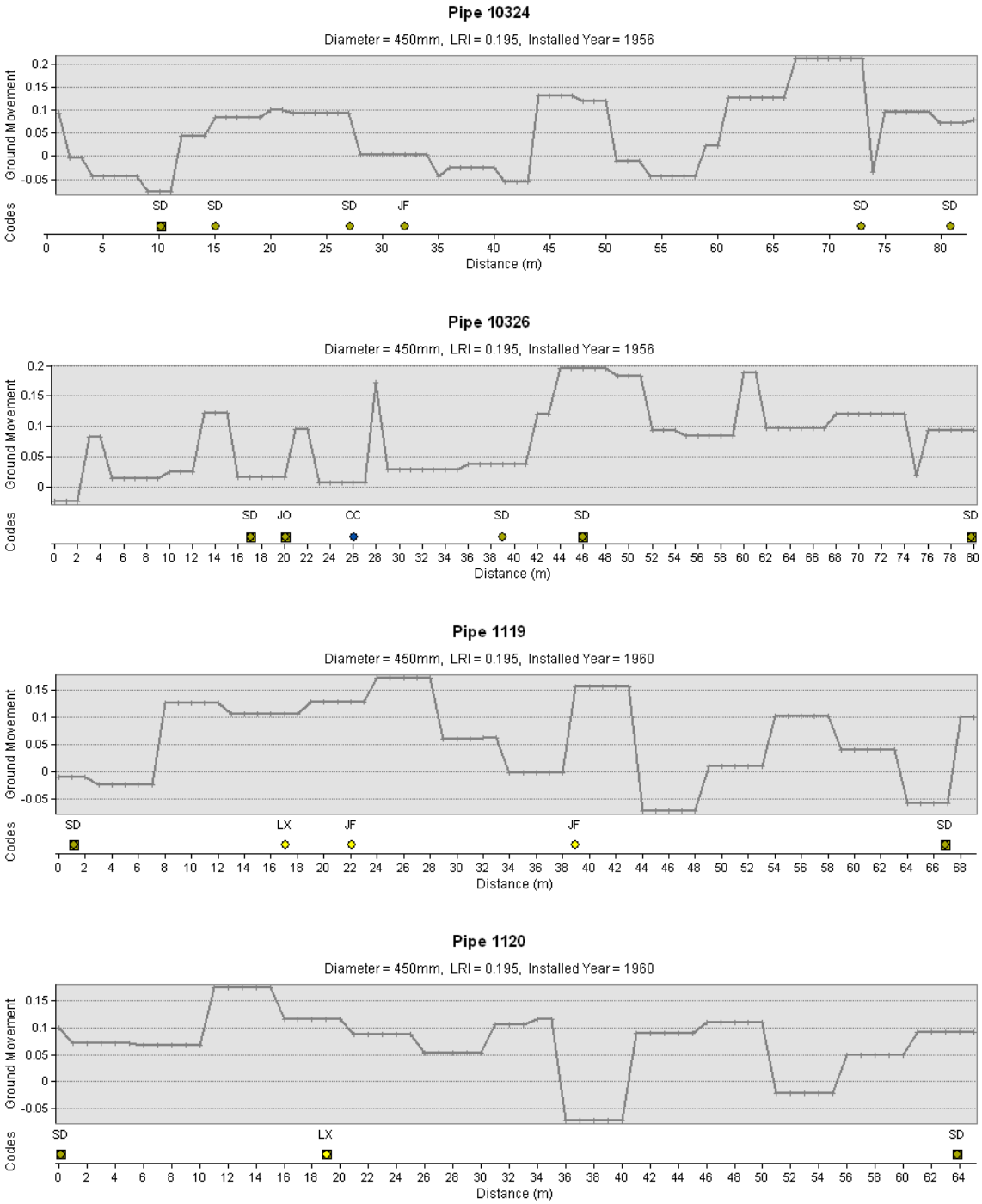

Figures B-47 to B-50. Individual pipe damage observation records

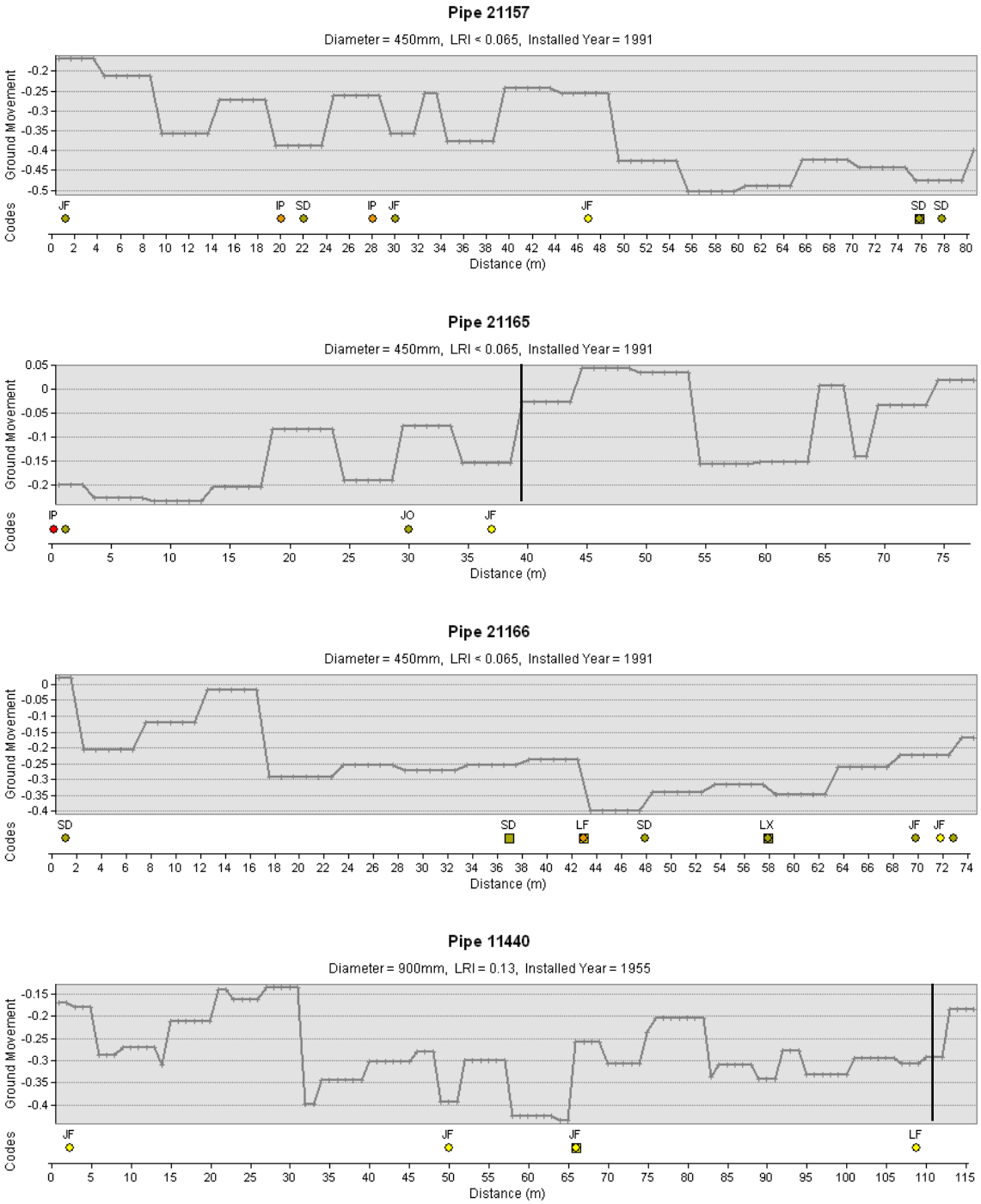

Figures B-51 to B-54. Individual pipe damage observation records

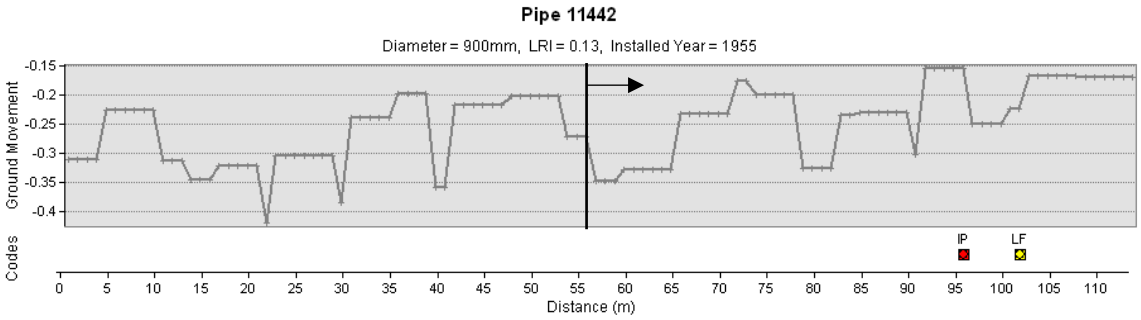

Figure B-55. Individual pipe damage observation records

Appendix C - Pipe Installation Information

This section features the information for specifying pipe bedding and installation using different methodologies.

CLASS A

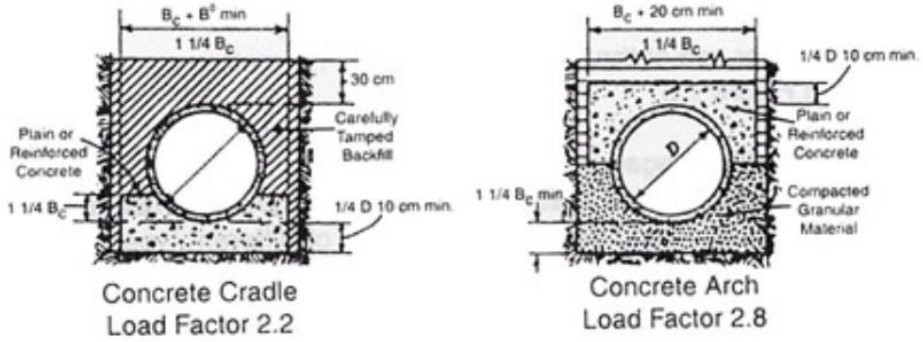

CLASS B

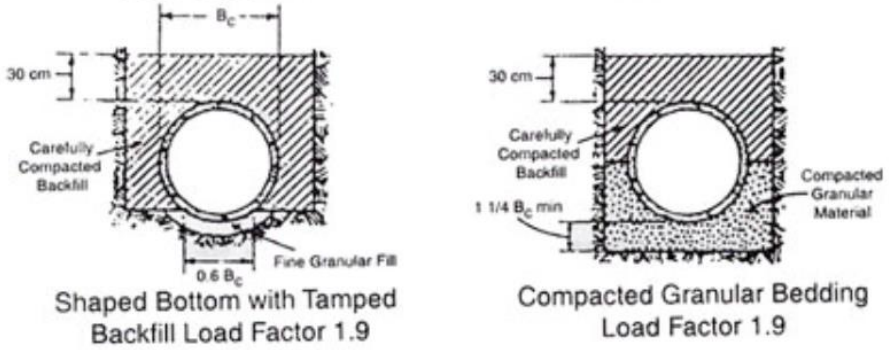

CLASS C

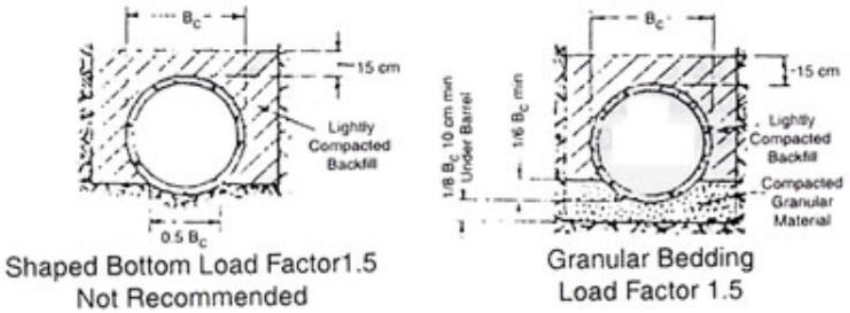

CLASS D

Figure C-1. Spangler's original bedding configurations for use with the Indirect Method (Al-Saleem & Langdon, 2015)

Table C-1. ACPA Standard Installation Types using the Direct Method (Al-Saleem & Langdon, 2015)

Installation Type	Bedding Thickness	Haunch and Outer Bedding	Lower Side
Type 1	Do /24 minimum, not less than 3 in. If rock foundation, use DO /12 minimum, not less than 6 in.	95% Category I	90% Category I, 95% Category II. or 100% Category III
Type 2	Do /24 minimum, not less than 3 in. If rock foundation, use DO /12 minimum, not less than 6 in.	90% Category I or Category II	85% Category I, 90% Category II, or 95% Category III
Type 3	Do /24 minimum, not less than 3 in. If rock foundation, use DO /12 minimum, not less than 6 in.	85% Category I, 90% Category II, or 95% Category III	85% Category I, 90% Category II, or 95% Category III
Type 4	No bedding required, except if rock foundation, use DO /12 minimum, not less than 6.0 in.	No compaction required, except if Category III, use 85% Category III	No compaction required except if Category III, use 85% Category III

Note. The percentage indicates compaction percent, and the Category is the Soil Category, refer Table C-2

Table C-2. Equivalent Unified Soil Classification System (USCS) and American Association of State Highway and Transportation Officials (AASHTO) Soil Classifications for Soil Designations using standard installations (Al-Saleem & Langdon, 2015)

	Representative Soil Types		**Percent Compaction**	
SIDD Soil	USCS	AASHTO	Standard Proctor	Modified Proctor
Gravelly Sand (Category I)	SW, SP GW, GP	A1, A3	100	95
			95	90
			90	85
			85	80
			80	75
			61	59
Sandy Silt (Category II)	GM, SM, ML Also GC, SC with less than 20% passing #200 sieve	A2, A4	100	95
			95	90
			90	85
			85	80
			80	75
			49	46
Silty Clay (Category III)	CL, MH GC, SC	A5, A6	100	90
			95	85
			90	80
			85	75
			80	70
			45	40